UDP-GLUCOSE:GLYCOPROTEIN GLUCOSYLTRANSFERASE (UGGT-1) AND UPR GENES MODULATE *C. ELEGANS* NECROTIC CELL DEATH

By

YURY ORLANDO NUNEZ LOPEZ

A Dissertation Submitted to The Graduate School of New Brunswick

Rutgers, The State University of New Jersey

and

The Graduate School of Biomedical Sciences

University of Medicine and Dentistry of New Jersey

in partial fulfillment of the requirements for the degree of

Doctor of Philosophy

Graduate Program in Cell and Developmental Biology

written under the direction of

Professor Monica Driscoll, Ph.D.

and approved by

_____

_____

_____

_____

New Brunswick, New Jersey
October 2009

ABSTRACT OF THE DISSERTATION

UDP-glucose:glycoprotein Glucosyltransferase (*uggt-1*) and UPR Genes Modulate *C. elegans* Necrotic Cell Death

By YURY ORLANDO NUNEZ LOPEZ

Dissertation Director:
Prof. Monica Driscoll, Ph.D.

Necrosis underlies the pathology of many neurodegenerative diseases, stroke, and traumatic injury. In the Driscoll Lab, necrotic cell death (NCD) mechanisms have been addressed for several years taking advantage of unique genetic and molecular biology tools developed in the model organism *Caenorhabditis elegans*. The necrotic paradigm we study the most involves initiation of cell death by hyperactivated ion channels expressed in six touch-sensory neurons and requires elevation of intracellular Ca^{2+}, which activates calpain and cathepsin proteases.

I exploited the unique features of our model system to uncover novel genetic factors influencing this process. To this end, I conducted a high-throughput forward genetic screen to identify mutations that block or delay necrotic cell death induced by MEC-4(d) channel hyperactivation, and genetically mapped novel mutations capable of blocking or slowing the death process. I exploited an automated mutational screening capacity that allows sorting of individual animals based on detection of fluorescent signals that, in our particular case, had been engineered to indicate neuronal viability. I focused on the

cloning of two novel mutant loci and dissected molecular mechanisms responsible for death suppression. In addition, I studied the impact of a major subset of calcium homeostasis genes in a *C. elegans* model of Aβ toxicity.

My research adds a new component to the current understanding of NCD, suggesting that inability to cope with endoplasmic reticulum stress (presumably induced by calcium depletion inside the ER, which affects chaperone functionality) plays an important role in progression through necrosis. I discovered that mild activation of an intact unfolded protein response (UPR), e.g., as induced by downregulation of UDP-glucose:glycoprotein glucosyltransferase (UGGT, an ER-resident enzyme involved in high-fidelity protein folding quality control) or mild increments in ambient temperature, can partially suppress necrosis in our *C. elegans* model, reminiscent of beneficial preconditioning effects in mammals. Additionally I found that several UPR transducers contribute to such modulation of cell death in a "tug-of-war" fashion. Our refined model of molecular mechanisms contributing and modulating necrosis suggests new strategies that could eventually limit the devastating effects of necrosis in human injury and disease.

ACKNOWLEDGEMENTS

My work as a graduate student and this thesis would not be complete if I do not acknowledge the many people that, one way or the other, have contributed to my development as a scientist, a labmate, and a simple person with big dreams.

First of all, I want to express my sincere and everlasting gratitude to my advisor Professor Monica Driscoll for her important guidance, support, and understanding during these interesting and complicated years. Dr. Driscoll has been, in addition to an excellent scientific advisor, a role model, a polite listener, and a life coach for me. I owe a great deal of my success while applying to very competitive fellowships to Dr. Driscoll mentorship, and I have no words to express, again, my appreciation for her constant support and advice. I am also very grateful to the members of my Thesis Committee: Professors Mary Konsolaki, Richard Padgett, and William Wadsworth, as well as to Professors Barth Grant and Garth Patterson for important scientific advice and guidance in relation to my work, both during Committee Meetings and lab meeting exchanges.

I dedicate a special note to a great colleague, Dr. Dewey Royal, who sadly for all of us just recently passed away in a brave battle against Multiple Sclerosis. Dr. Royal introduced me to the *C. elegans* work in the Driscoll laboratory, and together with his wife, Ms. Mary Anne Royal, developed in me necessary skills to succeed as a graduate student. I will always remember Dr. Royal as an example, a model of dedicated scientist

that will stop at nothing but discovering the truth behind the intricate pathways of biology, science, and life in general. I feel proud for having met Dr. Royal and with this thesis, I want to honor his memory.

Also special among my long-term interactions born here at UMDNJ and Rutgers University, is the one with Professor Michael Leibowitz, co-Director of the Molecular Biosciences Graduate Programs at Rutgers/UMDNJ and Executive Director of Graduate Academic Diversity at UMDNJ-GSBS. When I started at UMDNJ as a minority Pipeline fellow, Professor Leibowitz impressed me very much for his dedication to assisting underrepresented students. Today, I am very grateful to Professor Leibowitz for his sincere and encouraging guidance, for his effort to support and develop all of us minority as well as non-minority students, and for the multiple recommendation letters he has so willingly written for me. I am also grateful to Professor Evelyn Erenrich (Assistant Dean, Recruitment and Retention Rutgers/UMDNJ-GSBS) and Professor Jerome Langer (co-PI and Program Director for the "Initiative to Maximize Student Diversity" (IMSD) grant), for their mentorship during my initial years. I also thank Professor Charles Martin (Director of Education and the Molecular Biosciences Program, Division of Life Sciences at Rutgers) and Professor Vincent Pirrotta (Chair of the Molecular Biology and Biochemistry Department at Rutgers), as well as Graduate Program and Departmental Administrative Assistants: Mrs. Perry Dominguez, Mrs. Carolyn Ambrose, Mrs. Diane Murano, and Mrs. Barbara Nowakowski, for their efforts while supporting our graduate programs and students.

Very valuable to my development during this stage has also been my interaction with postdoctoral fellows Dr. Carolina Ibanez, Dr. Itzhak Mano (currently an Assistant Medical Professor at CUNY), Dr. Christopher Quinn (soon to join University of Wisconsin Milwaukee as an Assistant Professor), Dr. Peter Schmeissner (currently a Scientist at the US Department of Agriculture), Dr. Laura Bianchi (currently an Assistant Professor at University of Miami), Dr. Marton Toth, Dr. Berengere Pinan, and Dr. Brian Onken from whom I have learnt great science and received important advise and friendship. I am similarly grateful to all other research associates and student labmates in the Driscoll laboratory, as well as graduate school classmates with whom I had the privilege to interact, for their friendship and enthusiasm that made unique my graduate school experience. I am also thankful to the members of the Grant, Paterson, Konsolaki, and Barr Laboratories for providing important insights during our group meetings and seminars.

I want to express sincere gratitude to my former supervisors Professor Debra Bessen, now at the New York Medical College, and Professor Elizabeth Lacy, from Memorial Sloan Kettering Cancer Center, for giving me the opportunity to get back into science here in the USA and for encouraging and supporting my applications to graduate school and predoctoral fellowships.

I am also very grateful to my many good friends, teachers, professors, and colleagues from Cuba and the USA, that one way or another have contributed to and encouraged my development as a social being, a science lover, and a freedom-seeking individual.

Last yet most importantly, I thank all my family. In a special pedestal I have my wife Diamela for her love, understanding, and dedication; for believing in me, in the good and the bad times; for being considerate and supportive during these many years of sacrifice and hard work; and for giving me two special and lovely daughters: Nicole Gabriela and Emily Camila, who make special every one of our days and give us strength to keep our dreams alive. I have no words to thank my parents Marta Elsa and Santiago Orlando, my sister Marta Belkis, and my brother Santiago Alexander for their immense love and support, and for being always by my side (no matter how much land and sea could separate us) to encourage me and revive my strengths. I am also thankful to all other family members with whom I have shared many important moments. To the great family I am lucky to have, I am forever grateful.

DEDICATION

To my lovely daughters: Emily Camila and Nicole Gabriela

To my wife, my parents, my sister, and my brother

TABLE OF CONTENTS

LIST OF FIGURES

LIST OF TABLES

THESIS SUMMARY

In this thesis I document studies of molecular mechanisms of neurodegeneration conducted as PhD research in the Joint Graduate Program in Molecular Biosciences and the Cell and Developmental Biology Program from the University of Medicine and Dentistry of New Jersey and Rutgers, The State University of New Jersey.

In Chapter 1, I offer a short introduction to cell death mainly focusing on recent advances that underscore the continuity of the cell death space and the intricate cross-communication and interdependent regulation of processes governing the eventual death outcome. I also introduce the nematode Caenorhabditis elegans as a powerful and amenable model organism and describe how we have used this model to study necrotic cell death (NCD) in the laboratory.

In Chapter 2, I describe the implementation of a high throughput strategy for chemical mutagenesis and fluorescent screening of suppressors of *mec-4(d)*-induced necrotic-like cell death. Using an automatic sorting capability recently installed in the laboratory (the so-called worm sorter), I screened more than 56,000 haploid genomes, identified 107 mutant lines, and assigned them to 7 loci, 4 of which represented novel genes. In this chapter I also describe my initial mapping efforts regarding positional cloning of LGII-linked novel death suppressor locus (reference allele bz200).

Chapter 3 describes my work on mapping, positional cloning, and characterization of novel LGX-linked suppressor locus *uggt-1*. This gene encodes a UDP-glucose:glycoprotein glucosyltransferase (UGGT), which is an endoplasmic reticulum (ER)-resident enzyme highly conserved in the animal kingdom and a major sensor of protein folding quality. I show that loss or downregulation of *uggt-1* in *C. elegans* induces mild, chronic activation of the unfolded protein response (UPR) and general reprogramming of transcriptional networks and cellular homeostasis, with an overall protective effect reminiscent of preconditioned cellular states. I discuss my supporting data and relevant recent reports implicating ER calcium signaling, ER-stress preconditioning, and differential regulation of pro-survival versus death-inducing factors in cellular adaptation.

Lastly, chapter 4 describes a reverse genetic screen for calcium-binding, EF-hand motif-containing suppressors of Aβ-dependent paralysis in *C. elegans*, which I conducted in addition to my work on *mec-4(d)*-induced necrosis. Here I describe and discuss the identification of ten *C. elegans* genes, nine of which have human homologs, which could potentially be involved in the development and/or progression of Alzheimer's disease (AD). The identification of genes already well known for their involvement in AD, Huntington disease (HD), and bipolar disorder validates this approach and suggests that the interactions discovered in our simple model may hold pertinent value in the study of the etiology of the human disease.

The composite of multiple mutagenesis screens conducted in our lab during the last decade underscores a crucial role for the ER in the activation of necrosis in *C. elegans*, reminiscent of the fundamental role played by the mitochondria in apoptosis. In this view, I recommend that additional efforts be dedicated to better understand the basic roles that ER-to-nucleus signaling and ER-mitochondria crosstalk may be playing during NCD progression. Such studies will likely contribute insights into other degenerative diseases as well, such as those involving toxic protein aggregation.

CHAPTER 1. INTRODUCTION TO CELL DEATH

1.1. Cell death interplay: the cellular triple-play

In multicellular organisms, cell death plays an essential role paradoxically necessary for life of the organism as a whole. This is well evidenced, for example, by the fact that cell death is indispensable to selectively eliminate excess cells and to sculpt tissues and organs during development. In other instances throughout life, aging cells are sacrificed and contents recycled, in harmony with the proliferation of new cells that take over the needed functions. Such cellular homeostasis has marvelously evolved into a tightly regulated and highly orchestrated process, where “live or die” decisions, among others, are constantly implemented. Dysregulation of the control mechanisms ensuring cell death contributes to a variety of disease states such as neurodegenerative and inflammatory diseases (due to excess cell death), and cancer and autoimmune diseases (due to reduced cell death and excessive proliferation) (Henriquez et al., 2008).

Multiple types of cell death have been described in the scientific literature, but there is a main core of three mechanisms that includes: apoptosis, autophagy, and necrosis (Festjens et al., 2006; Hengartner and Bryant, 2000; Levine and Klionsky, 2004). These mechanisms could be understood as the more distant or independent outcomes in the cell death continuum, although accumulating evidence indicates considerable crosstalk and switchability between the three processes (Henriquez et al., 2008; Thorburn, 2008).

Figure 1 summarizes the more notable morphological features distinguishing apoptosis, necrosis, and autophagy.

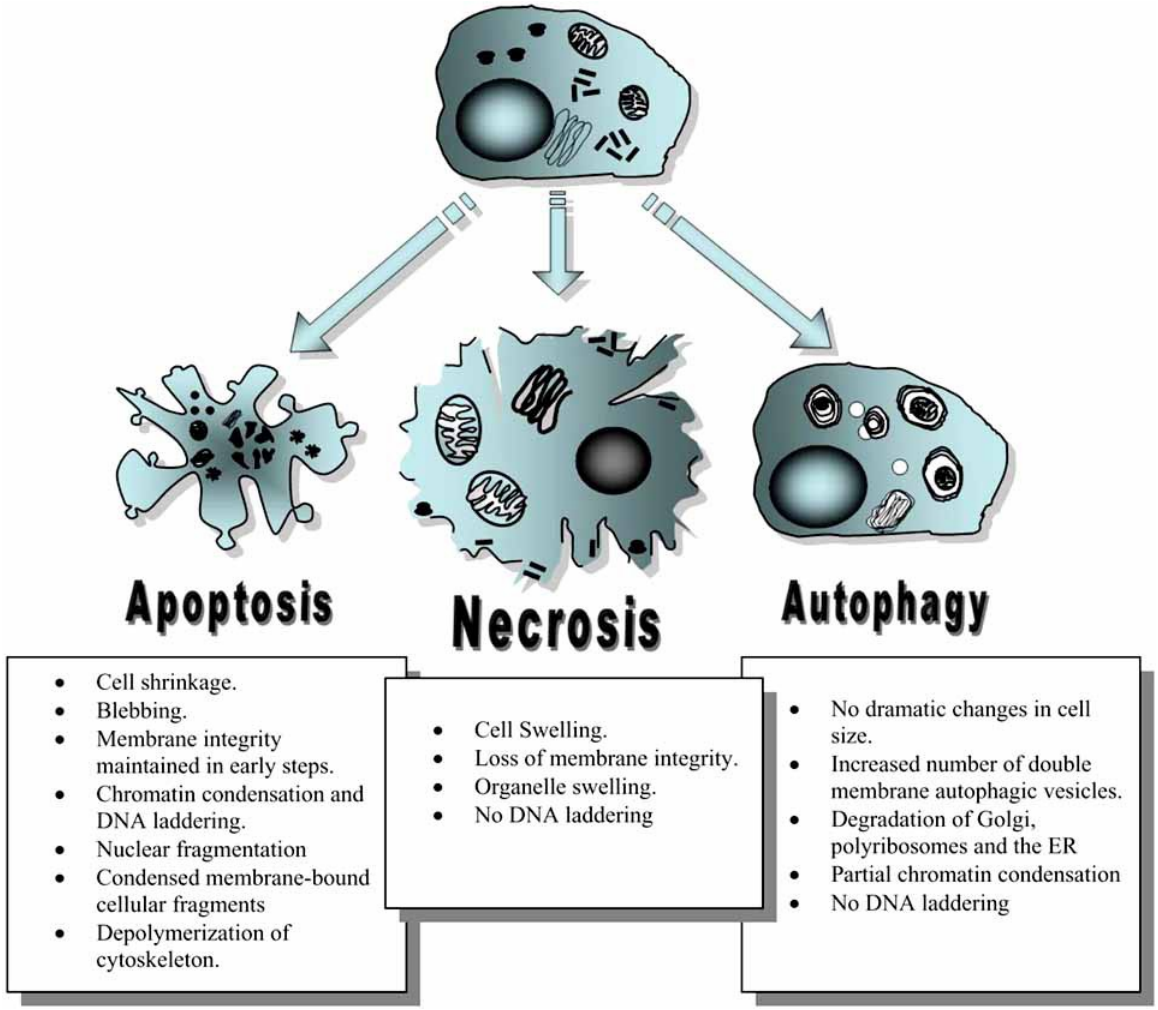

Figure 1. Morphological changes associated with the three modes of programmed cell death.

In the upper part of the figure a normal cell is shown; lower panels summarize schematically the morphological features associated with execution of apoptosis, necrosis and autophagy (Henriquez et al., 2008). Reproduced with permission from Dr. Andrew F.G. Quest, Universidad de Chile, Santiago, Chile).

1.1.1. Apoptosis

Apoptotic mechanisms have been intensely studied in the last few decades because of their involvement in development and cancer, and a well understood picture has emerged of the classical phenomenon, originally known as programmed cell death (PCD) but now more accurately referred to as PCD type I (PCD I). The term PCD referring only to apoptotic cell death arose as a logical consequence from an initial understanding of necrosis as an uncontrolled, chaotic series of events induced by acute cell injury. Nowadays evidence has accumulated and demonstrated that autophagy (PCD II) and necrosis (PCD III) are also highly regulated processes (Henriquez et al., 2008; Klionsky, 2007; Thorburn, 2008; Vanlangenakker et al., 2008).

A major contribution to the fundamental understanding of the basic apoptotic mechanism came from studies in the nematode *C. elegans*, pioneering work for which Dr. R.H. Horvitz was awarded a share of the 2002 Nobel Prize in Physiology and Medicine. In brief, the apoptotic pathway elaborated in nematodes involves the action of BH3 domain protein EGL-1, which influences globally-acting death suppressor CED-9 (a BCL-2 family member) and an executor caspase, CED-3 (Horvitz, 1999; Metzstein et al., 1998). Apoptotic death regulation, execution, and corpse removal mechanisms are strikingly conserved from nematodes to humans (Metzstein et al., 1998), though more simple and genetically tractable in nematodes.

Apoptosis can be executed through two different pathways. One pathway is denominated intrinsic or mitochondrial because is activated in response to intracellular stimuli that lead to permeabilization of the mitochondrial outer membrane (MOMP) and the release of cytochrome c and other apoptogenic proteins (Green and Kroemer, 2004). Released cytochrome c activates the apoptosome, which process pro-caspase-9 into activated caspase-9 (initiator caspase), which then activates executioner caspases (e.g. caspase-3, casapase-7, *etcetera*). The other pathway, denominated extrinsic or death receptor pathway, involves the activation of cell surface receptors upon ligand binding. Ligand-activated death receptors induce the formation of a multi-protein complex denominated the Death-Inducing Signaling Complex (DISC) that recruits and process pro-caspase-8 or pro-caspase-10 into the respective activated caspase (differently from the intrinsic pathway caspase-8 or caspase-10 are the initiator caspases in this case), which subsequently activates executioner caspases such as caspase-3 (Bredesen, 2008; Thorburn, 2004). Both, the intrinsic and extrinsic pathways converge on the activation of executioner caspases by initiator caspases.

1.1.2. Necrosis

Although researchers had traditionally considered necrosis as a chaotic, non-regulated type of death caused by overwhelming stress, growing evidence suggest the existence of an alternative programmed cell death mechanism characterized by necrotic morphology and specific biochemistry (Golstein and Kroemer, 2007; Yuan, 2009). A concept of programmed course and programmed occurrence is supported, for example, by reports

describing the occurrence of necrosis during development (Chautan et al., 1999; Roach and Clarke, 2000) and in adult tissue homeostasis (Barkla and Gibson, 1999).

Necrosis is typically associated with early signs of mitochondrial dysfunction (such as the production of reactive oxygen species (ROS) by mitochondria and swelling of mitochondria), ATP depletion, general disruption of ionic and internal homeostasis, cellular edema (swelling), perinuclear clustering of organelles, activation of calpain and cathepsin proteases, lysosomal rupture, and ultimately plasma membrane rupture (Golstein and Kroemer, 2007).

The release of the cytoplasmic content into the extracellular space due to the cell lysis causes a characteristic and potentially damaging inflammatory response from neighboring tissues (Orrenius et al., 2003). Interestingly, it has been suggested that the release of some intracellular molecules such as hepatoma-derived growth factor (HDGF) can function to activate signaling pathways that promote axonal sprouting and neurite outgrowth in the damage area, as well as cell migration and tumor cell metastasis from necrotic areas in solid tumors (Zhou et al., 2004; Zong and Thompson, 2006).

In contrast to apoptosis, which is recognized as the predominant form of cell death in immature neurons, necrosis appears to be the cell death of choice as neurons mature (Liu et al., 2004; Yuan, 2009). Mature neurons are one of the most precious cell types in

an organism because of their limited ability to regenerate, yet devastating neuronal losses can occur in pathologic conditions such as stroke, for which there is not direct therapy available yet.

1.1.3. Autophagy

Some authors refer to autophagy as a degradation pathway that complements the proteasomal pathway by degrading long-live proteins, protein aggregates, and organelles. The autophagic process recycles cellular material and produces energy and amino acids, and is therefore usually understood as a protective mechanism, as evidenced during nutrient starvation, for example (Bredesen, 2008). A role of autophagy in PCD is more controversial but direct and indirect observations have led to the concept of autophagy as a non-apoptotic form of PCD (Levine and Yuan, 2005; Shimizu et al., 2004; Yue et al., 2003).

Autophagy is normally mediated by the induction and nucleation of autophagic vesicles that expand and fuse with lysosomes. More than 30 genes have been implicated in autophagy in yeast, and at least 11 have orthologs in mammals (ATG1, 3, 4, 5, 6, 7, 8, 9, 10, 12, and 16) (Thorburn, 2008; Yorimitsu and Klionsky, 2005). Multiple upstream signaling pathways are able to modulate autophagy and most of them work through mTOR (mammalian target of rapamycin), which is a potent inhibitor of autophagy.

However, there are also mTOR-independent mechanisms that activate autophagy, e.g. trehalose-induced enhancement of autophagy (Sarkar et al., 2007; Thorburn, 2008).

Recently, it has been shown that direct molecular connections could simultaneously regulate autophagy and apoptosis. For example, apoptosis activator p53 can also activate autophagy through induction of DRAM, while activation of the PI3 kinase/Akt pathway can inhibit both apoptosis and autophagy (Arico et al., 2001; Crighton et al., 2006; Thorburn, 2008). While the apoptosis-autophagy crosstalk can sometimes result in the combined occurrence of both processes, in many other instances, the cell just switches between the two responses in a rather mutually exclusive manner, which is suggested to depend on variable activation thresholds (Maiuri et al., 2007).

1.2. *Caenorhabditis elegans* as a model for studying necrosis

1.2.1. Unique advantages of *C. elegans* as model organism

C. elegans is a microscopic, free-living, soil nematode highly amenable to genetic studies. Some key features of this model are a rapid, hermaphroditic life cycle of approximately 3 days at 20°C (progressing from a fertilized embryo through four larval stages to become an egg-laying adult), small size of approximately 1.5 mm long when adult, and transparent body that makes it ideal for *in vivo* differential interference contrast (DIC) microscopy. In addition, this nematode has a very simple and constant anatomical layout of only 959 cells in the adult hermaphrodite, of which exactly 302 are

neurons (Riddle et al., 1997). The constant cell number allowed researchers to develop a complete map of cell lineages from fertilized egg to adult (Sulston et al., 1983) and also the reconstruction of the whole nematode body from electron micrographs (White et al., 1976). All neuronal connections in *C. elegans* have been mapped, which makes it the only animal with a completely known wiring diagram (White et al., 1986).

Researchers easily and cheaply maintain *C. elegans* in the laboratory, on small agar plates (or in liquid cultures in multi-well plates), using *Escherichia coli* bacteria as a food source. Mutations can also be easily generated thanks to the fact that several mutagens work very efficiently in the worm, particularly ethyl methane sulphonate (EMS) (Hodgkin, 2005). The ability of *C. elegans* to reproduce by self-fertilization greatly simplifies the production of mutants, since homozygous F2 mutants segregate from mutagenized parents without requiring genetic crosses. In addition, the occurrence of some males in the population (males are generated by nondisjunction of chromosome X during meiosis) allows for the transfer of mutant alleles by mating, which makes complementation tests and construction of compound mutants straightforward.

C. elegans has a small genome of approximately 97 megabases, which is completely sequenced, and well annotated. The information on its approximately 19,800 predicted genes is publicly accessible through WormBase.org (Chen et al., 2005b). Remarkably, depending on the particular bioinformatics approach used, putative *C. elegans*

homologs have been identified for 60-80% of human genes (Kaletta and Hengartner, 2006). The vast amount of genomic information and molecular biology tools available are very useful, for example, to perform reverse genetics (Bargmann, 2001; Plasterk, 1992), mutation mapping (Fay, 2006; van der Linden and Plasterk, 2004), cloning and characterization studies (Nakamura et al., 2008; Wei et al., 2005), *etcetera*.

Reverse genetics has particularly gained popularity in the *C. elegans* field due to the remarkable simplicity with which double stranded RNA (dsRNA) can be introduced into nematodes. RNA interference (RNAi) is induced by simply feeding *C. elegans* with bacteria transformed to inducibly transcribe a gene of interest in both directions, hence producing sense and antisense RNA sequences that hybridize to make dsRNA (Timmons et al., 2001). Once the bacteria is eaten, the long dsRNA is absorbed through the intestine and endonucleolytically cleaved into 20-25 nucleotide-long small interfering RNA pieces (siRNA), which trigger a systemic and heritable gene knockdown effects (Grishok, 2005).

Production of transgenic *C. elegans* is also simple and cost-effective, mainly requiring good micromanipulation skills to obtain transformed lines just a few days after microinjecting the DNA of interest into the worm gonads. Biolistic transformation (also known as microparticle bombardment) is an alternative, very efficient method to

produce low copy, integrated transgenes (Evans, 2006; Praitis et al., 2001; Wilm et al., 1999).

Taken together, the broad range of genetic and molecular techniques applicable in the *C. elegans* model system allows unique lines of investigation into fundamental biological problems such as neuronal injury and cell death.

1.2.2. Necrotic-like cell death in *C. elegans*

Multiple genetic and environmental insults can trigger necrosis in *C. elegans*. Gain-of-function mutations in several genes, such as degenerin ion channels *mec-4(u231)*, *deg-1(u38)*, and *unc-8(n491)* (Chalfie and Wolinsky, 1990; Driscoll and Chalfie, 1991); nicotinic acetylcholine receptor *deg-3(u662)* (Treinin and Chalfie, 1995); and stimulatory α-subunit of trimeric G protein (Berger et al., 1998; Korswagen et al., 1997) can induce cell death that is morphologically similar to mammalian necrosis.

In the Driscoll lab, an elegant necrosis model (Figure 2) has been developed that involves death initiation by hyperactivation of Na^+/Ca^{2+} ion channel *mec-4(u231)* [gain-of-function mutant, commonly referred to as *mec-4(d)*]. As noted above, MEC-4 is a member of the *C. elegans* degenerin protein family, a group of ion channel subunits with homology to mammalian epithelial Na^+ ion channels (ENaC's), and is involved in mechanosensory transduction, being exclusively expressed in six touch sensory neurons.

Dr. Driscoll and collaborators have characterized in great detail this necrotic process at the cellular level by conducting an EM time course correlated with stages distinguished by light microscopic observation (Hall et al., 1997). Touch neurons initially develop normally and start to express toxic *mec-4(d)* about 4 hours after the neuron is born. About 4 hours later, first signs of necrosis are evident; necrotic corpses are eliminated by about 8 hours. *mec-4(d)*-induced necrosis involves initial formation of multilamellar whorl-like structures near the plasma membrane that appear to coalesce and internalize, later intracellular vacuolation that may correspond to mobilization of lysosomes, nuclear distortion associated with chromatin clumping, and eventual degradation of intracellular contents (Hall et al., 1997). Finally, neurons may lyse or be phagocytosed (Chung et al., 2000; Hall et al., 1997). This series of morphological changes resemble experimental excitotoxicity in rats (Rothstein, 1996). Channel hyperactivating mutations in flies and mice have also been found to induce neurodegeneration (Heintz and Zoghbi, 2000). The presence of unusual intracellular inclusions is also a common theme in many distinct human neurodegenerative disorders (Driscoll and Gerstbrein, 2003; Zoghbi and Orr, 2000). In the case of *mec-4(d)*, multilamellar inclusions are strikingly reminiscent of those found in lipid storage disorders such as neural ceroid lipofuscinoses (Driscoll and Gerstbrein, 2003).

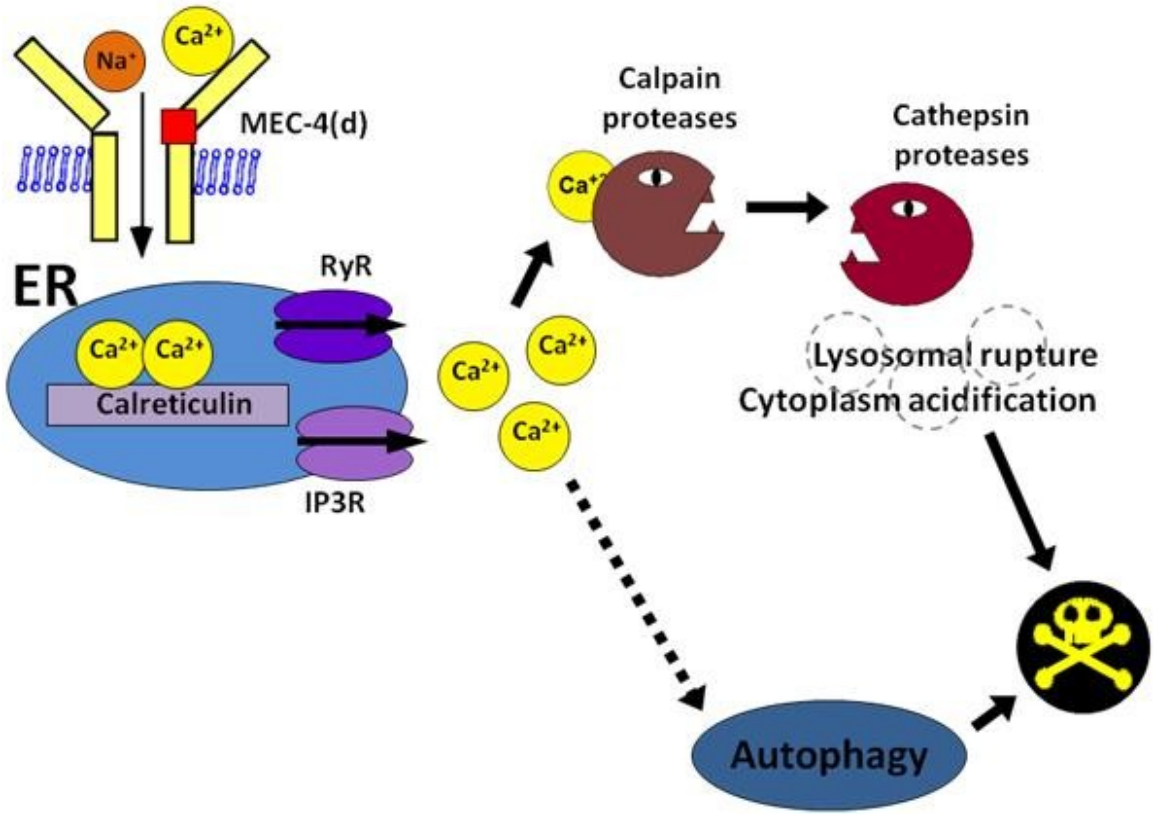

Figure 2. Model for MEC-4(d)-induced necrotic-like cell death in *C. elegans*. Hyperactivated MEC-4(d) channels induce elevation of intracellular Ca^{2+} concentration that activates calpain proteases CLP-1 and TRA-3, which in turn activates the cathepsin proteases ASP-3 and ASP-4, and eventually lead to death (Bianchi et al., 2004b; Driscoll and Gerstbrein, 2003; Hall et al., 1997; Syntichaki et al., 2002; Xu et al., 2001), consistent with the calpain-cathepsin hypothesis (Yamashima, 2004).

In our *C. elegans* NCD model, the toxic *mec-4(d)* subunit carries a large sidechain amino acid instead of a highly conserved small residue near the channel pore (AA713), which allows increased ion conductance through the channel (Adams et al., 1998; Driscoll and

Chalfie, 1991; Goodman et al., 2002; Hong and Driscoll, 1994). Recently, colleagues from our laboratory have demonstrated that, in addition to Na^+, hyperactive *mec-4(d)* channels conduct Ca^{2+}, and this may be the causative initial insult triggering Endoplasmic Reticulum Ca^{2+} release (CICR: calcium-induced calcium release) (Bianchi et al., 2004a). Interestingly, related mammalian family member ASIC1a (an acid-sensing ion channel predominantly expressed in the nervous central system) has been recently reported to conduct Ca^{2+} and to be largely responsible for acidosis-mediated, glutamate receptor-independent, neuronal injury (Xiong et al., 2006; Xiong et al., 2004; Yermolaieva et al., 2004).

It has also been reported that lysosomes contribute to necrosis execution in *C. elegans* by acidifying the cytoplasm and releasing hydrolytic enzymes into it. Such events were dependent on the action of vacuolar H^+-ATPase and lysosomal rupture (Artal-Sanz et al., 2006; Syntichaki et al., 2005). Coincidently, intracellular acidosis has been observed in ischemic astrocytes (Chesler, 2005).

Detrimental environmental conditions such as hypoxia, oxidative stress, and heat stress also induce necrosis in *C. elegans* (Hirsch et al., 2006; Luke et al., 2007; Tawe et al., 1998). These insults apparently activate necrosis through a related process involving calpain-induced lysosomal injury with consequent leakage of lysosomal peptidases into the cytoplasm, as inferred from recent findings that uncovered a pro-survival role for

srp-6 serpin (Luke et al., 2007). Such a role for *srp-6* was dependent on its ability to neutralize calpains and lysosomal cysteine peptidases. Provided sufficient levels within the cell, such inhibitory, anti-peptidase activity proved to counteract even massive lysosomal rupture, suggesting valuable strategies to halt necrosis. As Luke and collaborators conclude, serpin SRP-6 appears critically positioned at the center of the relevant stress response pathway (the one that mediates either adaptation or death by necrosis) by regulating both the induction and outcome of excessive lysosomal permeability.

Autophagy has also recently been implicated in *C. elegans* neuronal necrosis. In 2007, Toth and colleagues showed that three autophagy genes named *unc-51*, *bec-1*, and *lgg-1*, which are involved in cytoplasmic self-degradation, membrane trafficking, and cellular response to starvation, partially suppressed neurodegeneration induced by hyperactive ion channels (Toth et al., 2007). These authors also showed that TOR signaling, which normally downregulates autophagy in response to nutrient availability, protects *C. elegans* neurons from undergoing necrotic cell death, while the contrary expectedly takes place when animals are subjected to starvation (nutrient deprivation upregulates autophagy). Supporting this hypothesis, Samara and collaborators later showed that autophagosome formation occurs early during necrotic cell death in *C. elegans* and that, indeed, autophagy is required for necrosis. These authors additionally demonstrated that autophagy synergizes with lysosomal proteolytic mechanisms, and that calpains may also be implicated in induction of the autophagic response (Samara et

al., 2008). These results somehow contrast with well-known protective effects of autophagy, which, for example, can suppress neurodegeneration in mice (Hara et al., 2006; Komatsu et al., 2006). In this respect, it has been suggested that depending on the actual cellular environment, autophagy may perform a dual role: contributing to cell survival by clearing damage organelles and recycling nutrients, and contributing to cell demise presumably after prolonged over-activation of the pathway (Takacs-Vellai et al., 2006; Toth et al., 2007).

As we can see, this complex molecular choreography is common in many experimental models of necrosis. Necrosis can no longer be considered an accidental, chaotic, and irreversible type of cell death. Instead, it has been demonstrated to involve a variety of well-organized upstream signaling events that converge on a regulatable peptidase pathway. These discoveries could hold the secrets to designing appropriate therapies to interfere with the devastating outcomes of massive necrosis, which is characteristic, for example, in thromboembolic stroke and myocardial infarction in adults, and enterocolitis in preterm infants (Luke et al., 2007).

CHAPTER 2. SCREENING FOR SUPPRESSORS OF *mec-4(d)*-INDUCED CELL DEATH

2.1. Background and Significance

Forward genetics provides a way for scientists to eliminate bias while investigating biological phenomena. By searching for alternative phenotypes of a particular phenomenon and subsequently establishing causality by positional cloning of the responsible DNA variation, researchers can overcome the need for developing a specific hypothesis, which may be influenced by preconceptions. In essence, in isolating relevant mutants, nature reveals itself in the form of heritable variation. For these reasons, forward genetics regularly delivers unexpected discoveries of protein function that are rarely erroneous, and leads to testable hypotheses that are generally better founded than those based on observation alone (Beutler et al., 2007). Another benefit is that by analyzing allelic series generated from forward genetics screens, one can gain insights into relevant structure-function relationships. Secondary screens such as suppressor or enhancer screens are additional valuable tools for identifying genetically interacting genes. However, one limitation of the forward genetic approach is redundancy, which may limit or eliminate the probability of finding transmissible phenotypes induced by single mutations in genes that encode similar functions.

In our particular case, the long-term goal of the lab is to elaborate molecular mechanisms of necrosis by identifying all the genes critical for necrosis regulation and

execution. Toward this end, Dr. Driscoll and colleagues have conducted two preliminary classical forward genetic screens for suppressors of *mec-4(d)*-induced necrosis (see 2.1.1 and 2.1.2 below). Those two previous mutagenesis screens were not conducted to saturation and were focused on isolating only the strongest suppressors of the necrotic-like death. We came to appreciate that partial/weak suppressors are also highly likely to reveal important genes involved in the basic process of necrosis and thus we had a considerable interest in conducting a near-saturation screen for all mutations that influence necrosis, including those with partial suppression effects.

2.1.1. A GFP-based screen for restored touch neuron viability

The first GFP-based screen carried out in our lab was a highly labor-intensive GFP-based screen for restored touch neuron viability. A strain was engineered to express GFP in six touch receptor neurons, driven by the *mec-4* promoter (strain *Is[p_{mec-4}GFP]*). When the toxic *mec-4(d)* mutation is introduced into that background (strain *Is[p_{mec-4}GFP]*; *mec-4(d)*), the touch neurons die and are unable to produce GFP. This "dark" line was mutagenized and the F2 generation screened for rare occurrence of restored touch neuron fluorescence, indicating death suppression (Royal et al., 2005). In this initial screen, 10,000 animals were mutagenized and candidate suppressor lines in which fluorescence was observed in all six touch neurons were selected. These strong suppressors were found to be intragenic *mec-4* mutations that eliminated MEC-4 channel function (8 isolates) and mutations in *mec-6*, which is necessary for MEC-4 channel stability (4 isolates). These particular loci affected the channel death-inducing

stimulus rather than the postulated death pathway, and were thus not of interest for our long-term goal of identifying necrosis modulators. In addition, several mild suppressors were found with partially penetrant phenotypes in which several, but not all, touch neurons survived per animal. Of these, mutant allele *bz2* was the first of a studied subgroup of intragenic mutations in *mec-4(d)*. *mec-4(d,bz2)* appears to disrupt efficient channel trafficking to, or maintenance at, the plasma membrane. This mutant proved to have highly interesting properties, including that it is a strong temperature sensitive and that at 20°C affected touch neurons initially swell, just as in the *mec-4(d)* background, but instead of dying, about 13% recover and remain viable well into adulthood. Such findings indicated that extensive swelling could occur before commitment to death, and suggested a neuronal capacity of recovering after swelling (Royal et al., 2005).

2.1.2. A screen for suppression of death induced by ectopic expression of *mec-4(d)* in the ventral nerve cord

After finding that ectopic expression of the *mec-4(d)* channel can cell-autonomously kill the expressing neurons (Harbinder et al., 1997), colleagues in our lab designed a more efficient screen based on the expression of *mec-4(d)* under the control of the *unc-8* promoter in the ventral nerve cord. Cord neurons consequently swell and die and animals become fully paralyzed. However, animals are still able to self-fertilize and eat. After mutagenizing this strain, Xu and coworkers (Xu et al., 2001) looked for animals

that could move as well as wild type, which again narrowed the search to strong death suppressors. In this screen (45,000 haploid genomes) our lab identified many *mec-6* alleles (*mec-6* influences *mec-4* channel activity in ectopic sites as well as in touch neurons), four calreticulin (*crt-1*) alleles, and two other loci on chromosome I that are under analysis in other work. Since the focus at the time was on strong suppressors, weak ones were not saved, although they were definitely noticed.

From this "ectopic" suppressor screen, the analysis of strong death suppressor *crt-1* revealed several interesting findings. Null alleles of ER Ca^{2+}-binding chaperone calreticulin, which plays a major role in maintenance of intracellular Ca^{2+} stores (Michalak et al., 1999), are strong suppressors of death induced by several tested hyperactive degenerin channels and are also partial suppressors of $G\alpha_S$-induced death (Xu et al., 2001) and glutamate-induced excitotoxic death (Mano and Driscoll, 2009). Although effects on folding/assembly of the toxic MEC-4(d) channel appear to contribute to death suppression, calreticulin's function as a regulator of intracellular Ca^{2+} stores also appears critical. Mutations in ER Ca^{2+} release channels IP3 receptor *itr-1* and ryanodine receptor *unc-68* can also significantly suppress death, as can pharmacological manipulations that block ER Ca^{2+} release, such as dantrolene. Conversely, treatment with thapsigargin, which elevates intracellular Ca^{2+}, can restore degeneration even when calreticulin is absent. The implication is that for *mec-4(d)*-induced cell death, the intracellular Ca^{2+} concentration must rise to critical levels for progression through necrosis, similar to what occurs in mammalian excitotoxicity. Our

findings in nematodes implicate the ER as an important source or modulator of the extreme Ca^{2+} elevations required for necrotic cell death. Similar lines of evidence have been obtained using a mammalian model of traumatic spinal cord injury. Both dantrolene and ryanodine (inhibitors of the ryanodine sensitive receptor RyR) and 2APB (an inhibitor of ER Ca^{2+} release IP3 receptor) were shown to be significantly neuroprotective, suggesting a critical role for ER Ca^{2+} stores (Thorell et al., 2002).

2.1.3. Technological advances allowing for high throughput screening (HTS)

Until recently, fluorescent screening of transgenic *C. elegans* expressing GFP protein, for example, had to be done manually under the dissecting or compound microscopes. Such microscopic examination proved to be time consuming and not suitable for large saturation mutagenesis efforts focused on touch cells. With the advent of automatic COPAS Large Particle Flow Cytometers (Figure 3, Union Biometrica, Massachusetts), the tasks of in-flow analysis, sorting, and collection of objects and biological materials ranging in size from 20 to 1500 microns in diameter became possible. Since these instruments have been designed to accommodate larger objects while maintaining viability, their use is appropriate to screen and sort *C. elegans* specimens of all stages.

As stated in Union Biometrica website (http://unionbiometrica.com/products/overview.html), the patented COPAS technology platforms “are the only fully-automated systems for high throughput analysis, sorting, and dispensing of small model

organisms, seeds, pollen, as well as large particles such as combinatorial chemistry beads. The COPAS instrument enables researchers to measure objects by optical signatures including density and size, and by the presence of fluorescent markers".

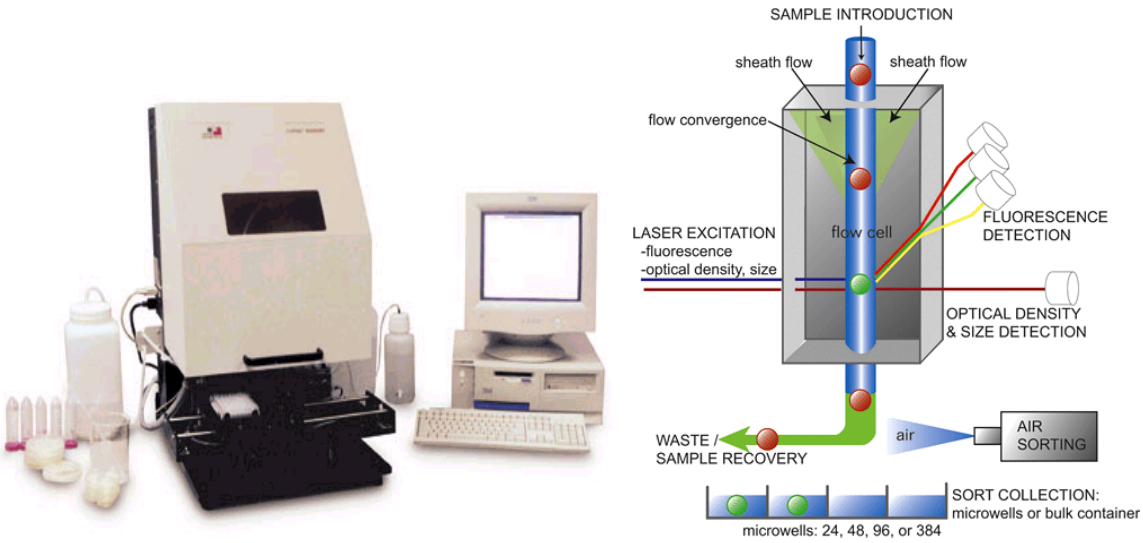

Figure 3. Particle Flow Cytometer System. Diagram of the particle flow and sorting principle.

COPAS stands for Complex Object Parametric Analyzer and Sorter. Objects flow from a continuously mixed sample cup to a pre-analysis chamber, where the sample is surrounded by a "sheath" solution to produce a stabilized laminar flow and focus the objects of interest in the center of the flow stream. Objects then pass through the flow cell where four optical parameters are measured for each organism using two lasers. A red diode laser is used to measure both the size and optical density of the objects, and a multi-line argon laser is used to excite user-selected fluorophores. The COPAS instrument then measures the emission signals. The real time-analysis of these

measured parameters is used to make sort decisions, and only those objects meeting the user-set sort criteria are dispensed into microtiter plates or stationary receptacles. Those organisms not meeting the sort criteria are gently sorted by a puff of air to a sample container, where they may be recovered, unharmed and viable (http://www.unionbio.com/products/copas2.html).

Although slower than I expected and often requiring attention from the user (to maintain proper liquid flow necessary for accurate sorting), this piece of equipment represents a valuable resource for those genetics laboratories engaging in, or willing to perform, high-throughput screens using small model organism such as *C. elegans*, *Danio rerio*, *Drosophila melanogaster*, and *Arabidopsis Thaliana* (seeds) among others.

In particular, using this automated sorting system I was able to rapidly conduct a near-saturation screen covering more than 56,000 genomes. I isolated 107 mutant lines that were assigned to seven loci, four of which represented novel genes.

2.2. Material and Methods

2.2.1. *C. elegans* strains and genetics

I followed standard procedures for *C. elegans* strain maintenance, crosses, and other genetic manipulations (Brenner, 1974). Nematodes were grown on standard nematode growth medium (NGM) plates seeded with *Escherichia coli* strain OP-50 as food source and incubated at 20°C.

Wild type worms were N2 strain Bristol isolate and CB4856 Hawaiian. Other strains used were: SK4005: *zdIs5[pmec-4::GFP] I*, TU253: *mec-4(u253) X*, ZB1028: *crt-1(bz29) V*, ZB1585: *mec-6(u450) unc-11(e47) I*, JT73: *itr-1(sa73) IV*, CB540: *unc-68(e540) V*, and mutagenesis strain ZB1259: *zdIs5 I; mec-4(u231) X*. Strains ZB2906: *zdIs5; rol-6(su1006) unc-4(e120) II; mec-4(d)* and ZB2972: *zdIs5; unc-4(e120) bli-1(e769) II; mec-4(d)* were used for three factor crosses, while SP619: *mnDf57/mnC1 dpy-10(e128) unc-52(e444) II*, SP542: *mnDf29/mnC1 dpy-10(e128) unc-52(e444) II*, SP645: *mnDf63/mnC1 dpy-10(e128) unc-52(e444) II*, B4077: *mnDf21 / mnC1 dpy-10(e128) unc-52(e444)* II, SP541: *mnDf28 / mnC1 dpy-10(e128) unc-52(e444) II* were used for deficiency mapping.

Lines generated for transgenic rescue experiments were constructed by microinjecting purified cosmid DNA and co-injection marker pRF4[*rol-6(su1006)*] into mutant *zdIs5; des(bz200) mec-4(d)* background (cosmid DNA concentration ranged from 1-10 ng/µl, while total DNA concentration was always adjusted to 125 ng/µl). Roller transformants

able to pass the extra-chromosomal array to the progeny were selected and used for further phenotypic characterization.

2.2.2. EMS mutagenesis and high-throughput strategy

I used strain ZB1259: *zdIs5[p_{mec-4}GFP]; mec-4(d)* for mutagenesis. In this strain, GFP signal is at a minimum since the majority of touch receptor neurons die (the average number of surviving, GFP-expressing neurons is 0.69 of 6 possible). L4/young adults were mutagenized using ethane methyl sulfonate (EMS) according to standard protocols (Brenner, 1974). This parental mutagenized population was allowed to lay eggs for three consecutive days at 20°C, and was transferred to fresh plates each day to generate synchronized F1 populations. F1 animals were allowed to grow for 3 days and were sorted by size through the COPAS Biosort (Complex Object Parametric Analyzer and Sorter, Union Biometrica, MA). Fifty L4 worms were sorted to each 100mm NGM plates for a total of 20-30 plates per run/day, depending on availability of L4 larvae. Four days later, sorted F1 animals had self-fertilized and produced the F2 generation, which was then subjected to an additional sorting run through the COPAS Biosort, this time gated to detect 3 or more fluorescent neurons. Stocks of candidate homozygous suppressor mutants with most animals harboring ≥3 fluorescent touch cells were generated for further study. The presence of at least 3 fluorescent neurons was chosen as primary criteria for automated sorting of suppressor mutants because 2 fluorescent, surviving touch cells can be found with a relatively high frequency in the mutagenesis strain, establishing the practical background.

To ensure independence of isolated mutants, I sorted only one F2 population (all the animals contained in a single 100mm plate) per run, hence 20-30 runs/day were needed. In addition, once a potential suppressor mutant was sorted, the siblings were cloned out to individual small plates and only one plate was kept later, ensuring the homogeneity of the population selected for further characterization. In this way (see flow diagram below in Figure 4), I screened 56,600 haploid genomes in 8 biweekly staggered runs as diagramed in Figure 5. I isolated 107 independent mutant death-suppressor lines that were furthered characterized by linkage assignment, complementation, and three factor crosses.

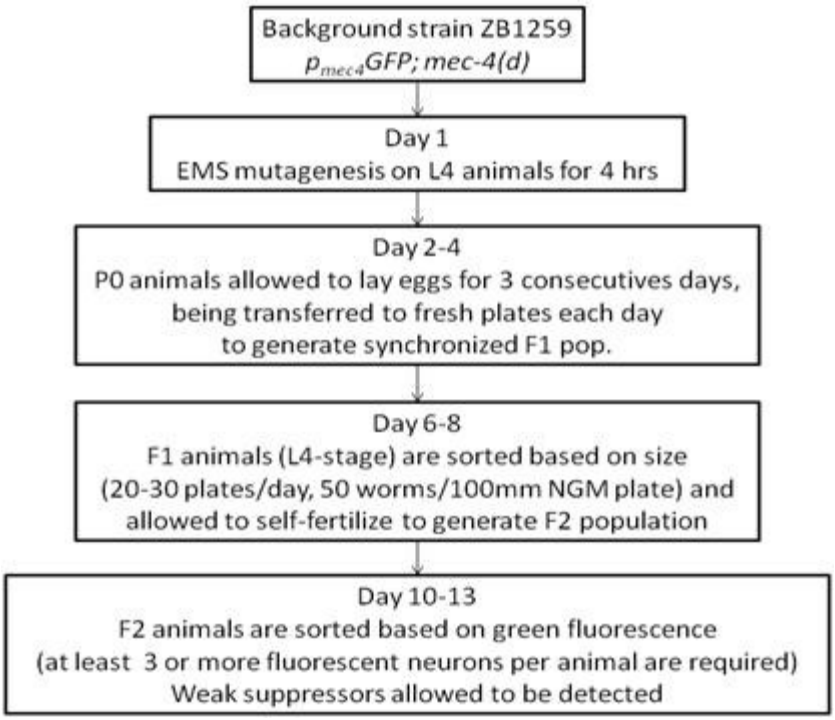

Figure 4. Flow diagram of high-throughput mutagenesis & sorting strategy.

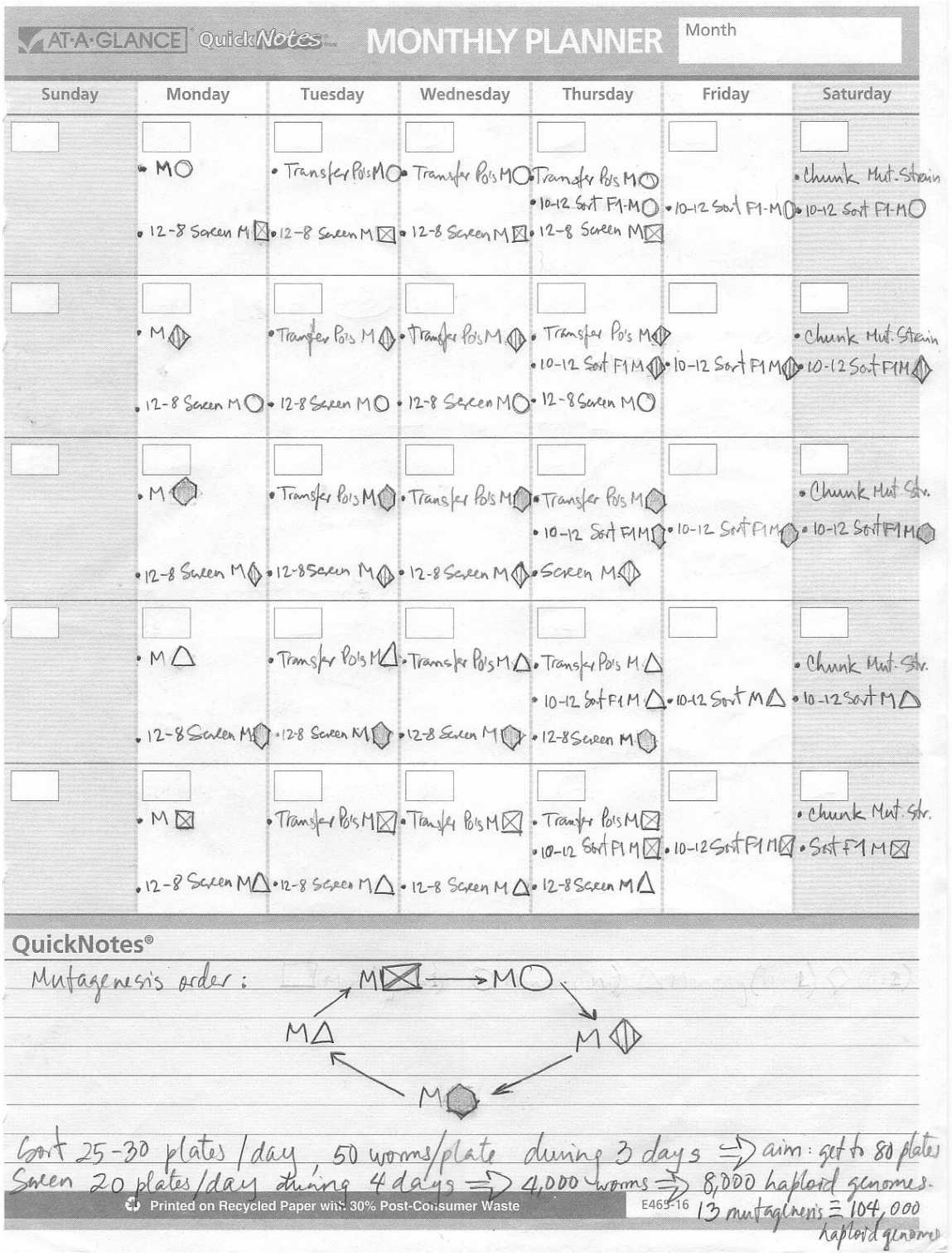

Figure 5. Scheduling diagram for high-throughput mutagenesis & sorting strategy.

2.2.3. Linkage and complementation analysis

First, I determined the dominance pattern of mutants and linkage to chromosome X. For this, mutant L4 hermaphrodites were crossed to males from the original "mutagenesis strain" *zdIs5[p$_{mec-4}$GFP]; mec-4(d)* ("non-glowing" phenotype, non-suppressed death, herein referred to as *zdIs5; mec-4(d)*). Hermaphrodite and male progeny were separately scored under the fluorescent microscope. The dominance pattern for the specific suppressor can be inferred by analyzing the glowing pattern of the heterozygous hermaphrodite progeny. On the other hand, by analyzing the glowing pattern of hemizygous male progeny, it can be inferred whether recessive suppressors are located on chromosome X (recessive mutations will only show a death-suppressing phenotype in male progeny if they localize to chromosome X). This is a helpful consequence of male hemizygocity in the nematode.

Many intragenic suppressors (2nd site mutations in *mec-4(d)* that render the mutant hyperactive channel non-functional, and thus unable to insult neurons to death) were expected as an inherent outcome of this particular screen. Since the *mec-4* gene is located on chromosome X, all recessive suppressors assigned to chromosome X were subjected to an initial round of complementation with the null allele *mec-4(u253)*. If the mutant suppressor happens to be an allele of *mec-4* (intragenic 2nd site mutation on the original *mec-4(d)* gene), the resulting heteroallelic hermaphrodite progeny *mec-4(new-mutant-allele)/mec-4(u253)* will fail to complement and the progeny will maintain the death-suppressing phenotype.

Some autosomal mutations were expected to fall into known suppressor categories such as: *mec-6* (strong suppressor located on LGI encoding a gene needed for *mec-4* channel function), *crt-1* (strong suppressor located on LGV encoding a ER chaperone that is also involved in ER Ca^{2+} storage), *itr-1* (partial suppressor located on LGIV encoding the ER IP_3 receptor Ca^{2+} release channel), and *unc-68* (another partial suppressor located on LGV encoding the ER ryanodine receptor Ca^{2+} release channel). Four additional rounds of complementation tests were therefore performed with the 16 suppressor lines that were not linked to chromosome X. Test alleles used in these cases were likely-null *mec-6(u450)*, null *crt-1(bz29)*, and partial loss-of-function alleles of *itr-1(sa73)* and *unc-68(e540)* (Mary Ann Royal and Mike Lizzio performed these crosses).

Additional rounds of complementation were performed between the novel mutations themselves, to define which ones represented alleles of a single locus and which ones defined distinct loci.

2.3. Results

2.3.1. High throughput screening

Fifty six thousand six hundred haploid genomes were screened, at approximately 8,000 (maximum) mutagenized haploid genomes per week, during a period of 8 “sorting-weeks”. An example of the COPAS Biosort output screen from a detected and sorted suppressor line is shown in Figure 6.

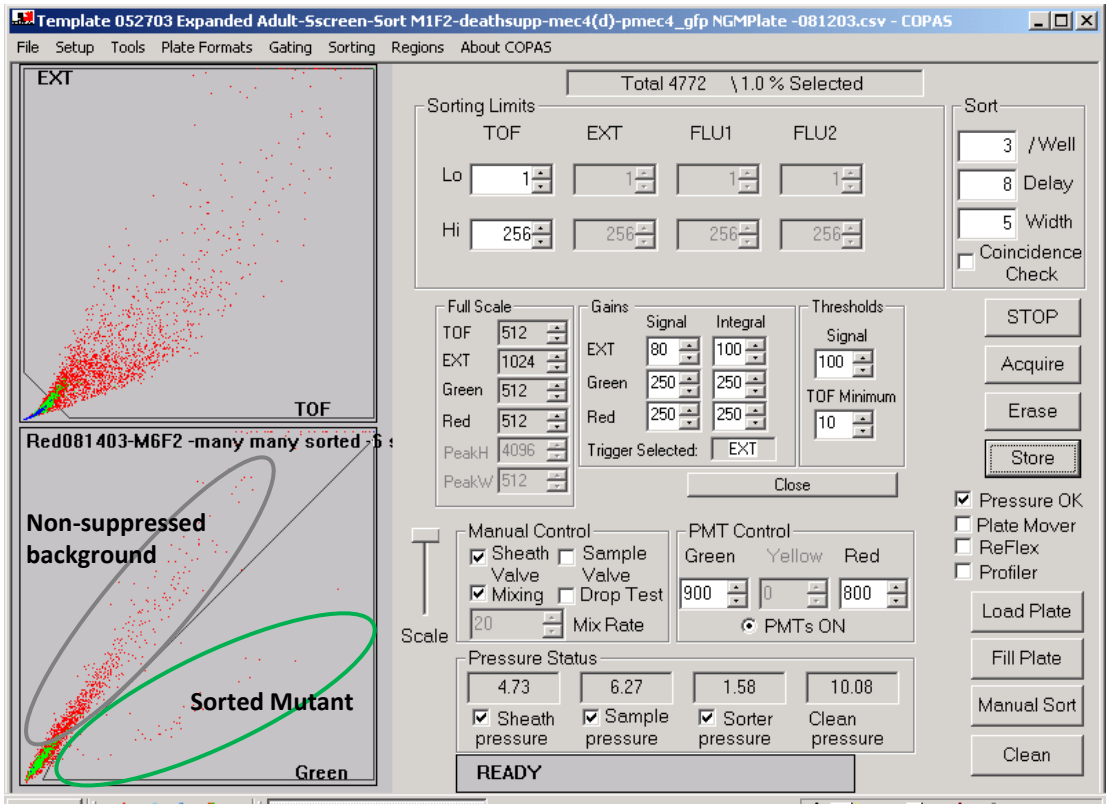

Figure 6. Example of COPAS biosorter output screen.

I isolated 107 mutant death-suppressors (hence loci designation *des*) and maintained them as individual strains. For each suppressor line, homozygocity of the population was ensured by cloning out individual worms with the highest number of fluorescent neurons and observing the "glowing" pattern of their respective descendants. Plates where all progeny had a consistent death-suppressed phenotype were maintained and considered homozygous, once the possibility of dominancy was eliminated (by analyzing the progeny from respective backcrosses to mutagenesis strain ZB1259: *zdIs5 I; mec-4(u231) X*).

Ninety one out of the 107 mutants appeared linked to the sex chromosome and recessive while 16 appeared autosomal. Out of those 16 autosomal alleles, 15 were recessive and one (*bz178*) was semi-dominant. Out of the 91 X-linked suppressors, 85 failed to complement null *mec-4* and presumably represent alleles of *mec-4*. The other six X-linked suppressors failed to complement each other, which suggested that they were alleles of the same gene and defined a novel suppressor locus on LGX. Alleles represent valuable and potentially informative reagents because their sequence analysis can help confirm gene identity, and because we can obtain functional information about putative domains in the specific protein. Alleles are also useful for comparisons between complete and partial loss-of-function phenotypes.

Eight autosomal mutants were alleles of *mec-6*, two were alleles of *crt-1*, and none were alleles of either *itr-1* or *unc-68*. The remaining six autosomal mutant alleles complemented the four known suppressors; therefore, they presumably represent previously unknown suppressor loci. After additional rounds of inter-complementation tests among the six novel mutants, four of them (*bz100, bz148, bz180, bz181,* and *bz200*) appeared to be alleles of the same gene (they failed to complement in the heteroallelic combination), which I later mapped to LGII. Allele *bz200* was chosen as reference for this locus because the strain had a tightly linked secondary roller phenotype that facilitated its initial linkage mapping. Semidominant allele *bz178* appeared unique and later mapped to LGIV. Allele *bz199* also appeared unique and later mapped to LGI. Table 1 summarizes the chromosomal allocation for all isolated mutants.

Table 1. Summary of *mec-4(d)*-induced death suppressor mutants isolated.

	# of mutants	**# of alleles**			**complementation groups**	**allele designations**
X linked	91	*mec-4*	85		1	***(Royal et al., 2005)***
		novel	**6**		**1**	***bz91, bz121, bz125, bz130, bz146, bz156***
Autosomal	16	*mec-6*	8		1	***bz88, bz92, bz140, bz142, bz152, bz166, bz169, bz194***
		crt-1	2		1	***bz190, bz197***
		novel	**6**	**4 in LGII** **1 in LGIV** **1 in LGI**	**1** **1** **1**	***bz100, bz180, bz181, bz200*** ***bz178*** ***bz199***
Total	107					

In summary, twelve novel suppressor lines that defined at least four suppressor loci were revealed by the complementation tests. Ten other lines failed to complement already known suppressor loci *crt-1* (2 lines) and *mec-6* (8 lines), and the remaining 85 were intragenic mutations in *mec-4(d)*. A brief description of this group of intragenic suppressors can be found in reference (Royal et al., 2005), on which I was an author.

This distribution indicates that this particular screen may be approaching saturation, since multiple alleles have been found for many of the loci apparently involved in the mechanism. Other important loci may still be missing from our list and may never be found following this particular strategy for a number of reasons, including cases where the suppressor mutant may be lethal and cases where redundancy may mask the effect of single gene mutations. Alternatively, non-overlapping expression patterns of genes may still hide novel necrosis suppressors from detection in our system (which follows necrosis in only 6 touch sensory neurons). For example, Luke and collaborators discovered that serpin *spr-6* is an important pro-survival regulator and suppressor of intestinal necrosis. However, *srp-6* (which appears able to suppress *mec-4(d)*-induced death in transgenic lines) could not be detected in our screen involving endogenous expression of *mec-4(d)* because *srp-6* is not expressed in the touch sensory neurons (Luke et al., 2007).

2.3.2. Efforts towards positional cloning of LGII-linked necrosis suppressor locus, comprised of alleles *bz100, bz180, bz181, bz200*

Mutant alleles of the LGII-linked locus behave as weak suppressor of necrotic cell death. Strain *zdIs5; des(bz200); mec-4(d)*, chosen as reference for the novel locus, has an average of 2.36 fluorescent neurons, which survived the necrotic insult by the L4 stage (mutagenesis strain *zdIs5; mec-4(d)* has an average of only 0.61 living neurons; maximum death suppression would allow the 6 touch sensory neurons to survive). Mutant allele *bz200* was initially isolated with a tightly linked secondary roller phenotype. This original *bz200* roller line was a useful reagent because it allowed me to quickly perform a first round of SNP mapping against CB4856 Hawaiian strain by following the secondary roller phenotype, then assessing selected polymorphic SNP markers on all chromosomes to determine linkage. This strategy was feasible due to the tight linkage between *bz200* and the roller marker. After conducting such initial SNP strategy and analyzing 23 recombinants, which all contained *bz200* as expected, the *bz200* mutation was mapped to the center of chromosome II, between genetic coordinates II:-1.80 and II:+3.34. By using complementation tests against roller genes around the center of chromosome II, I determined that the roller mutation was allelic to *rol-8* at position II:+0.50.

In order to narrow down the position of the *bz200* mutant gene, I conducted additional 3-factor crosses. I first constructed compound mutant strains *zdIs5; rol-6(II:+0.80) unc-4(II:+1.75); mec-4(d)* and *zdIs5; unc-4(II:+1.75) bli-1(II:+2.80); mec-4(d)* by crossing the

respective double mutants (obtained from CGC) into the *Is5* and *mec-4(d)* backgrounds. Then, I crossed these strains with zd*Is5; bz200; mec-4(d)* males (note that this is the outcrossed non-roller *bz200* strain) and recombinants of both types were isolated (from the F2 generation) and made homozygous by the F3 generation. Table 2 summarizes the results from these crosses and their implications while narrowing down the location of allele *bz200* to the interval between *unc-4* (II:+1.75) and *bli-1* (II:+2.80). Attempts to construct a compound mutant carrying the 2 visible markers and *bz200* (to be used in a fine SNP mapping strategy), using both kinds of recombinants from the *unc-4 bli-1* three-factor cross, were unsuccessful so I employed alternate mapping strategies in order to continue narrowing down the location of the mutant locus before proceeding with transgenic rescue experiments (wt cosmids injections), which could be difficult to interpret sometimes.

Table 2. Results from three-factor crosses while mapping allele *bz200.*

	II:+0.80	II:+1.75	II:+1.75	II:+2.80
	rol-6 non-*unc-4* recombinants	*unc-4* non-*rol-6* recombinants	*unc-4* non-*bli* recombinants	*bli-1* non-*unc-4* recombinants
bz200	13/13 (100%)	0/11 (0%)	3/5 (60%)	1/6 (16.7%)
conclusion	*bz200* is to the right of *unc-4*		***bz200* between *unc-4* and *bli-1***	

Deficiency mapping results shown in Table 3 suggested that *bz200* was located in the genetic interval II:+1.86..+2.12 (0.26 m.u.), which is covered by 5 cosmids (Figure 7).

Table 3. Results from deficiency mapping performed on mutant strain carrying allele *bz200*.

SP619 [mnDf57/mnC1 dpy-10(e128) unc-52(e444)II] (II:1.67-2.92) (failed to complement)
SP542 [mnDf29/mnC1 dpy-10(e128) unc-52(e444)II] (II:1.61-2.44) (failed to complement)
SP645 [mnDf63/mnC1 dpy-10(e128) unc-52(e444)II] (II:0.82-**2.12**) (failed to complement)
CB4077 [mnDf21/mnC1 dpy-10(e128) unc-52(e444)II] (II: 1.67-**1.86**) - (complemented)
SP541 [mnDf28/mnC1 dpy-10(e128) unc-52(e444)II] (II: 1.72-1.84) - (complemented)

Highlighted numbers in blue indicates location to the right of the specific position; highlighted numbers in red indicates location to the left of the specific position; underlined and **bold** numbers define the interval where *bz200* appeared to be located

Having narrowed down the location of allele *bz200* to a relatively short interval on chromosome II, covered by a handful of cosmids, transgenic rescue experiments were the next logical step. Initially, a pool containing five cosmids (F52H3, C18D1, ZK945, F27E5, and F33H1) covering the above-described interval and surrounding areas were injected as a means to corroborate previous mapping data and test the feasibility of procedure. After obtaining two transformed lines which demonstrated partial rescue-of-death, one pool of two and single cosmids were injected.

Cosmid F33H1 consistently showed partial rescue-of-death in the majority of several lines obtained, which was very encouraging. Nevertheless, not a single mutation was found after completely sequencing the genomic region from *bz200* covered by the cosmid. One possible explanation could be that the real mutation resides in a nearby regulatory sequence that regulates the expression of a gene contained in cosmid F33H1.

Alternatively, overexpression of a gene contained in that cosmid could induce death on its own, independently of the LGII suppressor locus. Interestingly, RFX-transcription factor *daf-19* is contained in cosmid F33H1, and this gene has been recently reported to induce degeneration when overexpressed (Yu et al., 2003). Discarding then cosmid F33H1, my results suggest that the LGII-linked suppressor locus may be located in one of the four remaining cosmids covering the above mentioned interval and comprised of 26 genes reported by WormBase curators (Figure 8, Table 4).

The fact that no transgenic rescue was achieved with the four remaining cosmids may indicate that a higher number of transgenic lines should be produced in order to find the elusive transformants. Another issue to consider is that cosmids have some tendency to rearrange and lose pieces of DNA, preferentially those with certain levels of homology. In such a case, one could be testing a cosmid thinking that it is complete but in fact, relevant DNA information may be missing. To address this issue, I checked restriction patterns of purified cosmid DNA before injection and compared them to theoretically expected ones, but there is still the possibility that small deletions in the cosmid sequence could have gone undetected, due to a lack of resolution inherent to agarose electrophoresis techniques.

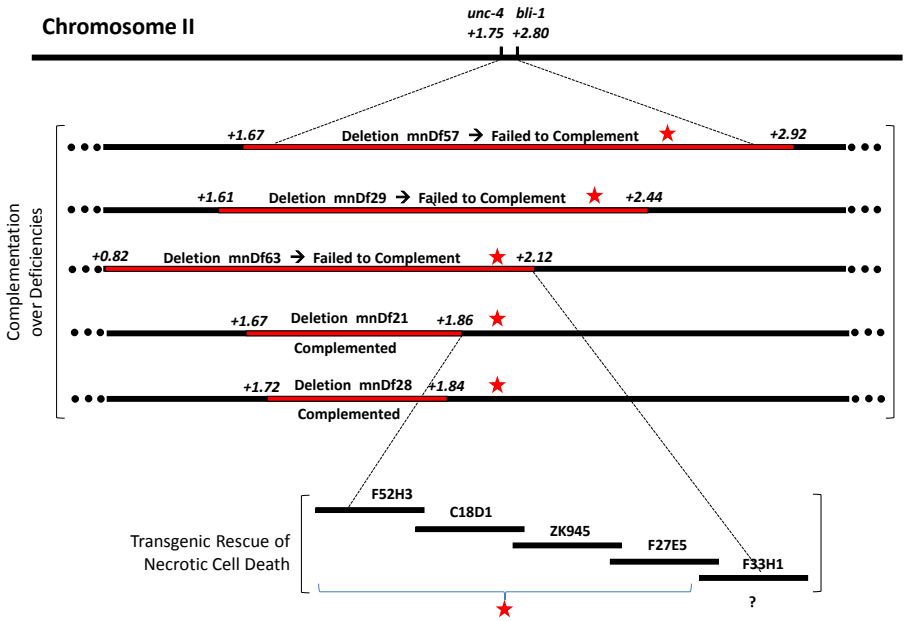

Figure 7. Efforts towards positional cloning of LGII-linked suppressor locus.

Initial SNP mapping strategy located allele bz200 on LGII and between genetic coordinates II:-1.80 and II:+3.34. Three-factor mapping additionally narrowed down the location of the mutant locus to area between genetic markers unc-4 (II:+1.75) and bli-1 (II:+2.80). Deficiency mapping further reduced the area of interested to the interval between II:+1.86 and II:+2.12, which is covered by 5 cosmids (F52H3, C18D1, ZK945, F27E5, and F33H1), one of which harbors no mutation (for cosmid F33H1, I sequenced the entire genomic regions from *bz200* and did not identify any sequence polymorphism).

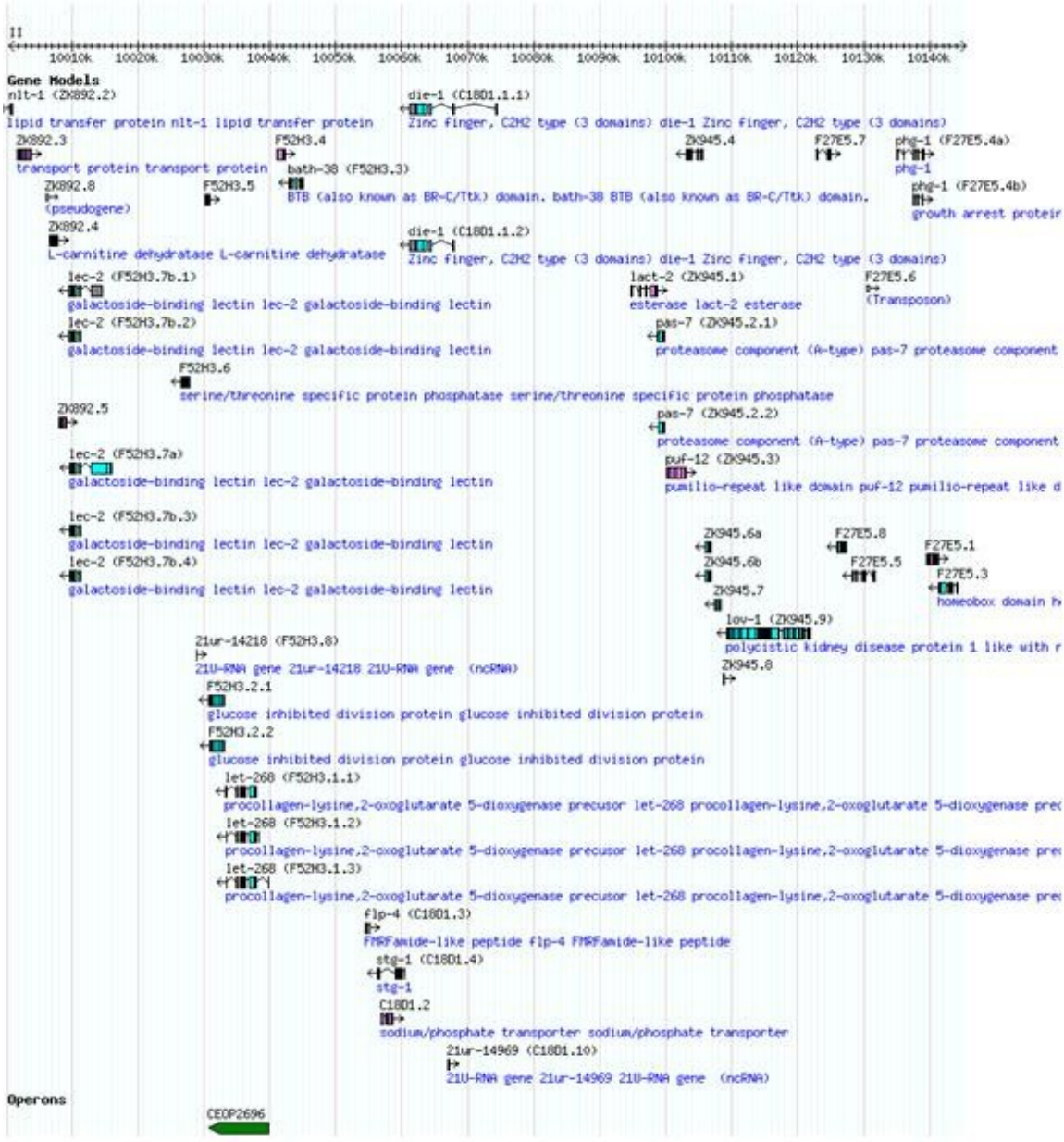

Figure 8. Zooming in the 4-cosmids area (F52H3, C18D1, ZK945, and F27E5). WormBase.org, release WS201. A list of the 26 genes covered in this genomic interval is presented in Table 4.

Table 4. Open reading frames (ORF) contained in genetic interval II:1.86 to II:2.12 (genetic interval as described in WormBase.org release WS201)

Name	Pos	Type	Description
let-242	1.8603	mapped mutant	Molecular identity unknown. Lethal.
21ur-14969	1.8712	mapped mutant	Molecular identity unknown. 21U RNA class.
evl-3	1.8714	mapped mutant	Molecular identity unknown. Abnormal eversion of the vulva.
C18D1.1 / die-1	1.8723	named gene	die-1 encodes a C2H2 zinc finger protein containing four fingers, homologous to CG18265-PA in Drosophila; DIE-1 is autonomously required in the posterior dorsal hypodermis for intercalation, for morphogenesis in other embryonic tissues, and for normal postembryonic growth and vulval development.
ZK945.1 / lact-2	1.8861	named gene	lact-2 encodes a beta-lactamase domain-containing protein that contains a predicted transmembrane domain in its N terminus.
ZK945.2 / pas-7	1.8873	named gene	pas-7 encodes a proteasome alpha-type three subunit of the core 20S proteasome subcomplex; loss of pas-7 activity via RNAi results in several defects including embryonic and larval lethality, sterility, and abnormal meiotic progression.
ZK945.3 / puf-12	1.8885	named gene	Pumilio/FBF domain-containing protein. RNA-binding protein
ZK945.4	1.8898	predicted gene	62% similarity to paralog *C. elegans* ADP-ribosylation factors (Arf family) (contains ATP/GTP binding P-loop), Zinc finger, C3HC4 type (RING finger)
ZK945.6	1.8908	predicted gene	Nematode specific gene. A protein complex that forms part of a proton-transporting two-sector ATPase complex.
ZK945.7	1.8915	predicted gene	No molecular description available. Nematode specific gene. Spermatogenesis enriched expression.
ZK945.8	1.8919	predicted gene	Protein phosphatase inhibitor domain.

			Homolog of human Protein phosphatase 1 regulatory subunit 11
ZK945.9 / lov-1	1.8951	named gene	lov-1 encodes an ortholog of human PKD1 (OMIM:601313; mutated in autosomal dominant polycystic kidney disease) that is expressed in the ciliated sensory endings of three types of male-specific neurons and that is required for two aspects of male mating behavior: response to hermaphrodite contact and vulva location; LOV-1 acts with PKD-2; EGL-44 and EGL-46 regulate cell-specific expression of lov-1 and pkd-2 to specify the behavioral function of the HOB neuron; *in vitro*, LOV-1 interacts, via its conserved PLAT domain, with the N-terminus of ATP-2, the beta subunit of ATP synthase that also localizes to cilia, suggesting that ATP synthase may play a role in C. elegans polycystin signaling.
F27E5.7	1.9185	predicted gene	No molecular description available. Nematode specific gene.
F27E5.8	1.9262	predicted gene	GPCR, chemoreceptor. 88% similarity to F27E5.5
F27E5.5	1.9357	predicted gene	GPCR, chemoreceptor. 82% similarity to F27E5.8
F27E5.4 / phg-1	1.9555	named gene	Pharynx-associated GAS (growth arrest protein) related. 45% similarity to human growth arrest-specific protein 1.
F27E5.1	1.9717	predicted gene	Acid ceramidase. 88% similarity to human N-acylsphingosine amidohydrolase 1 isoform b.
F27E5.3	1.9829	predicted gene	48% similarity to human isoform 1 of cell division cycle 2-related protein kinase 7.
mel-30	1.9891	mapped mutant	Molecular identity unknown. Maternal-effect lethality.
evl-4	2.0000	mapped mutant	Molecular identity unknown. Abnormal eversion of vulva.
mig-19	2.0000	mapped mutant	Molecular identity unknown. Abnormal cell migration.
let-243	2.0086	mapped mutant	Molecular identity unknown. Lethal.

let-244	2.0086	mapped mutant	Molecular identity unknown. Lethal.
F27E5.2 / pax-3	2.0154	named gene	pax-3 encodes a divergent paired-like homeodomain protein that does not belong to the Q50, K50, or S50 classes; PAX-3 is required for locomotion and vulval development; pax-3(RNAi) animals have consistent Pvl and Unc phenotypes (as well as less consistent Bmd, Rup, and Stp phenotypes).
stu-2	2.0394	mapped mutant	Molecular identity unknown. Sterile and uncoordinated.
F33H1.6	2.0682	predicted gene	No molecular description available. Integral to membrane.

2.4. Discussion and Future Prospects

In general terms, this high-throughput mutagenesis screen successfully identified multiple novel loci that are able to suppress necrotic cell death in *C. elegans*. Currently, two of these loci have been cloned and characterized (my work on X-linked locus *uggt-1* discussed in Chapter 3, and work of colleagues Dewey Royal and collaborators on LGIV-linked locus Y57G11C.15, a Sec61-homolog).

Most of the suppressor alleles detected by this particular screening strategy represent intragenic *mec-4(d)* mutations that disrupt the function of the hyperactive channel (85 out of 107, which account for 79% of the total). This result was expected based on previous smaller screen described in epigraph 2.1.1. Dr. Driscoll and collaborators have previously reported that EMS-induced nonsense mutations that disrupt MEC-4 channel function are generally dispersed along the length of the *mec-4* coding sequence, a 2307 nucleotide sequence that codes for a 768 aminoacid protein (Hong et al., 2000). Since EMS preferentially causes C to T and G to A transitions (Coulondre and Miller, 1977), it has the potential to affect 548 of the 768 amino acids in the MEC-4 protein (Hong et al., 2000). This supports the idea that EMS mutagenesis can generate an ample variety of intragenic, second site mutations in the *mec-4(d)* mutant gene that could potentially eliminate its function, hence the toxic insult and consequent activation of necrotic death. This type of suppressor directly and dramatically affects the channel function, so its effect in death suppression is generally strong, making its detection extremely

efficient in our fluorescence-based screening strategies. In addition, since *mec-4* is not an essential gene, all mutations could in principle be detected.

Some expected alleles were not identified in my screen. More precisely, we did not isolate *itr-1* or *unc-68* suppressor alleles, although existing partial loss-of-function alleles *itr-1(sa73)* and *unc-68(e540)* have previously been reported to mildly suppress necrosis (Xu et al., 2001). An explanation for this could be that weak alleles of these genes may not be detected by our screen strategy, while strong loss-of-function alleles could not be detected either, due to their detrimental pleiotropic effects (Kamath et al., 2003; Sonnichsen et al., 2005) that cause either embryonic lethality, or sterility, or slow growth, *etc*.

Further efforts are needed to identify the remaining two novel loci (LGI- and LGII-linked). Royal and collaborators are already working on positionally cloning the LGI-linked suppressor (unique allele *bz199*). I advanced related work on the LGII-linked locus as to mapping the responsible mutation to a 140 kb genomic interval comprised of 26 open reading frames (Figure 8, Table 4). With the advent of next generation sequencing (NGS) technologies, the sequencing of the above mentioned interval is already economically feasible. Identification of the relevant mutation would be straightforward, akin to a candidate gene sequencing approach.

A caveat to consider in my *bz200* mapping strategy is the fact that deficiency mapping may be at times problematic, since it is known that deficiencies may contain non-mapped alterations that might interfere with particular phenotypes. I would still consider that this is not a major problem in the *bz200* mapping case, since I obtained consistent results from the analysis of 5 distinct deficiencies (3 failing to complement and 2 complementing the *bz200* mutant phenotype), which make the possible effect of a specific unsuspected alteration less probable to affect the final conclusion.

In any case, if a strategy using NGS technologies were subsequently employed to identify this locus, it might be advisable to include a longer genomic interval containing the above referenced one, which is not at all a problem since NGS technologies are applicable to massive genomic areas (including full genomes) and we are targeting here just a very small portion of the *C. elegans* genome (e.g. 140 KB of sequence represents only 0.14% of the *C. elegans* genome).

Overall, this particular nearly-saturated screening approach indicates that there are about nine genes that can mutate to induce suppression of *mec-4(d)*-induced necrotic-like cell death in *C. elegans* touch neurons. Two of these genes, *mec-4(d)* and *mec-6*, do not directly affect the death pathway, but the functionality and availability, respectively, of the initiator toxic insult. Two other loci, linked to LGI and LGII remain to be identified and characterized, whereas the remaining five (*crt-1*, *itr-1*, *unc-68*, *uggt-1*, and

Y57G11C.15 –a Sec61 homolog) are all relevant to ER function. The latter observation suggests that the ER plays a crucial role in the activation of necrosis in *C. elegans*, akin to the fundamental role played by the mitochondria in apoptosis. I recommend therefore, that additional efforts be dedicated to better understand the basic roles that ER-to-nucleus signaling and ER-mitochondria crosstalk may be playing during NCD progression. Such studies will likely contribute insights into other degenerative disease models as well, such as those involving toxic protein aggregation.

CHAPTER 3. UDP-GLUCOSE:GLYCOPROTEIN GLUCOSYLTRANSFERASE 1 (UGGT-1): NOVEL *C. ELEGANS* NECROSIS SUPPRESSOR

The endoplasmic reticulum (ER) is a dynamic organelle that controls a wide variety of cellular processes including folding of newly synthesized proteins, sterol biosynthesis, Ca^{2+} storage, and signaling processes such as Ca^{2+} release, arachidonic acid release, and apoptosis regulation, *etc*. The ER structural organization is extremely varied: appearing as flattened sacks mainly when engaged in protein synthesis or existing as an interconnected meshwork of tubules, which are constantly remodeled and may contribute to microlocalized Ca^{2+} signaling inside the cell (Berridge, 2002). Such capacity to divide into autonomous signaling units enables the ER to create modular signaling systems such as those found in neurons and involved in memory, e.g. ER that enters individual spines can release Ca^{2+} independently of neighboring spines (Rose and Konnerth, 2001; Wang et al., 2000).

It is important to point out that ER functioning is tightly coupled to the mitochondria, which assist during Ca^{2+} signaling with the recovery phase by recycling Ca^{2+} back to the ER. In a normal equilibrium, the bulk of intracellular Ca^{2+} resides in the ER (millimolar concentration), where it also contributes to maintaining the activity of chaperones responsible for optimal protein folding.

As mentioned above, the ER is a major compartment where folding and sorting of newly synthesized secretory proteins takes place. This process is subject to a strict quality control surveillance that retains and eventually disposes of misfolded proteins before they can exit the ER. Central to this surveillance mechanism is the calnexin/calreticulin (CNX/CRT) cycle and ER-associated proteasomal degradation (ERAD). The CNX/CRT cycle functions as a kinetic trap that retains intermediates that are not properly folded while allowing native folded proteins to proceed along the secretory pathway (Dejgaard et al., 2004). ERAD on the other hand, plays a central clearance role inside the cell: terminally misfolded proteins are trimmed by ER α1,2-mannosidases and transported to the cytosol, via the Sec61p translocon complex, where they are poly-ubiquitinated and degraded by the proteasome (Fewell et al., 2001; Hampton, 2002).

Perturbations of ER functions can provoke dramatic consequences to the cells and the organism. For example, secretion defects of particular secretory proteins can cause severe diseases in humans, such as hemophilia, diabetes, phenylketonuria, alpha-1-antitrypsin deficiency, short-chain acyl-CoA dehydrogenase deficiency, and neurodegenerative diseases such as Parkinson's, *etc*. (Delepine et al., 2000; Gregersen et al., 2006; Nichols et al., 1998; Teckman and Perlmutter, 2000). Although each of these disorders has its own specific features, the common framework based on the cellular effects of protein misfolding contributes important insights into disease pathogenesis and development of clinical interventions.

3.1.1. Endoplasmic reticulum (ER) quality control and UGGT

When nascent peptide chains emerge in the ER lumen, they are covalently modified by olygosaccharyl transferase, which attaches a preassembled carbohydrate moiety onto specific asparagines in the nascent chains. The original glycan core contains three terminal glucose residues, two of which are quickly removed by the action of ER-resident α-glucosidases I and II. The monoglucosylated glycoprotein generated is then recognized by lectin chaperones calnexin (CNX) and calreticulin (CRT), which assist in creating a proper microenvironment for correct folding. Once the glycoprotein is released from CNX/CRT, the terminal glucose is removed by α-glucosidase II to avoid reassociation of the protein with the lectins and to trigger exportation.

To ensure maximum fidelity of this folding process, cells evolved a folding sensor (UDP-glucose:glycoprotein glucosyltransferase, UGGT) that ignores native proteins but selectively recognizes and reglucosylates nearly native folding intermediates that were prematurely released from CNX/CRT. The monoglucosylated intermediate is then resequestered by CNX/CRT and engaged in additional folding efforts (Caramelo et al., 2004; Solda et al., 2007) This is known as the Calnexin/Calreticulum Cycle, which is depicted in Figure 9. It should be noted here that UGGT also ignores terminally misfolded proteins as they will be recognized and handed off for degradation by BiP chaperone and ERAD systems (Cabral et al., 2002; Molinari et al., 2002; Solda et al., 2007).

UGGT is the only known component of the CNX/CRT cycle that can distinguish between optimally and suboptimally folded glycoproteins, ensuring high-fidelity ER quality control (Dejgaard et al., 2004; Jin et al., 2007; Parodi, 2000). It is also reported that UGGT recognizes folding defects at the level of individual domains and only reglucosylates glycans in the misfolded domains, which would allow CNX/CRT to only interact with such misfolded regions (Dejgaard et al., 2004; Ritter and Helenius, 2000; Ritter et al., 2005). Jin and collaborators recently discovered that mutations in the *Arabidopsis* UGGT homolog gene (*EBS1*) suppressed the growth defects of a brassinosteroid (BR) receptor mutant (bri1-9) in an allele-specific manner by restoring its BR sensitivity (Jin et al., 2007). These authors demonstrated that "*ebs1* mutations significantly reduce the stringency of the retention-based ER quality control, allowing export of the structurally imperfect yet biochemically competent bri1-9 to the cell surface for BR perception". These results strongly support a physiological role for UGGT in high-fidelity ER quality control.

As Jin and coworkers point out, overcoming such an overzealous retention-based ER quality control mechanism could lead, for example, to correct targeting of mutated yet functional ΔF508-CFTR to the apical membrane of epithelial cells, hence providing a promising cure for fatal genetic disease cystic fibrosis (Jin et al., 2007).

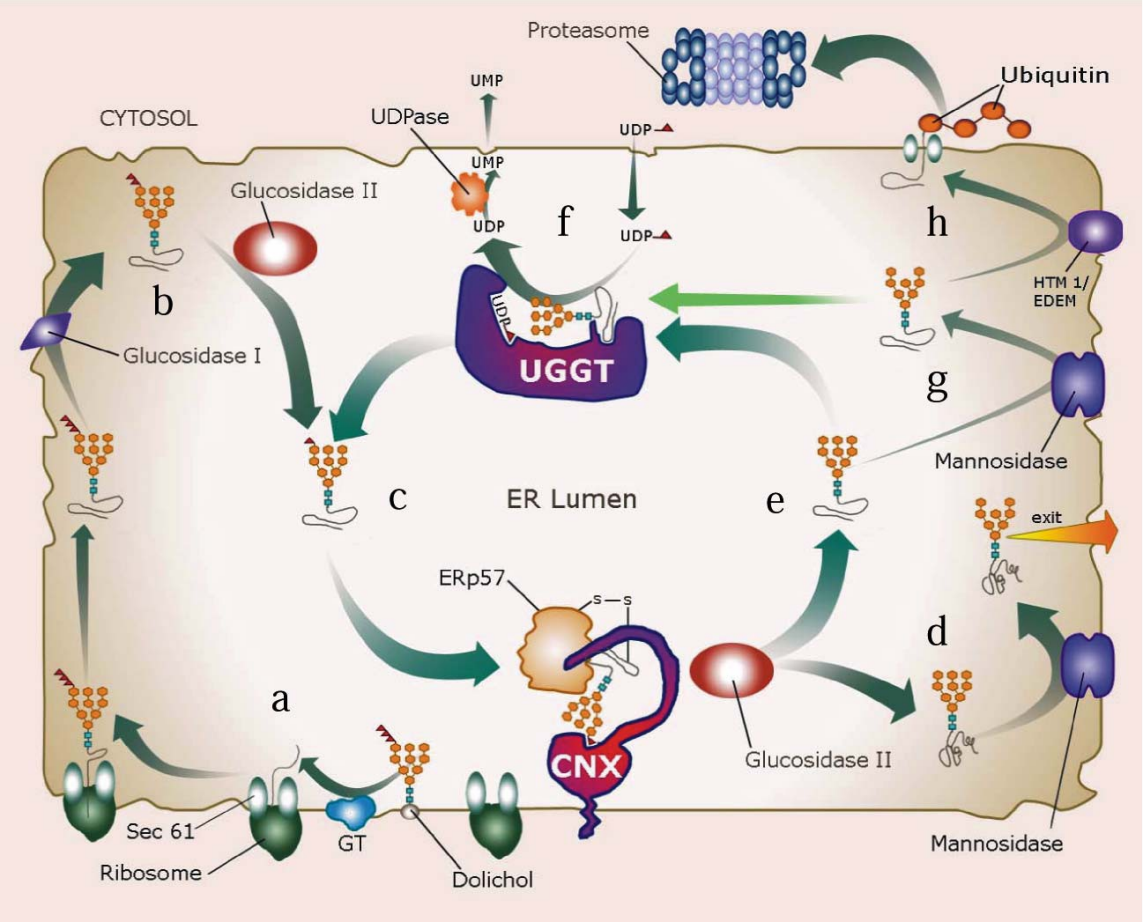

Figure 9. The calnexin/calreticulin (CNX/CRT) cycle.

In the ER, the action of two enzymes, glucosidase II and UGGT, regulate the release and binding of glycoproteins to CNX/CRT providing a unique quality control mechanism known as the CNX/CRT cycle for glycoprotein folding. (a) The precursor glycan (Glc3Man5-9GlcNAc2) linked to the lipid molecule, dolichol, is transferred to the NH2 group on the side chain of asparagine residues positioned in a consensus sequence Asn-X-Ser/Thr (where X is any amino acid except proline) in the growing, nascent polypeptide chain, as soon as it enters the ER lumen via the Sec61p translocon complex. The transfer is catalyzed by membrane-bound glycosyl transferases, which recognizes a specific conformation of Asn-X-Ser/Thr sequences. (b) Glucosidase I and II successively

trim two of the glucose residues leaving the Glc1Man9GlcNAc2 core oligosaccharide. (c) Calnexin and its lumenal paralogue calreticulin are lectins that specifically bind monoglucosylated oligosaccharides, and present them to the glycoprotein-specific thiol oxidoreductase, ERp57, which also bound to CNX/CRT. If the complete deglucosylation of glycoproteins occurs before the CNX-glycoprotein interaction, the monoglucosylated glycoproteins are also generated by reglucosylation through the action of UGGT. Trimming of the last glucose residue by glucosidase II terminates the calnexin-glycoprotein interaction. If the proteins are correctly folded (d) they proceed further into the secretory pathway, whereas incompletely folded proteins (e) are recognized by UGGT. (f) UGGT reglucosylates incompletely folded proteins by readdition of a single glucose residue from UDP-Glc thereby generating a substrate for the calnexin cycle. UDP-Glc is transported into the ER lumen from the cytosol and is exchanged to uridine monophoshate (UMP) by uridine diphosphatase (UDPase), and UMP is transported back to cytosol. (g) The CNX/CRT cycle continues until the proteins are correctly folded or directed to ER-associated degradation (ERAD) after trimming by ER α1,2-mannosidases. (h) An enzymatically inactive member of this protein family, ER Degradation Enhancing α-Mannosidase-like protein (EDEM) and the yeast homologue Mn11p (mannosidase-like protein) or Htm 1p (homologous to mannosidase I, shown as HTM 1) may participate as lectins and promote ERAD of incorrectly folded proteins that are then transported to the cytosol, via the Sec61p translocon complex, where they are proteolytically degraded by the proteasome system, in most cases following polyubiquitination (Dejgaard et al., 2004). Reproduced with permission of Dr. John Bergeron.

3.1.2. The unfolded protein response (UPR) pathway

The unfolded protein response (UPR) is an intracellular signaling cascade that is activated when misfolded proteins accumulate in the ER lumen. In these terms, the UPR is an adaptive, protective response to ER stress, but the UPR can also trigger apoptosis when the stress levels transcend putative unmanageable thresholds that exceed folding capacity of the ER. In a broad sense, activation of apoptosis by the UPR can also be considered a protective response, although at the organismal level. As Rutskowski and collaborators put it, this "ability to sense and respond to the accumulation of misfolded proteins is a central component of the cellular defense against environmental insult" (Rutkowski et al., 2006). Multiple insults such as nutrient deprivation, redox imbalances, changes in Ca^{2+} concentration, impaired post-translational modifications, or just augmented production of secretory protein, can lead to protein misfolding and ER stress (Rutkowski and Kaufman, 2004).

There are three main parallel subpathways involved in this cellular response, which are mediated by inositol-requiring protein-1 (IRE1/*ire-1*), activating transcription factor-6 (ATF6/*atf-6*), or double-stranded RNA-dependent protein kinase (PKR)-like ER kinase (PERK/*pek-1*) respectively. These subpathways/branches regulate the transcription and/or translation of numerous genes that assist not only in protein folding, degradation, and secretion, but also influence broad aspects of metabolism and cell fate (Ron and Walter, 2007).

Central to the activation of the three UPR branches is BiP (*hsp-3*/*hsp-4*), a member of the heat-shock protein (Hsp70) family. BiP binds the luminal portions of each of the transmembrane-located UPR transducers (IRE1, ATF-6, and PERK), inhibiting their respective activities unless unfolded proteins accumulates in the ER. When the latter occurs, BiP engages in its chaperonic functions and dissociates from its interaction with the UPR transducers, which can then dimerize and activate themselves and the respective signaling cascades (Bertolotti et al., 2000; Wu and Kaufman, 2006).

Although the three UPR branches are simultaneously activated upon severe ER stress, the immediate response occurs through the PERK/eIF2α branch (Wu and Kaufman, 2006), which is logical from a cellular viewpoint because activation of chaperone expression and synthesis would require a longer time span (20-30 minutes), so its stress-reducing effect will not be exercisable until later. Conversely, inhibition of translation occurs instantly, as in a just-in-time approach, preventing system overload with additional misfolded protein.

Recently, Trusina and collaborators applied a modeling approach to the study of translation attenuation (TA) in the context of the unfolded protein response and proposed that TA mechanisms allow for tighter adjustment of new peptide translation to chaperone levels in the ER, mainly due to the fact that the TA response is fast compared with chaperone up-regulation (Trusina et al., 2008). They also pointed out the

benefit of minimizing the amount of chaperones needed to deal with transient stress, and predicted that the activation of TA mechanisms will be particularly effective in (i) professional secretory cells where ER load and TA buffering capacity are high, and (ii) during acute stresses, where the fast timescale of the TA response is beneficial.

Upon dissociation from BiP, PERK dimerizes and auto-phosphorylates, activating its kinase activity on target eIF2α and inducing attenuation of general translation initiation (Harding et al., 1999). Interestingly and paradoxically, phosphorylation of eIF2α allows for preferential translation of less abundant mRNAs that contain inhibitory upstream open reading frames (uORF) within their 5' untranslated region. The cell, "intelligently" taking advantage of this finesse, evolved a subset of ER-stress responsive targets, the activating transcription factor 4 (ATF4) mRNA being the best-studied example in mammalian cells (Lu et al., 2004a).

Similarly to PERK, IRE1 also dimerizes and auto-phosphorylates after dissociation from BiP, which activates its site-specific endoribonuclease (RNAse) activity and splices a 26-base intron from XBP1 mRNA. This nonconventional splicing reaction creates a translational frameshift in the XBP1 mRNA that produces a potent transcription factor (Tirasophon et al., 1998). ATF6, on the other hand, is transported (also after BiP release) to the *cis*-Golgi compartment where it is cleaved by site-1 and site-2 proteases (S1P and

S2P respectively), producing a cytosolic N-terminal fragment that also becomes an active transcription factor (Haze et al., 1999; Yoshida et al., 2000).

Even when IRE1, PERK, and ATF6 are independently activated from each other, the three UPR branches communicate extensively with each other, and their transcriptional outputs overlap significantly (partly achieved through mutual positive reinforcement: e.g., XBP1 is transcriptionally activated by ATF6 and PERK signaling (Ron and Walter, 2007)).

The combinatorial transcriptional program activated by XBP1, ATF6, and ATF4 target genes that encode ER chaperones (e.g. BiP, calnexin, and calreticulin), protein-folding catalyzers such as disulfide isomerases (e.g. PDI, ERP57, and ERP72), and other proteins that stimulate ER expansion (e.g. choline phosphotransferase activity (Sriburi et al., 2004)) and ER-associated degradation (e.g. EDEM (Hosokawa et al., 2001) and Derlin (Oda et al., 2006)).

Regarding ER expansion, Ron and Hampton suggest that this phenomenon should be reserved by the cell “for situations in which the burden of client proteins heralds a long-term commitment to increased ER function” (Ron and Hampton, 2004). Sriburi and collaborators reported a key role for XBP1 in promoting the ER biogenesis by increasing the activity of key enzymes involved in phospholipid biosynthesis while maintaining

cholesterols levels unaffected (Sriburi et al., 2004), which is consistent with the cholesterol-deficient nature of ER membranes.

Translocation through the ER translocon is also reprogrammed under ER stress, as to keep proteins with weaker signal peptides preferentially excluded from the ER. This reduces the protein load in the stressed ER and clears the way for translocation of newly synthesized UPR target proteins (Kang et al., 2006; Ron and Walter, 2007).

3.1.3. ER stress: survival vs. death decisions

When the cell is incapable of handling the ER-stress through activation of the UPR, suicidal mechanisms are activated. It has been suggested that both mitochondrial-dependent and mitochondrial-independent apoptotic pathways are involved in response to uncontrolled ER stress. Evidence shows that proapoptotic Bcl2-related proteins Bak and Bax undergo conformational alterations in the ER membrane that induce Ca^{2+} efflux into the cytosol (Scorrano et al., 2003). The increase in cytosolic Ca^{2+} concentration, from micromolar to millimolar levels, leads to depolarization and permeabilization of the mitochondrial inner membrane, cytochrome *c* release, and activation of Apaf-1/procaspase-9-dependent apoptosis (Boya et al., 2002).

Apoptosis could also be triggered through transcriptional activation of CHOP (CEBP homolog protein), which is downstream of both ATF6 and PERK/eIF2α/ATF4 and works

by inhibiting the expression of Bcl-2 (Ma et al., 2002). IRE1 on the other hand, interacts with TRAF2 (TNF receptor-associated factor-2) and ASK1 leading to activation of ASK1 and JNK and subsequent cell death (Nishitoh and Ichijo, 2004; Nishitoh et al., 2002). The fact that the UPR activates effectors of cell death in addition to other factors involved in cell survival, highlights the complexity of these relationships.

A *C. elegans* homolog for CHOP has not been yet reported, neither have I been successful in identifying one while applying a variety of bioinformatic approaches in its quest. This absence may indicate that CHOP is a more recent evolutionary adaptation in metazoans. This reasoning is supported by observations of Zinszner and collaborators, recently reviewed by Ron and Walter (Ron and Walter, 2007; Zinszner et al., 1998). Based on the observation that activation of a CHOP-dependent process of programmed cell death appears to promote tissue regeneration in mice, these authors suggest that fitness of complex metazoans (where CHOP appears to have first evolved) is improved by the death of ER stress-damaged cells because the cleared cells are replaced through novel regenerative programs developed in long-lived higher eukaryotes.

3.2. Materials and Methods

3.2.1. *C. elegans* strains

I followed standard procedures for *C. elegans* strain maintenance, crosses, and other genetic manipulations (Brenner, 1974). Nematodes were grown on standard nematode growth medium (NGM) plates seeded with *Escherichia coli* strain OP-50 as food source and incubated at 20°C, unless otherwise specified (e.g. 25°C was required for specific experimental procedures).

Wild type worms were N2 strain Bristol isolate and CB4856 Hawaiian. Other strains used were: SK4005 *zdIs5[pmec-4::GFP] I*, ZB1259: *zdIs5 I; mec-4(u231) X*, *uIs22(pmec-3::GFP]; eri-1(mg366) IV; lin-15B(n744) mec-4(d) X,* SP66: *dpy-8(e130) unc-6(e78) X*, DR1290: *dpy-6(e14) unc-3(e151)* X, BC13719: *dpy-5(e907) I; sIs13291 [rCes F48E3.3::GFP + pCeh361] (McKay et al., 2003),* SP64: *unc-6(e78) dpy-6(e14) X, SJ4005 zcIs4[hsp-4::GFP] V,* TU1747: *deg-3(u662)V*, SJ30: *ire-1(zc14); zcIs4[hsp-4::GFP]*, RB772: *atf-6(ok551)*, RB545: *pek-1(ok275)*, MT1672: *unc-8(n491) dpy-4(e1166)IV*, PS1631: *itr-1(sy290) dpy-20(e1282)*, UA4: *baIn4[punc-54::Q82::GFP]* (Caldwell et al., 2003), CL4176: *smg-1(cc546ts) I; dvIs27 [pAF29(myo-3/AB1-42-long3'UTR)+pRF4] X*. Following standard genetic approaches, I constructed compound mutant strains: ZB1388: *zdIs5; unc-6(e78) dpy-6(e14) mec-4(d)*, ZB2922: *zdIs5; unc-6(e78) uggt-1(bz130) dpy-6(e14) mec-4(d)*, ZB1392: *zdIs5; unc-6(e78) uggt-1(bz130) mec-4(d)*, ZB2968: *pmec-4MEC-4::GFP; In30[rol-6(su1006)];* ZB3028: *zdIs5; deg-3(u662); uggt-1(bz146),* ZB2938: *zdIs5;*

ire-1(zc14); uggt-1(bz130) mec-4(d), ZB2933: *zdIs5; unc-6(e78) uggt-1(bz130) pek-1(ok275) mec-4(d)*, ZB2988: *zdIs5; unc-6(e78) uggt-1(bz130) atf-6(ok551) mec-4(d)*, ZB3004: *zdIs5; atf-6(ok551) mec-4(d)*, ZB2996: *zdIs5; atf-6(ok551)*, ZB3012: *zdIs5; pek-1(ok255) mec-4(d)*, ZB3014: *zdIs5; pek-1(ok255)*, ZB2992: *zcIs4; uggt-1(bz130)*, ZB3022: *zcIs4; uggt-1(bz146)*, ZB3020: *zdIs5; unc-8(n491) dpy-4(e1166); uggt-1(bz146)*, ZB3025: *zdIs5; itr-1(sy290) dpy-20(e1282); uggt-1(bz146) mec-4(d)*, ZB3024: *zdIs5; itr-1(sy290) dpy-20(e1282); mec-4(d)*, ZB3018: *zdIs5; itr-1(sy290) dpy-20(e1282)*.

3.2.2. General microscopy

I scored for touch receptor neuronal survival by observing GFP signals driven by *mec-4* promoter in L4 stage larvae, using epifluorescence capability installed on a Zeiss Stemi V6 stereomicroscope. I scored for degenerating (swollen, vacuole-like) PLM touch neurons by examining tails of L1 stage larvae with DIC optics installed on a Zeiss Axiovert 2, as previously described (Driscoll, 1995). Staged animals were immobilized using 10mM sodium azide.

3.2.3. Touch test assay

I performed touch test by gently stroking individual animals at anterior and posterior positions with an eyelash as previously described (Chalfie and Sulston 1981). Mean values were determined by averaging response ratios from all worms tested.

3.2.4. MEC-4::GFP punctae and protein level quantifications

For these experiments I constructed strain ZB2968: *pmec-4MEC-4::GFP; In30[rol-6(su1006)]; uggt-1(bz146)* and compared it to control strain *pmec-4MEC-4::GFP; In30[rol-6(su1006)]*. Pictures were taken using epifluorescence capabilities installed on a Zeiss Axiovert 2 microscope, using a 63x objective. I quantified the number of fluorescent punctae using the Particle Analysis capability (a multi-region detection and analysis routine) of NIH ImageJ software (Collins, 2007; Papadopulos et al., 2007). Previous to particle analysis, all pictures were subjected to automatic background subtraction and threshold adjustment to transform raw pictures into required binary format.

I estimated the relative protein levels using ImageJ's Integrated Density measurement capability (Multiple Measurements) after manually selecting the region of interest (ROI), in this case the cell bodies of fluorescent neurons, on background-subtracted images. I assumed protein levels were proportional to fluorescence intensity as measured in the cell bodies.

3.2.5. MEC-2 immunostaining

Goodman and collaborators showed, via GST (glutathione S-transferase) pulldown experiments, that the MEC-2 stomatin-like domain (AA141-361) interacts *in vitro* with

the N-terminus of MEC-4 (Goodman et al., 2002) and the Chalfie group later reported that the stomatin-like domain of MEC-2 is responsible for recruiting MEC-2 to MEC-4 (Zhang et al., 2004). I used MEC-2 immunostaining to reveal MEC-2 punctae in touch neuron processes, hence indirectly revealing the localization of MEC-4(+) and MEC-4(d) proteins. Pictures were taken by epifluorescent microscopy using a Zeiss Axiovert 2 and 63x objective. Punctae distribution patterns were visually analyzed.

3.2.6. Expression profiling by quantitative PCR

For this experiment I grew animals to the L4 stage as a synchronized population after bleaching gravid adults, then purified total RNA using MasterPure™ Complete RNA Purification Kit and synthesized cDNA using MonsterScript™ 1st strand cDNA Synthesis kit (Epicentre Technologies, Madison, WI). I accounted for growth developmental differences between wild type N2 and mutant *uggt-1(bz146)* strain by allowing *uggt-1(bz146)* animals to grow for eight additional hours before animals were processed for RNA extraction. Appropriate population stage was confirmed by microscopic evaluation. Transcript levels were quantified by RT-PCR using QuantiTect SYBR Green PCR Kits (Qiagen, Valencia, CA) and ABI PRISM 7900 cycler. Two independent samples per strain and four replicates per RT-PCR reaction were used. Data was analyzed using SDS2.2 software (Applied Biosystems, Foster City, CA). Primers used for RT-PCR are described in Table 5 and were designed using PrimerSelect software from the DNASTAR package (DNASTAR, Inc., Madison, WI).

Table 5. Primers used for RT-PCR

uggt-1.qPCRf	ACTTCACCCAGATTCCGTAGATGC	uggt-1.qPCRr	CTGCGCTGCTTGGTAACTGAGAT
pek-1.qPCRf	AATTGGCGAGCGGTCTTGA	pek-1.qPCRr	TGGGAGCTCCATCAGTTTTAGTTG
atf-6.qPCRf	TGTTCGCCAAAAGGGAGATACACT	atf-6.qPCRr	GAACACTAGGCAGGAGCAACGATA
ire-1.qPCRf	AGGGTTGGATGGCAGTTGGTAG	ire-1.qPCRr	TCGTAATAAATCCGCTTCTCTGTGA
xbp-1.qPCRf	GGATCGCCGTGCCTTTGAAT	xbp-1.qPCRr	ATACGACGGAGTTGGTTGCTGATG
crt-1.qPCRf	AGCGACGAACTCACTCATCTCTACAC	crt-1.qPCRr	AGTTTGGGCGCTTTCTCCGT
cnx-1.qPCRf	TATCGACGCAACAAATGAAAAACCA	cnx-1.qPCRr	TCCGAAGCAAAATACTCCGATAGCA
hsp-4.qPCRf	GTCGAAAATACCGGAGATGTTGTC	hsp-4.qPCRr	TATCGGCAGCGGTAGAGAAAA
dnj-7.qPCRf	ACATTGCGGCCGCTAAAG	dnj-7.qPCRr	ACCGCCGCCAAAATGAT
ero-1.qPCRf	AATCGCCGCAAAGAGTGTGG	ero-1.qPCRr	GCCGAGTGAAGTCCCGAAATC
pdi-1.qPCRf	GTTGCCGGTTCTGCTGAGGTTG	pdi-1.qPCRr	CTTAAGAGCGATGGTGTTGGTGATTTC
itr-1.qPCRf	TCGAGGGCATTGTGGGAAGTA	itr-1.qPCRr	TGTGATGGCTCTGCGGAAAGGTA
unc-68.qPCRf	GCGTGGCAACTTTCCCTCTACC	unc-68.qPCRr	TTTTTCCATGCTTGCGACAGTTG
sca-1.qPCRf	CCGCCGAAGAGGGAAAATC	sca-1.qPCRr	AACGCCGTCACTGCTTCTGTC
ckb-2.qPCRf	ATCGGTGCAATCTTCCCACTCTATC	ckb-2.qPCRr	CACCACCTCCAAGACTTTCGTATCC
ckb-4.qPCRf	ACTCCGCCAGGTCTCGTCATT	ckb-4.qPCRr	CTTCGGGTTAGCGGTTTTCATC
ubc-13.qPCRf	TGGTCGCCGGCTCTTCAAAT	ubc-13.qPCRr	TGCTCGGCGACATCAGTTGC
sel-1.qPCRf	CTGGAGGCACCGACAAAATGATA	sel-1.qPCRr	TAGACCCGAGTAGGCTGATGTGAATA
C47E12.3.f	CCTCCTACTCCGCCATCTCAATA	C47E12.3.r	TGAAGAACCGAATCAACTCCAATAACT
erd-2.qPCRf	CGCCATCGCCATCGTTGTT	erd-2.qPCRr	GGTAGAAGATCTTCATCGCAGTGTTGTA
unc-51.qPCRf	TCGTCGCCGGTGGTTCAG	unc-51.qPCRr	GTTGTTCGGCGATGGTTTTGT
bec-1.qPCRf	TTGGGTTGATGGAATTGTTGGTG	bec-1.qPCRr	TGGCGACGGGCATCAGTT
lgg-1.qPCRf	GACCGTATTCCAGTGATTGTTGAG	lgg-1.qPCRr	GGATGCGTTTTCTGATGAGGA
lgg-2.qPCRf	GAAATCCGCAGCCAACAACC	lgg-2.qPCRr	TGGAGGCGTCGTCTAACAAT
nsf-1.qPCRf	TCCGCTTACCGCTCAATCATCAAC	nsf-1.qPCRr	CGAAGGCACGGCGGAAAATA
C33D9.8.f	CGAGAAATCAACAAATCTGCAACTAATG	C33D9.8. r	TGATAACGCGCTTCCAATCCAT
rab-11.2.f	GAGGCCAAAATCTACGCTGAAAG	rab-11.2.r	TGGACGCTGTCGAAGGAATGAT
T28H10.3.f	GATCGCGTTTTTGTTTACTTCACTG	T28H10.3.r	GCTTCCAGATTCACAGGCTTCA
nas-38.qPCRf	GCGCCAATCGAAGGAAGAGTG	nas-38.qPCRr	TGGAAGCAGCGAGCAACAGTATC
cht-1.qPCRf	CTTCTTGTAACCGCCGCTGTC	cht-1.qPCRr	GCCCATGCTCCGAAGAAATC
F55C5.2.f	CATACAGCGATGATCACAGAAAAAGTC	F55C5.2.r	CACATCAACTCCTAGAAATCTGGGTAAA
lips-11.qPCRf	GGAGGAAACTGCGTGGATACTAATGA	lips-1.qPCRr	GTCGCACAGAATACCTCCGTTTTG
gst-1.qPCRf	ATCCGTCATCTCGCTCGTCTT	gst-1.qPCRr	TTGCCGTCTTCGTAGTTTCTGTAG

T20D4.7.f	TGGCTGGAATGAAACTTGAAAAACT	T20D4.7.r	CCGCGGCATGGTGGACA
nlp-28.qPCRf	GTCTTCCTTCTCGCTTGCTTCAT	nlp-28.qPCRr	CTATGGACGCGGAATGTATGGT
srp-7.qPCRf	CTATTGGCGGCTGAAAGAGGA	srp-7.qPCRr	TTGCGCCAGCGTTGTAAAGT
F40F12.7.f	TTTATGTCATTTCGCTCATTGTGC	F40F12.7.r	TCCGTTGGCGCCTATCAGAC
Y113G7B.14.f	GATGAAACCGGTGAAAAAGTGAGC	Y113G7B.14.r	GGAATGGTGCGGCGGTAAC
R02D3.8.f	TCGACGGCTGATTGGAGTGA	R02D3.8.r	TTGTGGAAGCGTCGGTTTTT
let-607.f	TTTGCAGTAGCGGACCTCTTCTTG	let-607.r	AGGACTCTCGGTTGGCTGGATTTA
rrf-2.qPCRf	GTCGCCGGTGCTGGTTG	rrf-2.qPCRr	TGCCTCATCCGTCATCTGCT
clec-67.f	GGATGCCACTACGCGAAAGATA	clec-67.r	GTGGCCGATTGAACATTGCTAA
tbb-6.qPCRf	CAAACTGACGGGACATACAAAGGAG	TBB-6.qPCRr	TACCAAAATCGCACGAGGAACATA
fipr-24.qPCRf	GTCACCACCACCAAAATGAAGATG	fipr-24.qPCRr	ACCGTATCCACCGTATCCTCCAT
col-89.qPCRf	CACCGGGACCACCAGGAGAG	col-89.qPCRr	GGGCACGTGATAGGAGCAAATGTA
act-1.qPCRf	GCCCCAGAAGAGCACCCAGT	act-1.qPCRr	CCGGAAGCGTAGAGGGAGAGG
act-3.qPCRf	CGCCGGAATCCACGAGACTT	act-3.qPCRr	ATGGGGCAAGAGCGGTGATT
ama-1.qPCRf	GCCGACGATGAAGCCCAATAAT	ama-1.qPCRr	GCGCACAACGTCTTCCGAGTAG
rrn-1.1.qPCRf	ACCGGGGGCATTCGTATCAT	rrn-1.1.qPCRr	ACGGTCAGAACTAGGGCGGTATC
Y105E8B.5.f	CAAGGGGAAAAGTGTGCTCGTT	Y105E8B.5.r	AGGGCGGTCCAGGTCTTCTC
gpd-2.qPCRf	TTCCGTGTCCCAACCCCAGAT	gpd-2.qPCRr	CAGCGGCAGCCTTGATAACTTTCT
ctl-1.qPCRf	AATGCGCTCTTCGATTTCTGGA	ctl-1.qPCRr	TTTCCCTCCTTGTTGACCATCTTG
ctl-2.qPCRf	GTCCGGATGTCAAGGATACCAC	ctl-2.qPCRr	CGGCCCTGCAAAGTTCTG
ctl-3.qPCRf	AACGCGATGGTGCAATGGCTTAT	ctl-3.qPCRr	CGTGGCTGCTCGTAGTTGTGAT

3.2.7. Quantification of Q82::GFP polyglutamine aggregates in strain UA4

For reverse genetics experiments I used feeding RNAi following standard protocols (Kamath et al., 2001), on strain UA4: *baIn4[punc-54::Q82::GFP]* (Caldwell et al., 2003). This transgenic strain (better known as Q82::GFP) expresses a track of 82 glutamine residues fused to GFP and driven by the *unc-54* promoter. Fluorescent aggregates are readily detectable in body wall muscles of this animals. I took pictures using epifluorescence capabilities installed on Zeiss Axiovert 2 microscope and quantified the

number and size of aggregates using the Particle Analysis capability (a multi-region detection and analysis routine) of NIH ImageJ software (Collins, 2007; Papadopulos et al., 2007). Previous to particle analysis, all pictures were subjected to automatic background subtraction and threshold adjustment to transform raw pictures into required binary format.

3.2.8. Brood size quantification

Synchronized L4-stage animals were transferred to individual plates and the number of progeny produced by each scored over a period of 6 days with daily transfer of the parent. The total number of progeny was calculated for each individual and averaged over the total number of animals tested. This average measurement was considered the brood size for the strain.

3.2.9. Life span determination

Young adult animals used for life span experiments were picked from well-fed synchronized populations. About 20-25 young adults were distributed per plate, for a total of 75-100 per experiment. Although *uggt-1* mutants have a slight developmental delay, about 8 additional hours to reach young adulthood, animals have reached this stage by day 3 after egg deposition. Since the young adult stage is a short one (lasting only a few hours), selections of this stage for life span experiments ensures well-synchronized and comparable populations. Plates were maintained at 20°C and the

percentage of surviving animals was calculated every 1-2 days until all the test animals died. Bagged worms were eliminated from the data statistics. The experiment was repeated twice and an average percentage of surviving animals per day calculated.

3.3. Results

3.3.1. Positional cloning of X-linked necrosis suppressor locus (alleles *bz91, bz121, bz125, bz130, bz146,* and *bz156*)

Mutant alleles of the LGX-linked locus behave as moderate suppressors of necrotic cell death. Strain *zdIs5; des(bz130) mec-4(d)*, which represent the series' mildest allele, has an average of 3.86 surviving neurons by the L4 stage, while *zdIs5; des(bz146) mec-4(d)*, the strongest allele, has an average of 4.61 fluorescent neurons of a maximum of six. I observed that, although not always, the AVM and PVM neurons survive most of the time. ALMR/L and PLMR/L neurons die randomly and preferentially (as compared to AVM and PVM).

Three-factor cross between *zdIs5; des(bz130) mec-4(d)* and strain SP66: *dpy-8(e130) unc-6(e78)* produced 16/16 *Is5/?; dpy-8/dpy-8 mec-4(d)/mec-4(d)* (Dpy non-Unc) recombinants carrying allele *bz130*, which suggested that *bz130* is to the right of *unc-6*. A three-factor cross between *zdIs5; des(bz130) mec-4(d)* and strain DR1290: *dpy-6(e14) unc-3(e151)* produced 20/20 *Is5/?; dpy-6/dpy-6 mec-4(d)/mec-4(d)* (Dpy non-Unc) recombinants that did not carry allele *bz130*, which suggested that *bz130* is to the left of *dpy-6*. These results (see Table 6) indicated that the suppressor locus on LGX maps between *unc-6* and *dpy-6.*

To confirm the mapping results, gather additional data, and produce necessary reagents for the construction of a triple mutant for fine SNP mapping, I performed an additional 3-factor cross between *Is5; des(bz130); mec-4(d)* and *Is5; unc-6(e78) dpy-6(e14) mec-4(d)*. Note that this time the Unc Dpy double mutant was transferred into the *Is5; mec-4(d)* background to be able to extract information from both kind of recombinants. 6/18 (33%) *unc-6 non-dpy-6* recombinants and 14/24 (58%) *dpy-6 non-unc-6* recombinants carried allele *bz130*, indicating that the novel suppressor on LGX was indeed located between *unc-6* and *dpy-6*, approximately in between -1.13 and -1.35 m.u. (Table 6).

Table 6. Results from three-factor crosses while mapping allele *bz130*.

	X:-6.19 *(dpy-8)*	X:-2.00 *(unc-6)*
	dpy-8 non-*unc-6* recombinants	*unc-6* non-*dpy-8* recombinants
bz130	16/16 (100%)	Not scored because they did not carry *mec-4(d)*
conclusion	*bz130* to the right of *unc-6(X:-2.00)*	

	X:0.00 *(dpy-6)*	X:+21.34 *(unc-3)*
	dpy-6 non-*unc-3* recombinants	*unc-3* non-*dpy-6* recombinants
bz130	0/20 (0%)	Not scored because they did not carry *mec-4(d)*
conclusion	*bz130* to the left of *dpy-6(X:0.00)*	

	X:-2.00 *(unc-6)*	X:0.00 *(dpy-6)*
	unc-6 non-*dpy-6* recombinants	*dpy-6* non-*unc-6* recombinants
bz130	6/18 (33%)	14/24 (58%)
conclusion	*bz130* is to the between *unc-6* & *dpy-6* (on interval X:-1.13 & -1.35 m.u.)	

In order to precisely map the position of the mutant gene, I performed fine SNP mapping. For this purpose, I constructed compound mutant strain *Is5; unc-6(e78) des(bz130) dpy-6(e14) mec-4(d)* and used it against a derivative *zdIs5; mec-4(d)* which

had been backcrossed 10 times into the Hawaiian background. After two rounds of fine SNP mapping (comprised of 90 recombinants analyzed for 10 SNPs covering the *unc-6*--*dpy-6* interval), the map location of allele *bz130* was narrowed down to 0.05 m.u., a small genomic region covering about 72 kb of sequence between SNPs pkP6129 and pkP6134. Only 10 ORFs were annotated in the interest area in WormBase.

Next, I amplified long PCR products from candidate ORFs (the products from 3 independent amplification replicas were pooled to reduce the effect of polymerase-induced errors, which could be confused with original mutations otherwise) and used them for DNA sequencing. ORF F48E3.3 was found to carry mutations in all alleles (see Table 7 and Figure 10). The F48E3.3 ORF from each allele was sequenced in its entirety.

Table 7. Specific nucleotide sequence changes in F48E3.3 mutants

Allele designation	**Nucleotide change**	**Amino acid change**
bz91	C4024T	R1342OPA
bz121	G206A	W69AMB
bz130	81 nt [3319..3400] deletion	27 AA [1107..1137] in-frame-deletion
bz125	G3111A	W1037OPA
bz146	G848A	W283OPA
bz156	C2875T	Q959AMB
Stop codons are referred to by their respective names: UAG is amber (AMB), UGA is opal (OPA), and UAA is ochre (OCH).		

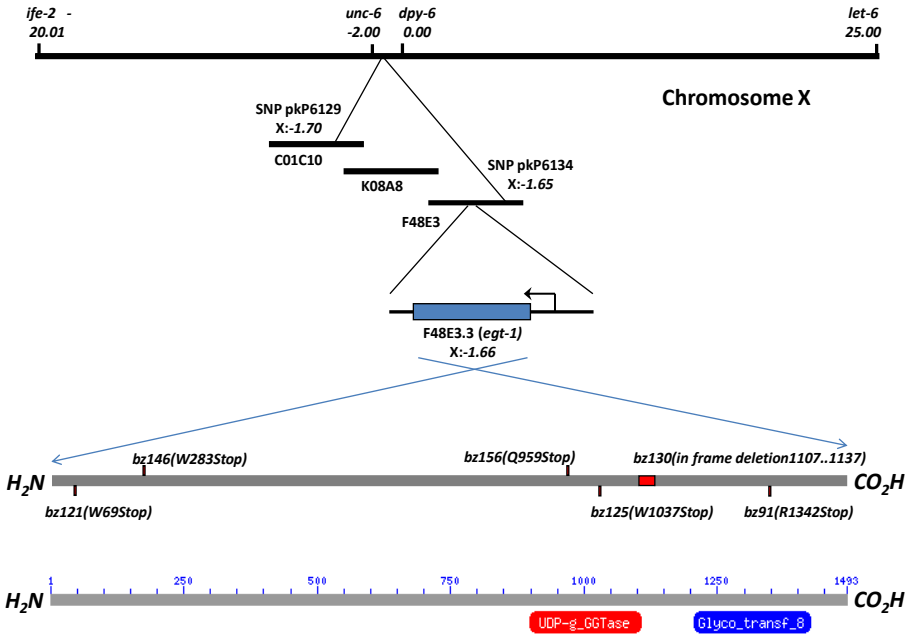

Figure 10. F48E3.3 (assigned name: *uggt-1*) is the death suppressor locus on LGX.

(A) Genetic and physical map of *uggt-1*. (B) Amino acid changes in six isolated alleles and gene domain architecture as represented by NCBI Conserved Domain Database (CDD). UDP-g_GGTase: UDP-glucose:Glycoprotein Glucosyltransferase domain (pfam06427); Glyco_transf_8: Glycosyl transferase family 8 domain (pfam01501).

Necrosis-suppressing effects were phenocopied by F48E3.3 RNAi on RNAi hypersensitive strain *uIs22[pmec-3::gfp]*; *eri-1(mg366); lin-15B(n744) mec-4(d)*, which corroborated the identity of the F48E3.3 as the gene responsible for the death-suppressing phenotype (Figure 11) and suggested reduction-of-function as responsible for the phenotype. Since death suppression was not observable when RNAi was performed on strain *zdIs5; mec-4(d)*, which neurons have little sensitivity to RNA interference, we can infer that the

necrosis-suppressing effect of F48E3.3 downregulation is most likely due to a neuron-dependent process, most likely acting cell autonomously in the touch receptor neurons.

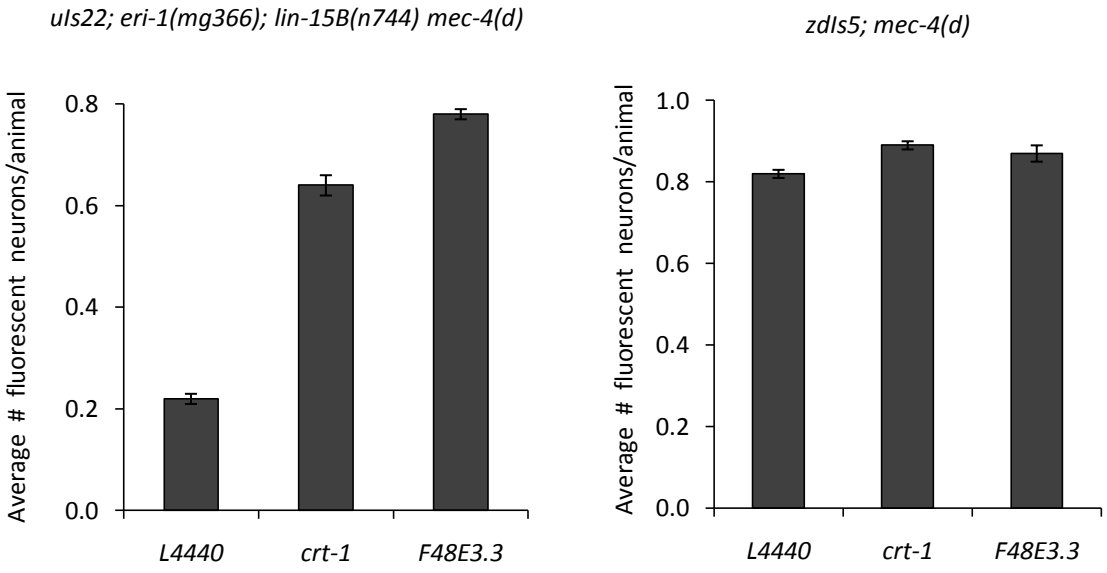

Figure 11. F48E3.3 knockdown by RNA interference phenocopies necrosis suppression. F48E3.3 knockdown phenocopies necrosis suppression observed in mutant F48E3.3 when RNAi is performed on hypersensitive strain *uIs22; eri-1(mg366); lin-15B(n744) mec-4(d)* (A) but not when RNAi is performed in *zdIs5; mec-4(d)*. Animals scored are: for RNAi on hypersensitive *uIs22; eri-1(mg366); lin-15B(n744) mec-4(d)*: 99 L4440, 95 *crt-1*, 111 *F48E3.3* and for RNAi on regular *zdIs5; mec-4(d)*: 98 L4440, 92 *crt-1*, and 103 *F48E3.3*. Error bars represent the standard error. Student's t-Test used to evaluate statistical significance: P(*eri-1; lin-15B mec-4(d)_L4440vs.F48E3.3*)= 7.93×10^{-05}, P(*zdIs5; mec-4(d)_L4440vs.F48E3.3*)= 0.5679.

3.3.2. Gene F48E3.3 is homologous to UDP-glucose:glycoprotein glucosyltransferases

F48E3.3 codes for a 1493 aminoacid protein that has high homology to UDP-glucose:glycoprotein glucosyltransferases (UGGTs). The alignment of the complete protein sequence using Vector NTI AlignX capability showed a 63.6% sequence similarity among the group, which is impressive considering that it covers organisms from protozoa to humans (see Appendix 3.A for sequence alignment and phylogenetic tree). Furthermore, there is 90% similarity between the *C. elegans* and the human homologs. There is a closely related paralog in *C. elegans*, gene F26H9.8 (with 90% homology to F48E3.3), which appears to be only expressed in a tissue-specific manner and at low levels, as reported in AceView (Thierry-Mieg and Thierry-Mieg, 2006), a comprehensive cDNA-supported gene and transcript annotation database. It has been suggested that higher eukaryotes such as worms, rodents, and humans, have evolved two UGGT genes with only one predicted to be catalytically active (Dejgaard et al., 2004). Interestingly, colleagues in the Driscoll Lab have recently identified a candidate missense mutation in ORF F26H9.8 in our parental strain *zdIs5; mec-4(d)* used for the mutagenesis (personal communication). Such secondary mutation appears closely linked to the transgene *zdIs5* on LGI and most likely for that reason, it was not removed by outcrossing. Dr. Royal and coworkers showed this mutation does not modify necrosis on its own and I observed that removal from the *zdIs5*; *bz146 mec-4(d)* background does not affect F48E3.3 death suppression either.

Sequence analysis of F48E3.3 reveals a signal peptide sequence but no transmembrane domain and thus the protein would be predicted to localize to the secretory pathway as indicated by CBS Prediction Server bioinformatic softwares: SignalP v3.0, TMHMM v2.0, and TargetP v1.1. In addition, F48E3.3 contains an HTEL C-terminal sequence closely related to the characteristic H/KDEL endoplasmic reticulum retrieval sequence. The fact that the putative ER retrieval sequence does not perfectly match the consensus sequence might indicate that the protein might also localize to other cellular compartments of the secretory system. Since the primary sequence information suggests that F48E3.3 may indeed function as an ER-resident UDP-glucose:glycoprotein glucosyltransferase we assign the new name *uggt-1* to this *C. elegans* gene (hence UGGT-1 the respective protein). By the same token, paralog F26H9.8 will be designated as *uggt-2*.

3.3.3. *uggt-1* is upregulated when temperature increases

The role that the UGGT enzyme could exert on ER protein-folding quality control prompted us to address its expression pattern under different folding stress levels, as induced by a temperature increase. As shown in Figure 12, *uggt-1* fluorescent reporter (strain BC13719: *dpy-5(e907)I; sIs13291 [rCes F48E3.3::GFP + pCeh361] (McKay et al., 2003)*) expression appears to be ubiquitous at all larval and adult stages, although present at very low or undetectable (by epifluorescent microscopy) levels in early stage embryos. This is consistent with *in-situ* hybridization data reported online by the Kohara Laboratory in the Nematode Expression Pattern Database (NEXTDB 4.0, see Appendix

3.B). Activity of the *uggt-1* reporter is upregulated when temperature is increased (Figure 13), which is expected for a protein with a role as a folding sensor.

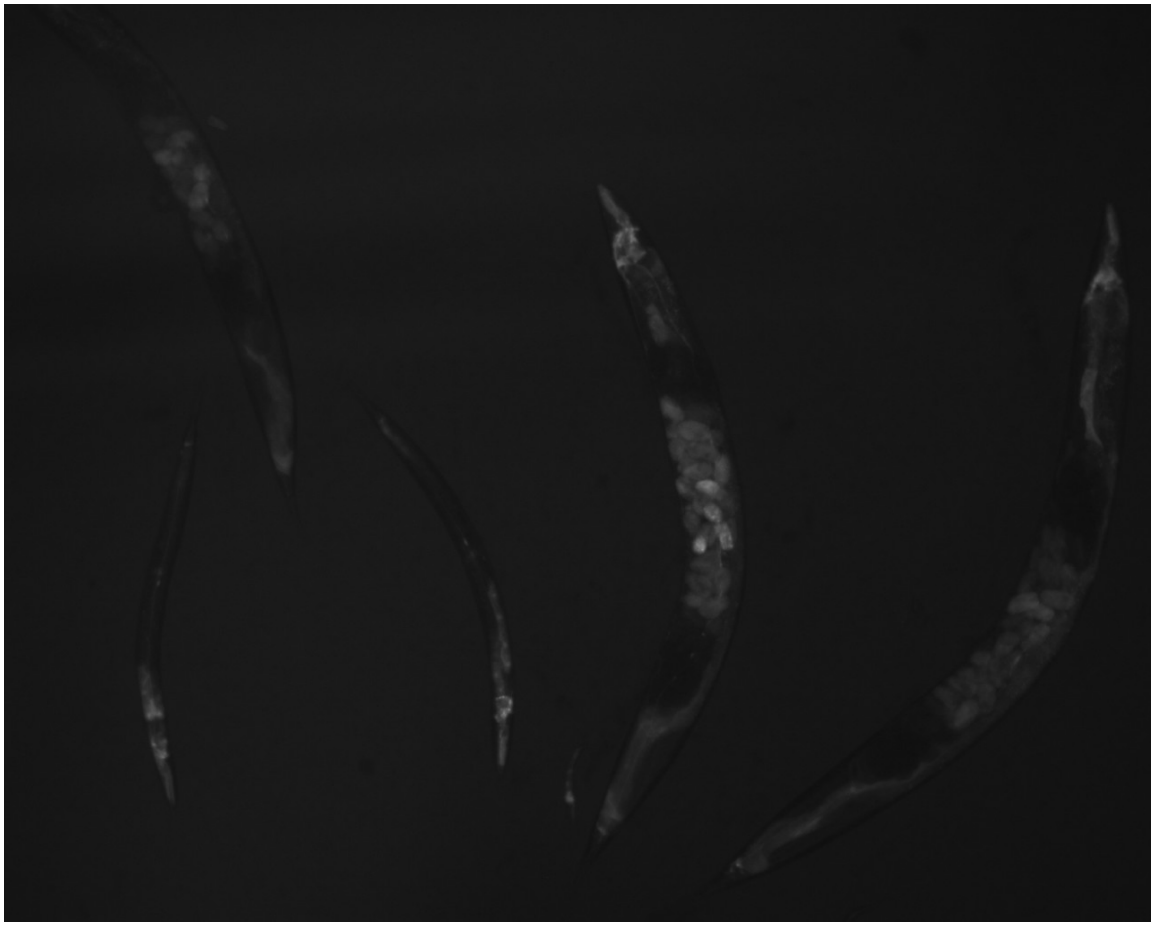

Figure 12. A *uggt-1* GFP reporter expression pattern at 20 °C.

Strain BC13719: *dpy-5(e907)I; sIs13291 [rCesF48E3.3::GFP + pCeh361]* carries an F48E3.3::GFP transcriptional fusion reporter, which had been stably integrated by X-ray irradiation *(McKay et al., 2003)*.

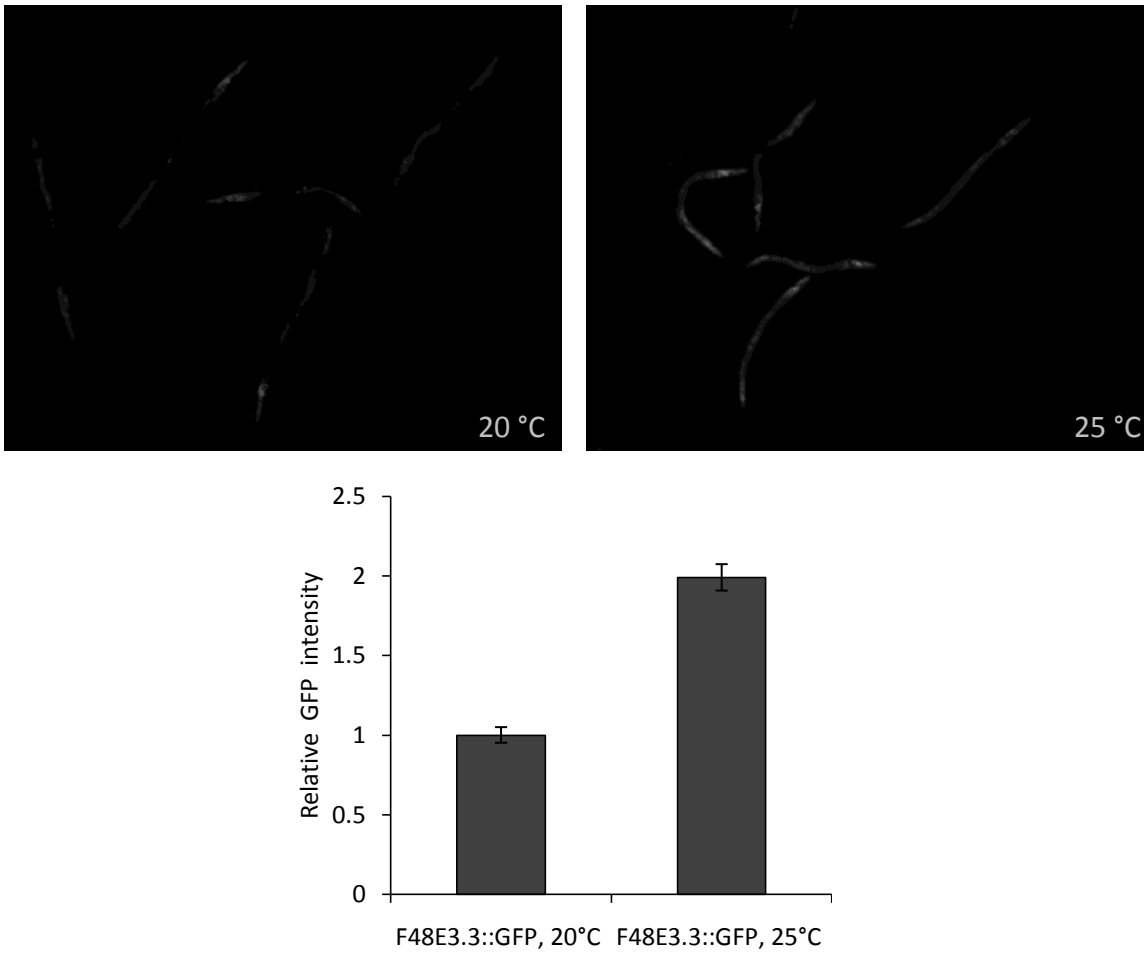

Figure 13. A *uggt-1* GFP reporter is upregulated when temperature increases.

L4 stage animals grown at 20°C and 25°C (n=28 & n=24 respectively) were anesthetized with 10mM sodium azide and photographed using epifluorescent optics in a Zeiss Axiovert 2 compound microscope (5x objective, long exposure time of 5.38 seconds). Quantification was performed using NIH ImageJ's integrated density calculation for the target areas (whole animals). Integrated density is a densitometric measurement, which in this case, describes the intensity of GFP fluorescence. Absolute integrated density values were made relative to the average F48E3.3::GFP integrated density at 20°C and referred to as Relative GFP fluorescence intensity. Animals analyzed were 28 at 20°C

and 24 at 25°C. Error bars represent standard error. Student's t-test was used to evaluate statistical significance: P(20°vs.25°C)= 8.60E-10.

3.3.4. *uggt-1* mutants constitutively and mildly activate the UPR, and such activation correlates with the increase in death suppression

The role that UGGT could exert on the unfolded protein response (UPR) pathway prompted us to address whether downregulation of *uggt-1* could activate UPR genes and whether such activation could play a role in the transduction of the death-suppressing effect in our mutants. As shown in Figure 14, we found that indeed *uggt-1* alleles *bz130* and *bz146* activate the UPR reporter *zcIs4(hsp-4::gfp)*. Note the higher intensity levels of reporter activation in mutant *uggt-1* backgrounds as compared to the *zcIs4* background strain. The increase in death suppression given the increase in temperature (from 20°C to 25°C) strongly correlates with the corresponding increase in UPR activation levels (R^2=0.97), which suggest an associative relationship between these two phenomena.

The differences in UPR activation levels between alleles *bz130* and *bz146* were expected and supported by my interpretation that allele *bz130* (carrying an in-frame deletion and behaving as a weaker death suppressor) may represent a partial-loss-of-function allele, while *bz146* (carrying a premature stop codon and inducing stronger death suppression) may behave closer to a complete loss-of-function allele (highly reduced *uggt-1* mRNA

levels in strain carrying allele *bz146* suggest that this is indeed the case, see Figure 24). Additional *uggt-1* RNAi experiments could be performed on *uggt-1* mutant strains in order to evaluate this interpretation. Transcript knockdown by RNAi should enhance any *uggt-1*-dependent phenotype in those cases where the specific mutation only partially eliminates *uggt-1* function.

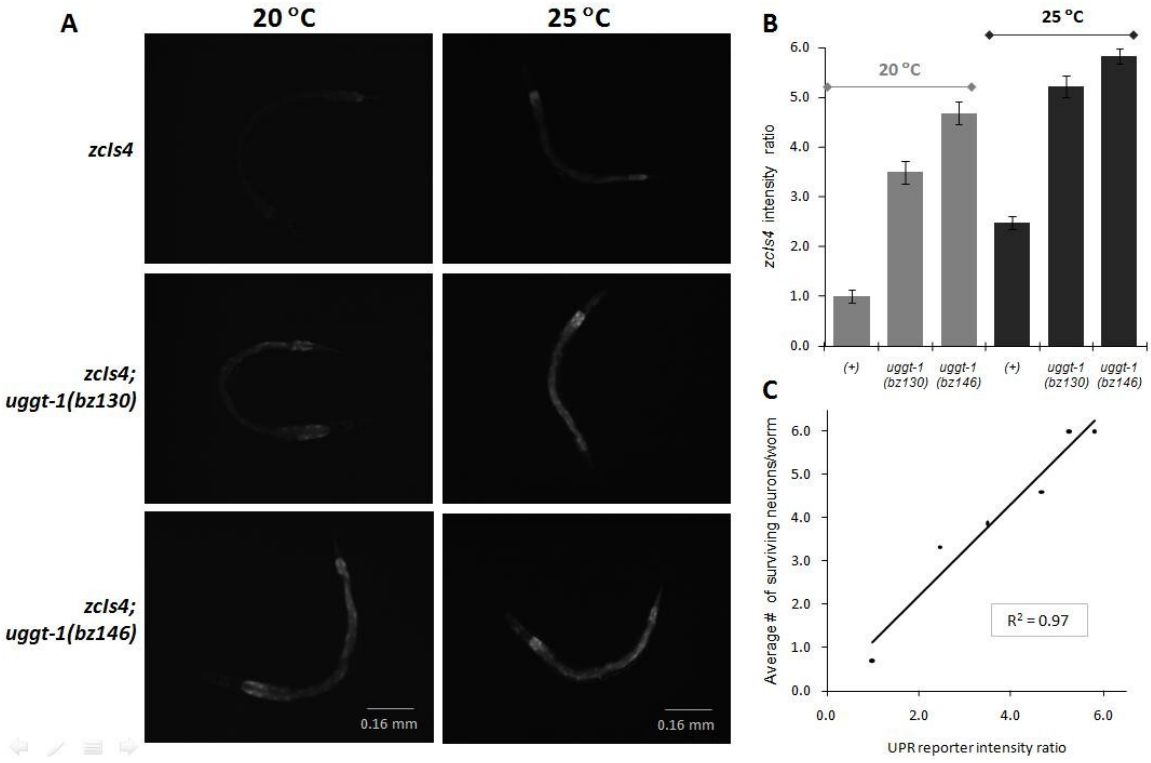

Figure 14. UPR reporter activation levels at 20°C and 25°C.

Representative animals were grown at the respective temperatures and pictures were taken at L4 stage using Zeiss Axiovert 2 compound microscope (A); *zcIs4(hsp::GFP)* transcriptional reporter was used to detect activation of the Unfolded Protein Response (UPR). Quantification of reporter fluorescent intensity (measurements performed using

NIH ImageJ software) is shown in (B), while correlation between such UPR reporter activation levels and respective necrosis-suppressing levels are shown in (C). Error bars represent standard error. Student's t-test was used to evaluate statistical significance: P(*Is4;bz130vs.Is4*_20°C)= 5.01×10^{-13}, P(*Is4;bz146vs.Is4*_20°C)= 3.48×10^{-19}, P(*Is4; bz146 vs. Is4; bz130*_20°C)= 0.0006, P(*Is4; bz130 vs. Is4*_25°C)= 3.15×10^{-16}, P(*Is4;bz146vs.Is4*_25°C)= 3.28×10^{-25}, P(*Is4;bz146vs.Is4;bz130*_25°C)= 0.0211.

3.3.5. *uggt-1* mutation does not affect localization of MEC-4 protein or functionality of the wild type or hyperactive channels

To address the possibility that *uggt-1* mutants may be suppressing *mec-4(d)*-induced death by impairing the proper folding and/or functionality of MEC-4 channels, I used four different approaches, which were: (1) determination of localization pattern of a MEC-4(+)::GFP fusion protein reporter in wt and *uggt-1* backgrounds; (2) localization pattern of MEC-2 protein by MEC-2 immunostaining in both *mec-4(+)* and *mec-4(d)* backgrounds when *uggt-1* is wt or mutant; (3) comparative touch sensitivity assays on *mec-4(+)* background when *uggt-1* is wt or mutant; and (4) presence of vacuoles in *mec-4(d)* background when *uggt-1* is wt or mutant.

One possibility for death suppression is that the MEC-4 channel is not expressed and distributed to punctae when *uggt-1* is mutant. To address this possibility, I first counted the number of MEC-4(+)::GFP punctae along axonal processes in wild type and *uggt-1*

mutant backgrounds, as well as fluorescence intensity in the cell body (an indicator of protein expression levels). My analysis did not show significant differences between MEC-4(+)::GFP wild type and *uggt-1* mutant backgrounds (Figure 15), indicating that the general localization pattern and protein levels of a MEC-4(+)::GFP fusion protein are not grossly altered in the *uggt-1* mutant background.

This conclusion was further supported by functional touch assays (Figure 16). Regarding touch sensitivity behavior, *uggt-1* mutants remain sensitive to gentle touch, which is an indication of the proper functioning of the touch-transducing channel in this mutant background. This suggests that impairment of *uggt-1* function does not significantly affect the proper folding and/or trafficking to the membrane (hence function) of the wild type MEC-4 protein.

I also considered a complementary test for MEC-4 expression at the proper sites in *uggt-1* mutant neurons, MEC-2 distribution. MEC-2 is a stomatin-like channel subunit that interacts with the MEC-4 subunit for proper localization to the plasma membrane (Zhang et al., 2004). MEC-2 distribution in punctae along the touch receptor process thus depends on *mec-4* activity. As another indicator of whether MEC-4 appears to reach its proper localization when *uggt-1* is mutant, I used MEC-2 antibody staining and quantitated signals +/- *mec-4*. The MEC-2 immunostaining pattern quantification (used here as an indirect reporter for MEC-4 localization) did not significantly change either in

the *mec-4(+)* vs. *mec-4(+) uggt-1(bz146)* (Figure 17a), further suggesting that *uggt-1* does not affect general expression level or localization of the MEC-4(+) channel.

One must keep in mind however, that the MEC-4(d) subunit is different from wt, and could interact with UGGT-1 in a different manner. A key question is what happens to the MEC-4(d) channel, which has substitution A713V, a change that could present an added folding challenge. Testing in a MEC-4(d) background is somewhat challenging, since touch cells normally die. To address potential differences in MEC-4(d) mutants, I also examined MEC-2 protein distribution in animals that were *mec-4(d) +/- uggt-1(bz146)* (Figure 17b). Although the distribution of MEC-2 punctae is more dispersed in surviving *mec-4(d)* neurons as compared to *mec-4(+)*; the presence of *uggt-1* mutation did not significantly change the pattern in death-suppressed *mec-4(d)* neurons (and the pattern is distinct from that seen in *mec-4* null mutants (Figure 17c)). This suggests that *uggt-1* does not markedly change the distribution and expression level of the *mec-4(d)* channel—possibly suppression is not attributed to a major change in abundance or position of mutant channel complexes.

(A) MEC-4(+)::GFP Punctae Quantification (ImageJ Processing)

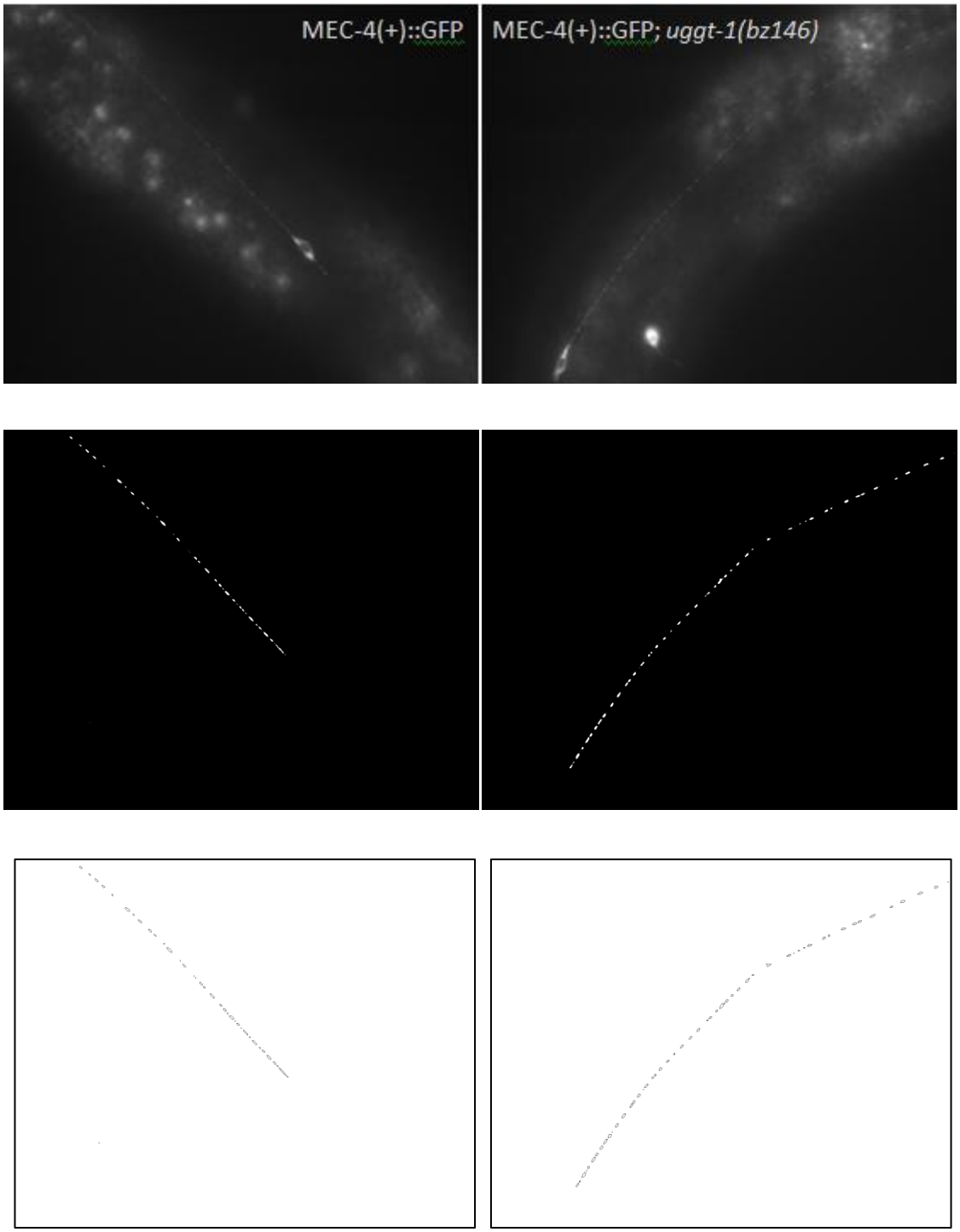

(B) MEC-4(+)::GFP Punctae & Fluorescence Expression Level Quantifications

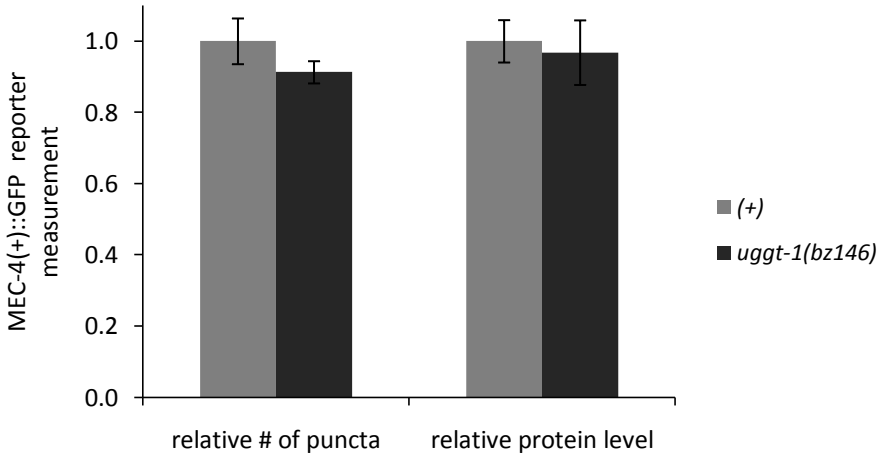

Figure 15. Punctae and fluorescence level quantification in the processes and cell bodies (respectively) of *MEC-4(+)::GFP*-expressing touch sensory neurons.

Strains used were *Is(pmec-4::MEC(+)::GFP)* vs. *Is(pmec-4::mec-4(+)::GFP); uggt-1(bz146)*. Pictures were taken using epifluorescence capabilities installed on Zeiss Axiovert 2 microscope. Punctae quantification was done by automatic Particle Analysis using ImageJ (shown in A, from top to bottom: raw, then subtracted background and adjusted threshold, followed by analysis of particle images). Estimation of relative protein levels was performed using Integrated Density measurement capability of ImageJ software (protein levels assumed proportional to fluorescence intensity as measured in the cell bodies). Shown in B, quantification charts for both relative number of punctae and fluorescence levels in cell body. Scored are, for punctae quantification: 24 *Is(pmec-4::MEC(+)::GFP)* processes accounting for total length of 990 µm and 15 *Is(pmec-4::mec-4(+)::GFP); uggt-1(bz146)* processes accounting for a total length of 840 µm; for protein level quantification: 33 *Is(pmec-4::MEC(+)::GFP)* and 15 *Is(pmec-4::mec-4(+)::GFP); uggt-*

1(bz146) cell bodies. No significant difference was found for either of the quantifications performed. Error bars represent standard error.

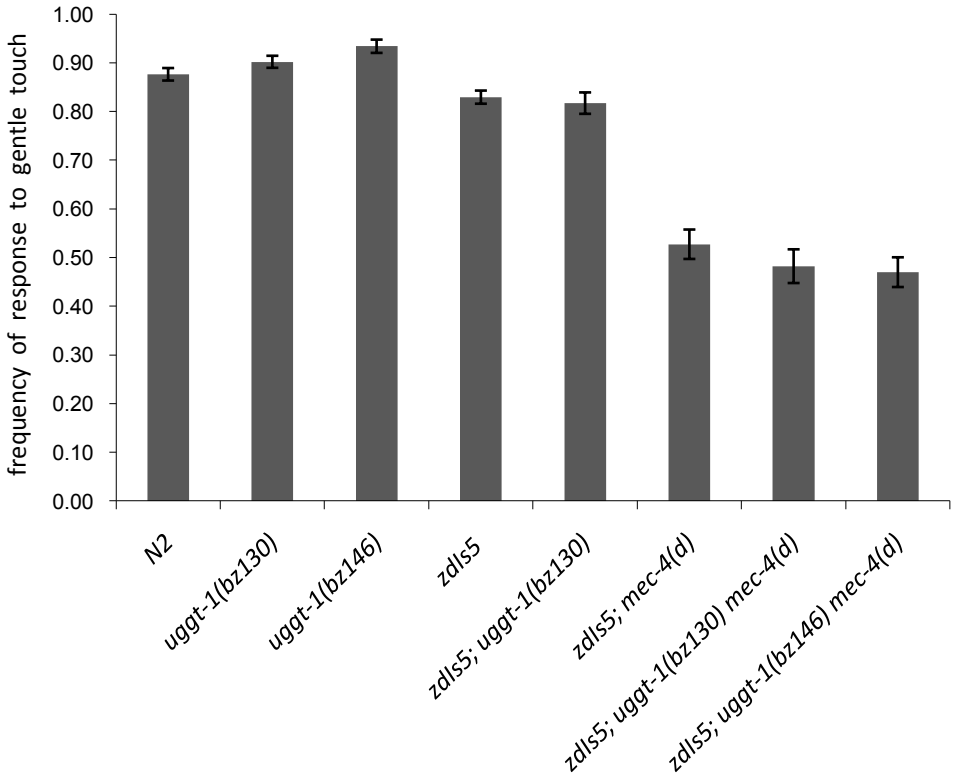

Figure 16. Gentle touch sensitivity tests for *uggt-1* alleles.

Scores were calculated as the frequency of response to 6 gentle touches (3 in the anterior and 3 in the posterior parts of the body). Animals scored are: 89 N2, 80 *uggt-1(bz130)*, 48 *uggt-1(bz146)*, 86 *zdIs5*, 31 *zdIs5; uggt-1(bz130)*, 61 *zdIs5; mec-4(d)*, 61 *zdIs5; uggt-1*(*bz130) mec4(d)*, 61 *zdIs5; uggt-1*(*bz146) mec4(d)*. Error bars represent standard error. t-Test probabilities are P(*uggt-1(bz130)* vs. N2)=0.119413; P(*uggt-1(bz130)* vs. *uggt-1(bz146))*=0.088763, P(*zdIs5* vs. N2)=0.001025; P(*zdIs5* vs. *zdIs5;*

mec4(d))=3.7187x10^{-16}; P(*zdIs5; uggt-1*(*bz130) mec4(d)* vs. *zdIs5; mec4(d)*) = 0.332599; P(*zdIs5; uggt-1(bz146) mec4(d*) vs. *zdIs5; mec4(d)*) = 0.187956.

If necrosis is not initiated in the *uggt-1 mec-4(d)* mutant, we would not expect to find the necrotic vacuoles that are typical of *mec-4(d)* touch neurons. To address whether necrosis initiation is impacted by *uggt-1*, I examined early larvae for the presence of vacuolar touch neurons. I found that swollen neurons (vacuolated appearance under DIC optics) are found during the L1 larval stage in the *uggt-1* mutant backgrounds (Figure 18), suggesting that the death-initiating competency of MEC-4(d) channels persist in the *uggt-1* mutant background. Notably, although the total number of swollen neurons at L1 is reduced compared to wild type, there is not a significant difference between the two *uggt-1* mutant backgrounds (allele *bz130* vs. allele *bz146*), which indicates that the different suppression levels observed in those strains might be due to different capacities to cope with and survive the initial insult, rather than eliminating the insult itself. Indeed, we can notice that by L2 stage there is a significantly higher number of swollen neurons remaining in the *bz146* background (the stronger suppressor) as compared to *bz130*, which may be indicative of an improved capacity of *bz146* strain to deal with the ionic imbalance and swelling. I reason that the reduced number of swollen neurons in *uggt-1* mutant larvae might be the consequence of an early interference with the death pathway (presumably before swelling takes place) rather than a consequence of elimination of the initial insult (see additional lines of reasoning in next paragraphs).

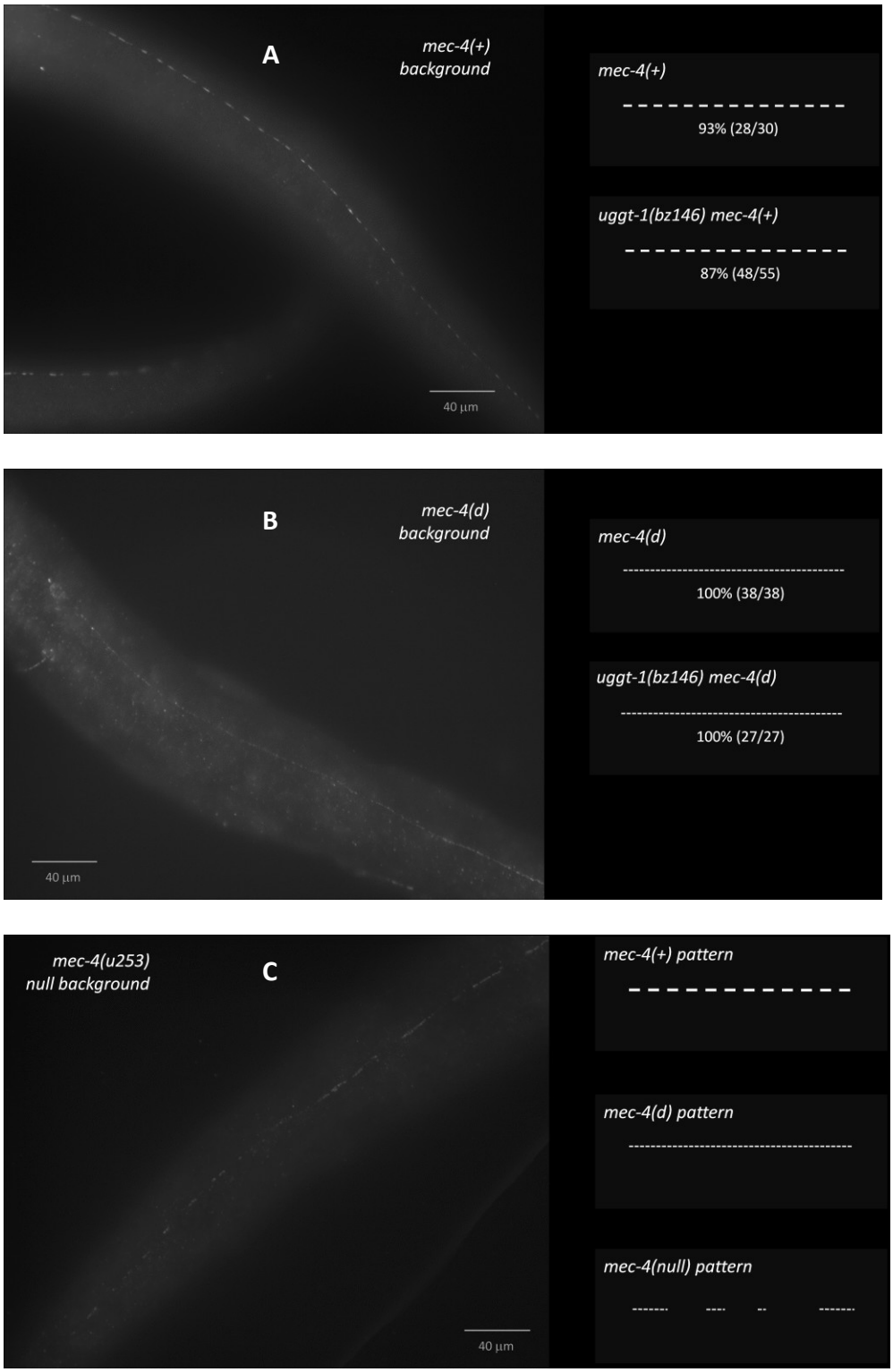

Figure 17. Quantification of the MEC-2 immunostaining punctuated pattern in axonal processes of touch sensory neurons.

Cartooned patterns to the right of the representative picture example indicate the percentage of pictures matching the specific pattern (absolute number of observations is given in the parenthesis: 30 pictures analyzed for *mec-4(+)* strain, 55 for *uggt-1(bz146) mec-4(+)*, 38 for *mec-4(d)*, and 27 for *uggt-1(bz146) mec-4(d)*). The Chi-squared test was used to test significance between pattern frequency differences between mutant *uggt-1* and control background.

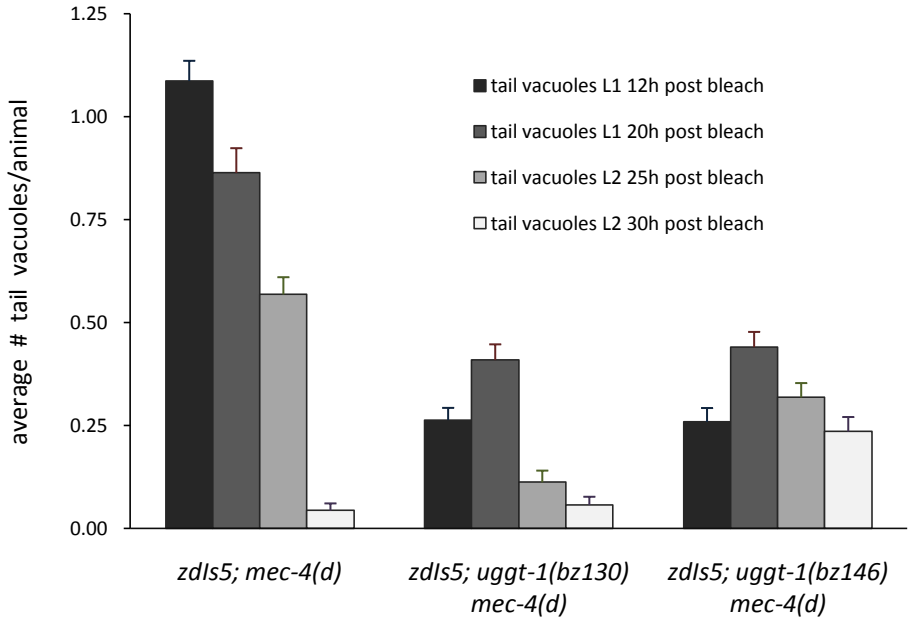

Figure 18. Time course scoring of vacuole phenotype in distinct *mec-4(d)* backgrounds. Average number of tail vacuoles at 12h L1, 20h L1, 25h L1/L2, 30h L2, Temp. 20°C. Vacuoles were scored using the Oblique Coherence Contrast (OCC) capability of Nikon SMZ1500 stereomicroscope. Maximum number of swollen neurons (vacuoles) in the tail is two. Developmental timing is slightly delayed in *uggt-1* mutants, taking about 8 additional hours for embryos to develop up to the L4 stage (this would be equivalent to

an approximate delay of 480min/48hrs= 10 min./developmental hour during larval stages). Animals scored are: 670 *zdIs5; mec-4(d)*, 698 *zdIs5; uggt-1(bz130) mec-4(d)*, and 761 *zdIs5; uggt-1(bz146) mec-4(d)*. Error bars represent standard error. Student t-test was used to evaluate statistical significance: P(*bz130vs.bz146*,L1,12h)= 1.0, P(*bz130vs.bz146*,L1,20h)= 0.5966, P(*N2vs.bz130*,L2,30h)= 0.4798, P(all other pairwise comparisons)< 0.0001.

These results might have been expected because UDP-glucose:glycoprotein glucosyltransferase appears to be involved only in "fine tuning" optimal protein folding in the ER, intervening in only the latest stages of the process. In these terms, it is expected that in the mutant *uggt-1* background, proteins would only harbor minor folding defects, if at all, which may not dramatically affect their respective functionalities. We also need to keep in mind that alternative chaperonic activity could compensate for an altered CNX/CRT cycle (Lee et al., 2006).

Supporting this line of reasoning is evidence that mutations in the *Arabidopsis* UGGT homolog gene suppressed the growth defects of a brassinosteroid (BR) receptor mutant by allowing the export of the structurally sub-optimal yet biochemically competent mutant receptor (Jin et al., 2007). Extrapolating to our *mec-4(d)* mutant scenario, I would expect that *uggt-1* mutations (e.g. *zdIs5; uggt-1(bz146) mec-4(d)*) would allow equal or even higher amounts (but not less) of MEC-4(d) protein to effectively reach the

plasma membrane, hence inducing a similar or even stronger necrotic insult. Equivalently, I would also expect that export of hyperactive MEC-4(d) channels would be in any case, reduced in an intact wild type UGGT-1 background (e.g. strain *zdIs5; mec-4(d)*), since the overzealous, intact ER-quality control mechanism would retain and possibly dispose of a certain amount of MEC-4(d) channel subunits. To highlight the relevance of this interpretation, I would like to refer again to its implications: it is reasonably expected that MEC-4(d) hyperactive channels were more lethal in the *uggt-1* background because a higher amount of functional protein would reach the plasma membrane. This may be the reason why the *uggt-1* suppressors cannot achieve maximum inhibition of necrosis. It seems unlikely then, that a MEC-4(d)-specific folding challenge could render these channels nonfunctional (non-hyperactive in such case).

3.3.6. *uggt-1* mutation suppresses death-inducing capacity of the hyperactive *unc-8(n491)* mutant channel

An important question is whether *uggt-1* mutations generally suppress against other known necrotic insults, or are rather specific to *mec-4(d)* mutations. Gene *unc-8* encodes another member of the amiloride-sensitive DEG/ENaC family of cation-selective channels. Allele *n491* encodes substitution G387E situated within an extracellular domain previously implicated in channel closing (Garcia-Anoveros et al., 1995; Tavernarakis et al., 1997). This mutation renders the *unc-8* channel hyperactive and the nematode becomes severely uncoordinated. In this background, ventral nerve cord motorneurons swell and disrupt function, although they do not extensively

degenerate (Shreffler et al., 1995; Tavernarakis et al., 1997). As observed in Figure 19, *uggt-1* mutation dramatically improves the uncoordinated phenotype, supporting that *uggt-1* can affect multiple hyperactivated degenerin channel subunits, in multiple cell types.

3.3.7. *uggt-1* mutation does not affect functionality (death-inducing capacity) of the non-desensitizing acetylcholine receptor *deg-3(u662*) mutant channel

I also tested for potential death-suppressing effects of *uggt-1(bz146)* in a non-desensitizing AChR mutant background *deg-3(u662)* that causes degeneration of a small set of neurons in the *C. elegans* (Treinin and Chalfie, 1995). I found that the *uggt-1* mutation does not suppress necrotic death induced by the non-desensitizing mutation in the nicotinic receptor *deg-3(u662)* (Figure 20). On the contrary, the *uggt-1* mutation appears to enhance *deg-3(u662)*-induced necrotic death (although not statistically significantly), as indicated by the consistently higher average number of vacuolated neurons found in the head and tail of the animals. This result indirectly supports my previous reasoning, discussed in Section 3.3.5, that *uggt-1* mutations might allow equal or even higher amounts of hyperactive channel protein to effectively reach the plasma membrane, hence inducing a similar or even stronger necrotic insult (as a consequence of a less overzealous ER quality control surveillance).

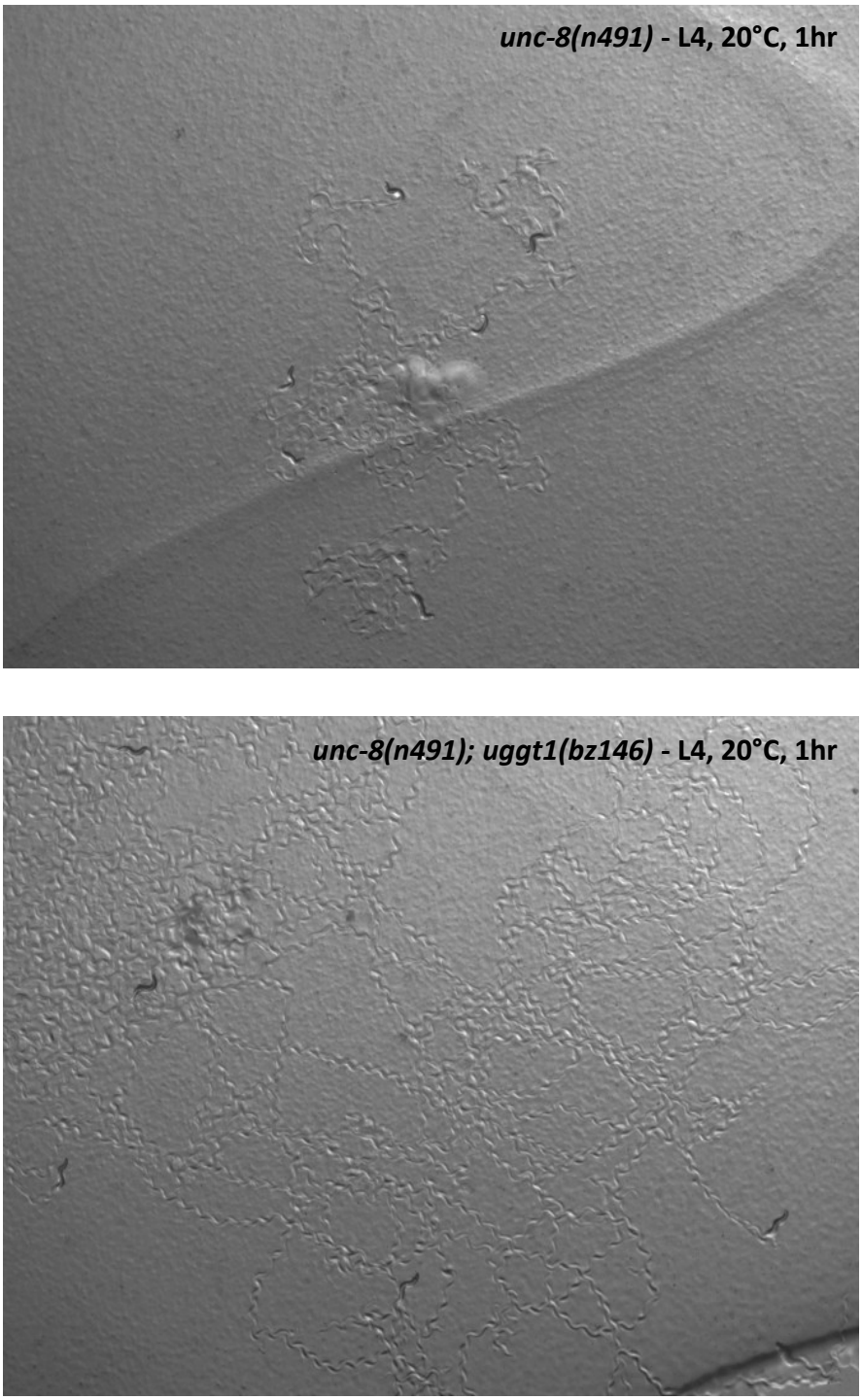

Figure 19. *unc-8(n491)* locomotion capacity is improved in a *uggt-1* mutant background. L4 stage worms were transferred to the center of a freshly seeded plate and left to wander for 1 hour, at which time pictures were taken under a stereo microscope.

Furthermore, this indicates that the *uggt-1* mutation does not interfere with the function, or consequences of, the *deg-3* mutant channel. Since *deg-3(u662)* conducts an excess of Ca^{2+} ions inside the cell, it may bypass any required contribution for calcium release from the ER, hence necrotic death could proceed independently from any endoplasmic reticulum calcium contribution.

These results support the idea that *uggt-1* mutations do not dramatically affect the general function and expression of membrane proteins (as we also observed in the case of MEC-4(+) and MEC-4(d) in previous section 3.3.5), which was a reasonable assumption based on its role in quality control of only the latest stages in folding and on the basic viability of the mutant strains. Data on *deg-3(gf)* do not rule out that *uggt-1* could change the nature of the ER calcium signal involved in *mec-4(d)*-induced necrosis.

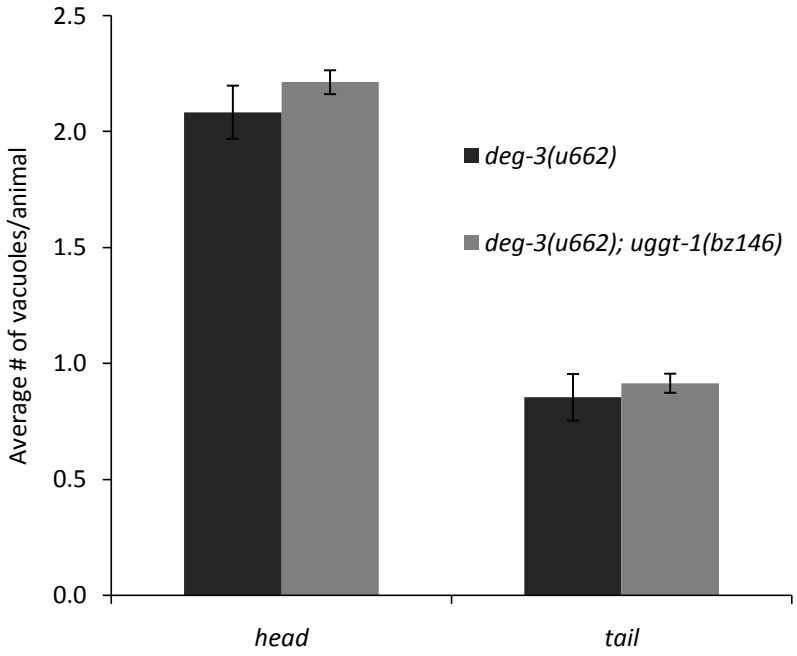

Figure 20. Quantification of *deg-3(u662)*-induced degeneration in wt and *uggt-1 backgrounds*.

Number of tail vacuoles at L1 stage was quantified by observation in Zeiss Axiovert 2 compound microscope using DIC optics. Scored were 48 *deg-3* animals and 47 *deg-3; uggt-1*. Error bars represent standard error. Student's t-test was used to evaluate statistical significance: P(*wt.vs.bz146.head*)= 0.3990, P(*wt.vs.bz146.tail*)= 0.3604.

3.3.8. UPR genes genetically interact with *uggt-1* to modulate *mec-4(d)*-induced necrosis

My observations that *uggt-1* mutation activates the UPR lead me to question the role of UPR genes in necrosis. First, I tested the effects of each major player in each downstream UPR branch for potential effects on *mec-4(d)*-induced necrosis. When

individually put into the *mec-4(d)* background, *pek-1(ok275)* and *ire-1(zc14)* alleles did not show any enhancement of necrotic death at 20°C (though necrosis already transpires at a very high rate), but mutations in these genes increased *mec-4(d)*-induced death at 25°C (Figure 21). The temperature-dependent death suppression effect induced when worms are grown at 25°C is dramatically impaired in both *pek-1* and *ire-1* mutant backgrounds, which corroborates important roles for *pek-1* and *ire-1* in transducing necrosis-suppressing signals when temperature is high. On the other hand, *atf-6(ok551)* suppressed necrotic death by itself in the *mec-4(d)* background, which suggests that *atf-6* may normally transduce necrosis-promoting signals.

To assess then suspected genetic interactions between *uggt-1* and members of the UPR pathway, I constructed triple mutants for *mec-4(d)* carrying allele *uggt-1(bz130)* and UPR genes *ire-1(zc14)*, *pek-1(ok275)*, or *atf-6(ok551)*. I was unable to construct compound mutants carrying the stronger death suppressor allele *bz146* because progeny from such crosses were not viable (which is evidence itself of genetic interaction between *uggt-1* and the UPR transducers).

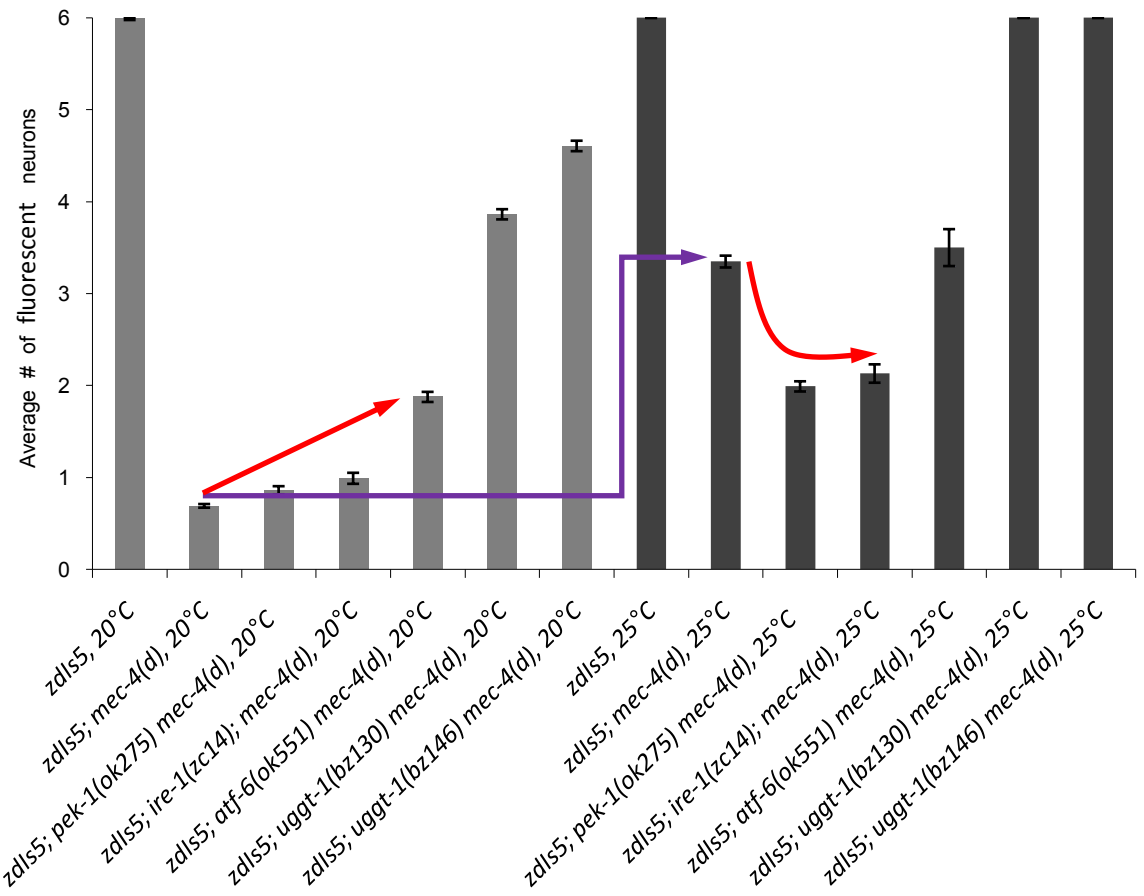

Figure 21. Genetic evidence for a role of unfolded protein response (UPR) genes in the suppression of *mec-4(d)*-induced necrotic cell death.

Red arrows highlight changes in neuronal survival levels in compound mutant strains as compared to control strain *zdIs5; mec-4(d)* at specified temperatures. The purple arrow highlights the increase in death suppression induced by an upshift in temperature from 20°C to 25°C. Scored at 20°C are: 192 Is5 animals, 316 *Is5; mec-4(d)*, 118 *Is5; pek-1(ok275) mec-4(d)*, 268 *Is5; ire-1(zc14) mec-4(d)*, 273 *Is5; atf-6(ok551) mec-4(d)*, 342 *Is5; uggt-1(bz130) mec-4(d)*, and 198 *Is5; uggt-1(bz146) mec-4(d)*. Scored at 25°C: 140 Is5 animals, 158 *Is5; mec-4(d)*, 222 *Is5; pek-1(ok275) mec-4(d)*, 225 *Is5; ire-1(zc14) mec-4(d)*,

150 *Is5; atf-6(ok551) mec-4(d)*, 171 *Is5; uggt-1(bz130) mec-4(d)*, and 165 *Is5; uggt-1(bz146) mec-4(d)*. Error bars represent standard error. Student's t-test was used to evaluate statistical significance: P(*Is5; pek-1(ok275) mec-4(d) vs. Is5; mec-4(d)*_20°C)= $1.02x10^{-02}$, P(*Is5; ire-1(zc14); mec-4(d) vs. Is5; mec-4(d)*_20°C)= $1.92x10^{-03}$, P(*Is5; atf-6(ok551) mec-4(d) vs. Is5; mec-4(d)*_20°C)= $8.62x10^{-07}$, P(*Is5; pek-1(ok275) mec-4(d) vs. Is5; mec-4(d)*_25°C)=$1.73x10^{-05}$, P(*Is5; ire-1(zc14) mec-4(d) vs. Is5; mec-4(d)*_25°C)= $5.70x10^{-04}$, and P(*Is5; atf-6(ok551) mec-4(d) vs. Is5; mec-4(d)*_25°C)= 0.4766.

Figure 22 shows that *ire-1(zc14) uggt-1(bz130)* and *uggt-1(bz130) pek-1(ok275)* restore *mec-4(d)*-induced death. That I found reduced levels of *uggt-1* suppression of *mec-4(d)*-induced death when *ire-1* and *pek-1* are mutant suggests that *ire-1* and *pek-1* act downstream of *uggt-1*. On the other hand, the triple *mec-4(d)* mutant carrying *uggt-1(bz130)* and *atf-6(ok551)* showed enhancement of suppression of *mec-4(d)*-induced death, compared to the level of necrosis when *atf-6* only is present. In addition, the above-mentioned triple mutant strains exhibited additional phenotypes such as reduced brood size, slow growth, and partial developmental arrest during larval stages (data not shown).

Altogether, this data supports that the UPR gene activities are capable of modulating the transduction of *mec-4(d)*-induced death signals, and that death-suppression induced by loss/reduction of *uggt-1* function may be mediated by activation of the unfolded

protein response and its respective signaling cascades (this might be direct or indirect, such as by influencing levels of molecules that participate in neurotoxicity). In this regard, *pek-1* and *ire-1* appear to transduce necrosis-inhibiting signals, while *atf-6* counteracts by activating necrosis-promoting ones.

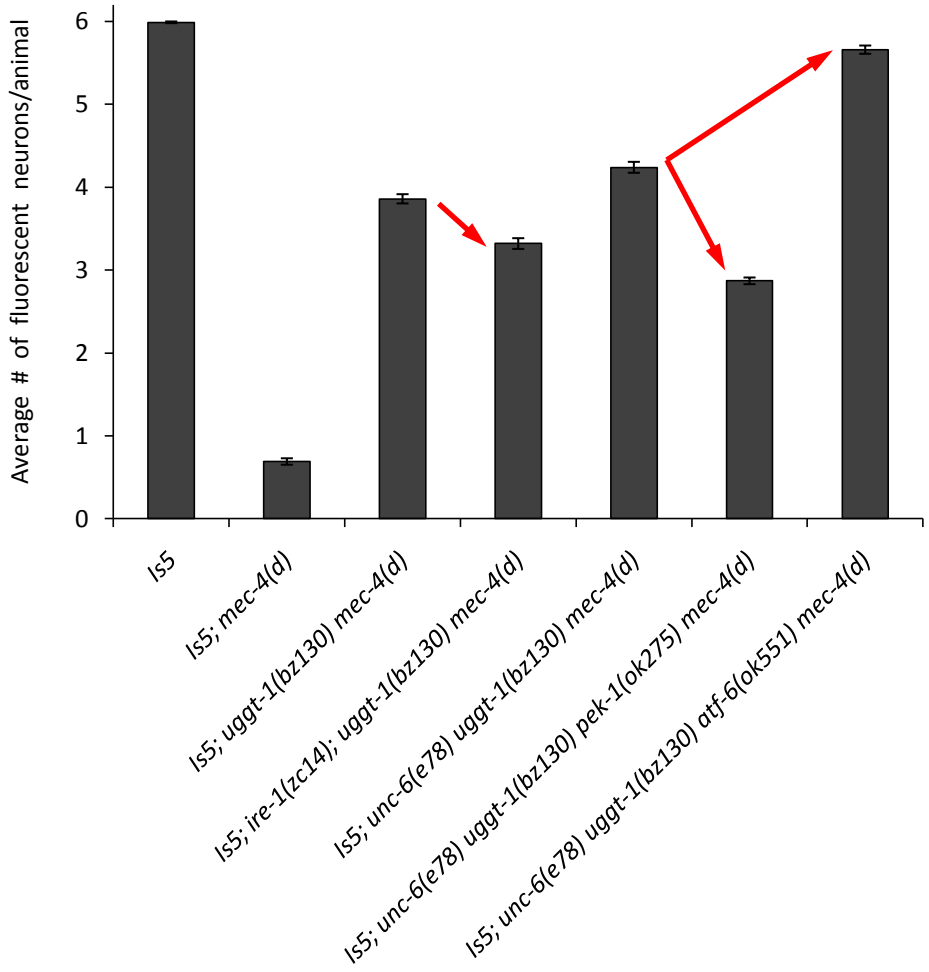

Figure 22. Genetic evidence for a role of unfolded protein response (UPR) genes in the transduction of *uggt-1* mutation-induced suppression of necrotic cell death.

Red arrows highlight changes in neuronal survival levels in compound mutant strains as compared to respective control strain. Scored under Zeiss SV11 epifluorescence optics:

102 Is5 animals, 316 *Is5; mec-4(d)*, 342 *Is5; uggt-1(bz130) mec-4(d)*, 287 *Is5; ire-1(zc14); uggt-1(bz130) mec-4(d)*, 220 *Is5; unc-6(e78) uggt-1(bz130) mec-4(d)*, 508 *Is5; unc-6(e78) uggt-1(bz130) pek-1(ok275) mec-4(d)*, and 149 *Is5; unc-6(e78) uggt-1(bz130) atf-6(ok551) mec-4(d)*. Error bars represent standard error. Student's t-test was used to evaluate statistical significance: P(*ire-1; uggt-1 vs. uggt-1*)= $1.35x10^{-04}$, P(*pek-1; uggt-1 vs. uggt-1*)= $3.22x10^{-11}$, P(*atf-6; uggt-1 vs. uggt-1*)= $1.75x10^{-08}$.

From a molecular perspective, the question of how the different branches of the UPR pathway modulate *mec-4(d)*-induced necrotic death remains intriguing with no obvious answer from published literature. The fact that opposite UPR contributions (*atf-6* vs. *ire-1* and *pek-1* in this case) modulate the final adaptation/survival vs. necrotic death outcome is consistent with the well-known properties of the pathway, which commonly perform in tug-of-war activities among its transducers.

3.3.9. Calcium release from the ER appears to be downregulated by loss of *uggt-1* function

I reasoned that the availability of substrate for calreticulin and calnexin (monoglucosylated glycoproteins) should be dramatically reduced in *uggt-1* mutant backgrounds; hence, the expression of these lectins might be downregulated by putative feedback mechanisms. Such downregulation of *crt-1* for example, could result in a reduction in calcium release from the ER, hence slower increases of intracellular

calcium concentrations that would delay and/or suppress necrotic death. To assess this potential contribution from calcium signaling downregulation, I constructed compound mutant strain *zdIs5; itr-1(sy290) dpy-20(e1282); uggt-1(bz146) mec-4(d)* carrying a gain of function mutation in the *itr-1* gene, the IP3R channel gene in *C. elegans*. The *itr-1(gf)* mutation is thought to increase ER calcium release.

Interestingly, the gain-of-function *itr-1* mutation rescued cell death to a statistically significant extent at 20°C in the *uggt-1* background, but not in an otherwise wild type or *mec-4(d)*-only backgrounds (Figure 23), which suggests that *uggt-1* deficiency can downregulate calcium release from the ER. Therefore, *uggt-1* deficiency can contribute to death suppression in part through that mechanism.

Although this effect cannot be readily detected at 25°C, it does not rule out my previous conclusion based on the 20°C experimental data. I reason that even when the *itr-1(gf)* mutation appears to increase touch neuron death in the *mec-4(d)* background at 25°C (as indicated by increased degeneration in the *mec-4(d)*-only background, Figure 23), the enhancement of *uggt-1*-induced suppression at 25°C could be such that the *itr-1* effect is not perceptible in the *uggt-1* background.

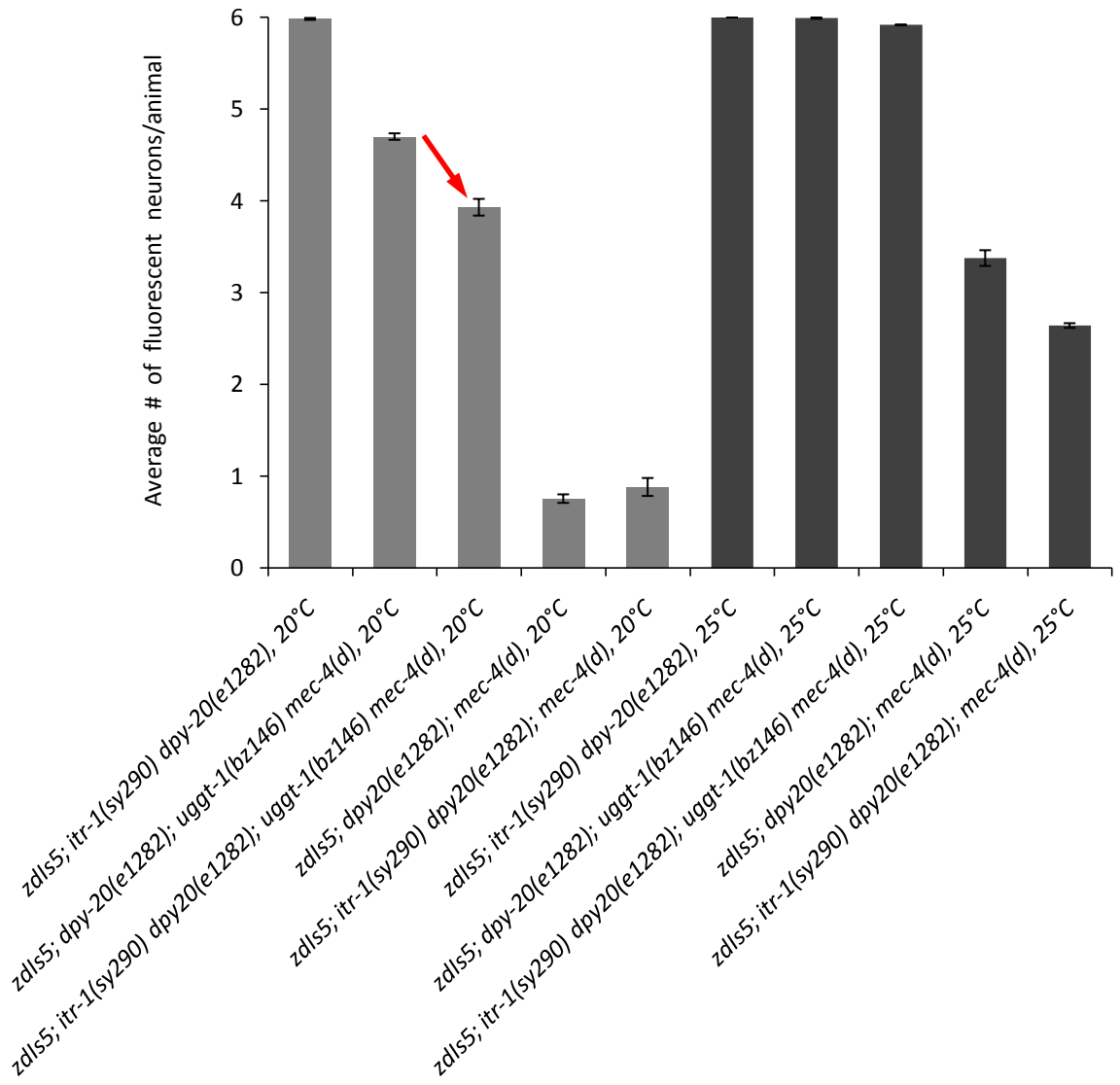

Figure 23. Ca^{2+} release upregulation by the gain-of-function *itr-1(sy290)* allele modestly increases necrotic cell death in the *uggt-1* background.

Fluorescent neurons were scored under a Zeiss SV11 stereomicroscope. Scored under Zeiss SV11 epifluorescence optics are 192 *zdIs5*; 166 *zdIs5, itr-1(sy290) dpy-20(e1282)*, 234 *zdIs5; dpy-20(e1282); uggt-1(bz146) mec-4(d)*, 403 *zdIs5; itr-1(sy290) dpy20(e1282); uggt-1(bz146) mec-4(d)*, 182 *zdIs5; itr-1(sy290) dpy20(e1282); mec-4(d)*, 122 *zdIs5; dpy20(e1282); mec-4(d)*, and 316 *zdIs5; mec-4(d)*. Error bars represent standard error.

Student's t-test was used to evaluate statistical significance: P(*itr-1; uggt-1 vs. uggt-1*_20°C)= 0.00025, P(*itr-1; uggt-1 vs. uggt-1*_25°C)= 0.0155.

These data suggest that mutations in *uggt-1* may suppress *mec-4(d)*-induced death, in part, due to a reduction in calcium release from the ER. Alternatively, *itr-1* gain of function mutation may indirectly (in parallel) promote death while *uggt-1* mutation promotes survival. In that case, the compounded effect would be subtractive, i.e. a reduction in *uggt-1*-induced death suppression as observed, but this seems unlikely since *itr-1(sy290)* mutation on its own neither induce death of the touch sensory neurons nor does it enhance *mec-4(d)*-induced death in an otherwise wild type background.

3.3.10. Differential gene regulation in F48E3.3 mutants

In order to assess alterations in expression levels of UPR inducible genes that might modulate necrosis outcome, I created a qPCR array comprising 54 genes of interest (Table 8) and performed expression profiling by real-time PCR in our *uggt-1* mutant and control backgrounds.

Table 8. Genes targeted for expression profiling

PROCESS	GENE NAME	NOTE ON FUNCTION
Protein Folding QC	uggt-1	UGGT enzyme
UPR signaling	pek-1	PERK pathway
	atf-6	ATF6 pathway
	ire-1	IRE1 pathway
	xbp-1	
protein folding	crt-1	chaperone/calcium
	cnx-1	chaperone
	hsp-4 (§)	chaperone
	dnj-7 (§)	P58IPK
	ero-1 (§)	oxidoreductase
	pdi-1 (§)	proline di-isomerase
ER calcium signaling	itr-1	IP3R channel
	unc-68 (§)	RyR channel
	sca-1 (§)	SERCA
membrane biogenesis (choline synthesis)	ckb-2 (§)	choline kinase
	ckb-4 (§)	choline kinase
ubiquitination	ubc-13 (§)	Ub ligase
QC & ERAD	sel-1 (§)	HRD complex
	C47E12.3 (§)	EDEM-1 glycosyl hydrolase
	erd-2 (§)	ER retention-signal receptor
autophagy	unc-51	Ser/Thr kinase
	bec-1	beclin1
	lgg-1	MAP-LC3 subunit
	lgg-2	MAP-LC3 subunit
secretory pathway	nsf-1 (§)	membrane & vesicle fusion
	C33D9.8 (§§)	vesicle docking
	rab-11.2 (§§)	RAS GTPase
protein degradation	T28H10.3 (§§)	endopeptidase
	NAS-38 (§§)	metalloprotease
metabolism	cht-1 (§§§)	hydrolase
	F55C5.2 (§§)	P-diesterase
	lips-11 (§§§§)	lipase class 2
oxidative stress	gst-1 (§)	GST
	T20D4.7 (§§)	thioredoxin
host defence	nlp-28 (§§§§)	antimicrobial peptide/osmotic stress response
	srp-7 (§)	serpin, protease
cuticle synthesis	fipr-24 (§§§§)	fungus induced
	col-89 (§§§§§)	collagen

Gene Expression:	F40F12.7 (§§)	CBP/p300
	Y113G7B.14 (§§)	transcription termination factor
	R02D3.8 (§§)	exonuclease
	let-607 (§)	CREBH
	rrf-2 (§)	RNA pol
cytoskeleton	clec-67 (§§§§§)	C-type lectin
	tbb-6 (§§)	tubulin β
housekeeping controls	act-1	structural
	act-3	structural
	ama-1	RNA pol II
	rrn-1.1	ribosomal RNA
	Y105E8B.5	HPRT
	gpd-2	GAPDH major isoform
	ctl-1	cytosolic catalase
	ctl-2	peroxisomal catalase
	ctl-3	neuronal catalase

(§) expression of these genes was previously reported to be positively regulated by *ire-1* only; (§§) expression of these genes was previously reported to be negatively regulated by *ire-1* but positively regulated by *pek-1*; (§§§) expression of this gene was previously reported to be positively regulated by *atf-6* only; (§§§§) expression of these genes was previously reported to be negatively regulated by *pek-1* but positively regulated by *ire-1*; (§§§§§) expression of these genes was previously reported to be negatively regulated by *atf-6* but positively regulated by *ire-1* (Shen et al., 2005). Housekeeping genes were used as control group for RT-PCR reactions: *ctl-1* was chosen to normalize the Ct data because it was one of the few housekeeping genes maintaining an invariable level of expression independent of the genetic background under scrutiny.

I found that expression of the UPR transducers is mildly but significantly upregulated (Figure 24), as is the expression of distinct ER chaperones and other genes involved in

the adaptative UPR response. My data support a role for the activation of this protective, anti-ER stress response in the *uggt-1* mutant background. Another important observation was that expression of genes involved in Ca^{2+} release from the ER is significantly downregulated in the *uggt-1* mutant background (Figure 24). Since ER Ca^{2+} release plays a central role in necrosis activation, these results implicate Ca^{2+} signaling downregulation as an additional factor contributing to death suppression in the *uggt-1* mutant, in accordance with genetic interaction data reported in the previous section.

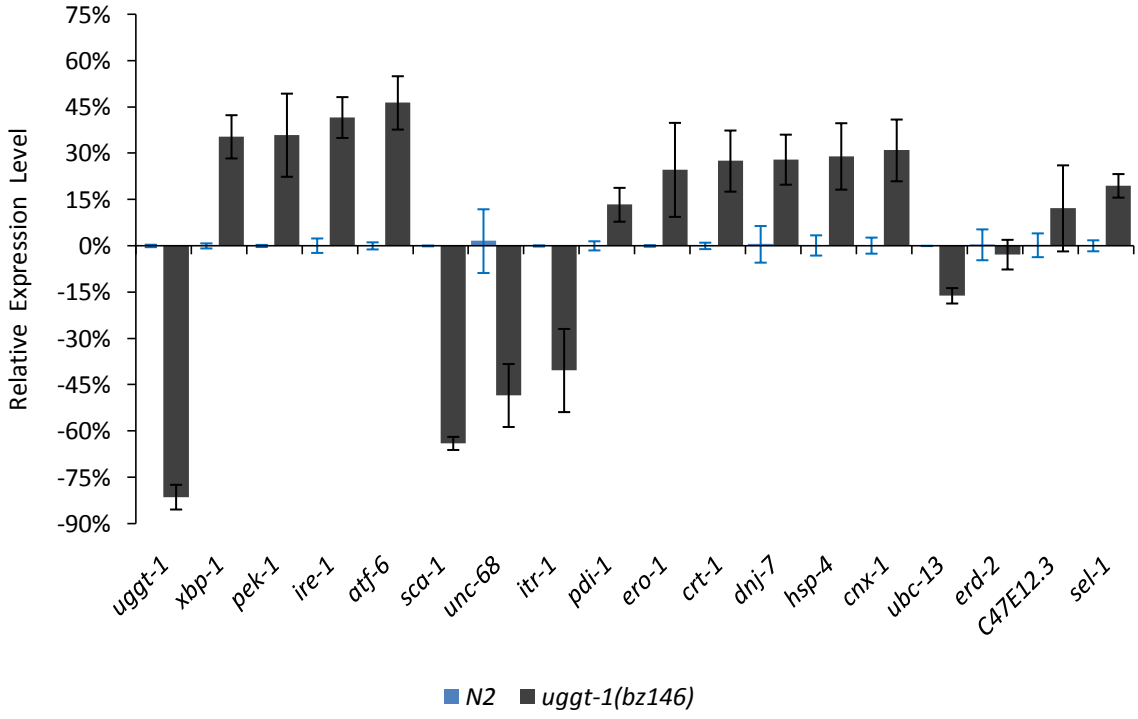

Figure 24. RT-PCR expression profiling of UPR-inducible and ER-related genes. Transcript levels were quantified by RT-PCR using QuantiTect SYBR Green PCR Kits (Qiagen, Valencia, CA) and ABI PRISM 7900 cycler. Two independent samples per strain and four replicates per RT-PCR reaction were used. Data was analyzed using SDS2.2 software (Applied Biosystems, Foster City, CA). Error bars represent standard error.

Additional expression profiling results shown in Figure 25 and Figure 26 document high upregulation of membrane biogenesis-related gene *ckb-2* (a choline kinase), tubulin β gene *tbb*-6, and T20D4.7 thioredoxin homolog (possibly involved in anti-oxidative stress responses), as well as milder but significant downregulation of metabolism-related genes (*lips-11, cht-1, nas-38, T28H10.3,* and *F55C5.2*) and general transcription activity (RNA polymerase II gene *ama-1* and transcription cofactor CBP/p300 homolog F40F12.7 were downregulated, whereas transcription termination factor *Y113G7B.14* and exonuclease *R02D3.2* were upregulated), among others.

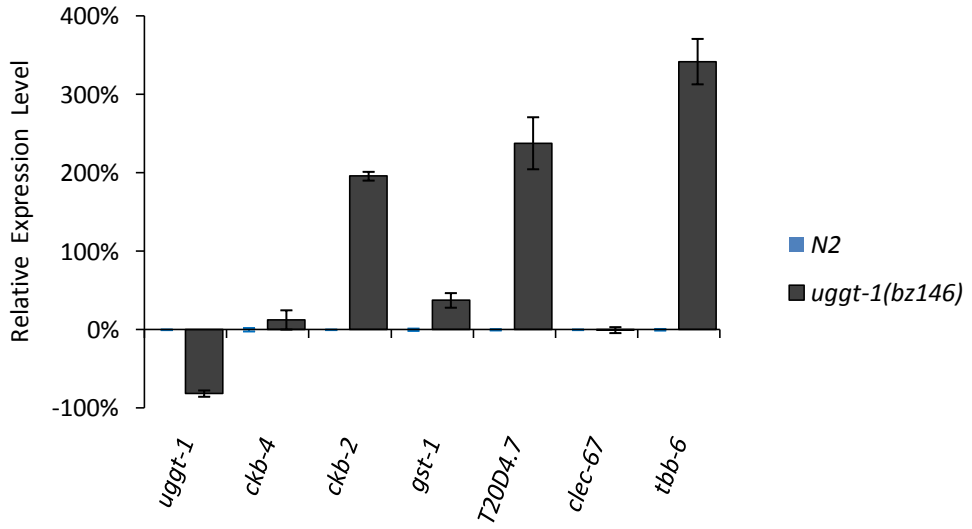

Figure 25. Highly upregulated UPR-inducible genes.

Choline kinase *ckb-2* was 3-fold (200% in the graph) upregulated, thioredoxin homolog T20D4.7 was upregulated more than 3-fold, and tubulin β gene *tbb-6* was upregulated more than 4-fold (>300% in the graph). Experiment performed as described in Figure 24 (and material and methods). Error bars represent standard error.

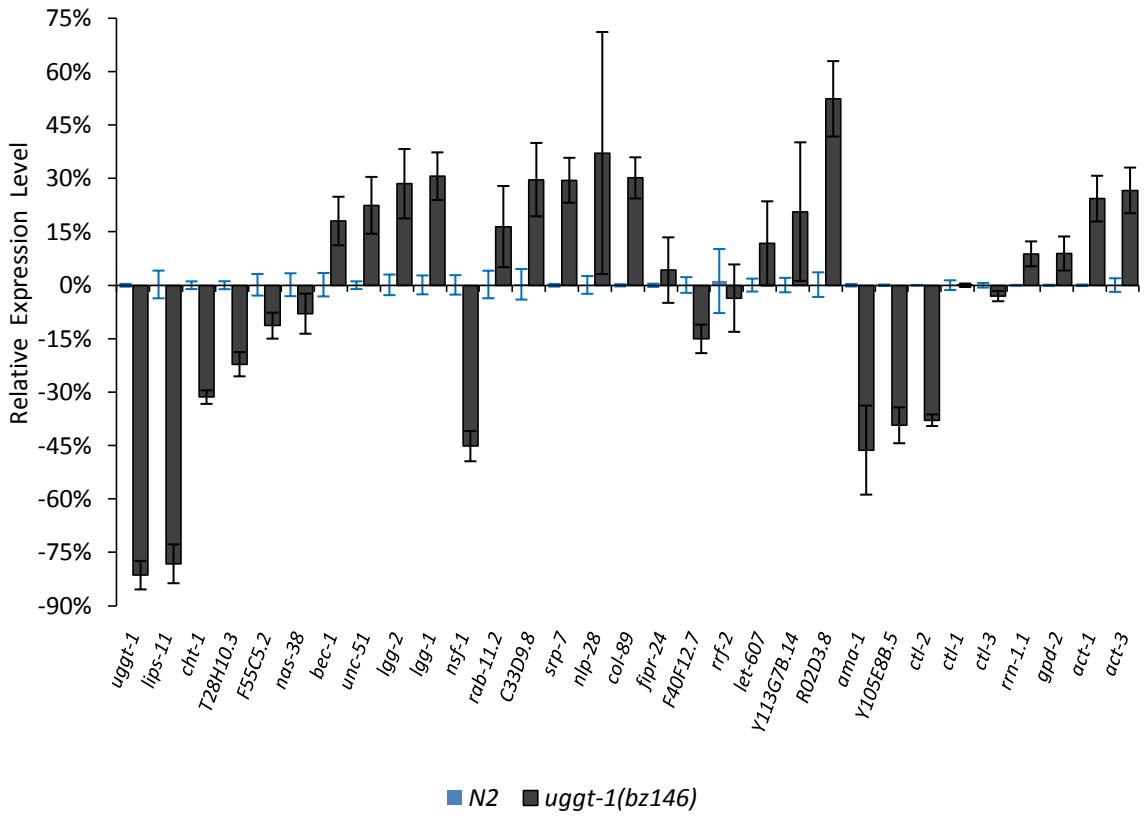

Figure 26. RT-PCR expression profiling of UPR-inducible and housekeeping genes. Experiment performed as described in Figure 24 (and material and methods). Error bars represent standard error.

Autophagy genes *bec-1, unc-51, lgg-1,* and *lgg-2*, were also mildly upregulated (Figure 26). This result appears contradictory at first sight, since autophagy has been implicated in necrosis progression in *C. elegans*. Nevertheless, if we consider that autophagy is primarily an adaptive cellular mechanism, we could reason that the observed mild levels of activation of these genes might only favor a protective autophagic response.

Expression of *nsf-1*, the nematode homologue of N-ethylmaleimide-sensitive factor (NSF), which is a key component of the vesicular fusion machinery on early endosomes (Haas, 1998; Haas and Wickner, 1996), was downregulated in the *uggt-1* mutant (refer to Figure 26 again), in contrast to the upregulation of C33D9.8 and *rab-11.2*, which are presumably involved in vesicle docking (Shen et al., 2005) and vesicle budding (Chen et al., 1998), respectively. Interestingly, *nsf-1* was recently implicated in phagosome maturation during engulfment of apoptotic cells (Kinchen et al., 2008), a function that might also play a role in autophagosome formation and/or maturation, hence be relevant to our necrotic paradigm, in which autophagy contributes to cell death. Impairing or delaying autophagosome formation and/or maturation, could directly interfere with necrosis progression.

In addition, expression of genes involved in host defense (*nlp-28* and *srp-7*), osmotic-stress response (*nlp-28*), and cuticle synthesis (*col-89*) were mildly upregulated in the *uggt-1* mutant background (Figure 26).

Overall, my transcriptional analysis suggests a potential role for general reprogramming of cellular homeostasis in the *uggt-1* mutant background. Interestingly, a picture emerges reminiscent of a preconditioned cellular state where the selective regulation of stress-responsive, pro-survival genes allows for cellular adaptation to chronic or

recurrent insult. Coincidently, ER stress preconditioning has been recently documented and associated with improved resistance to ischemia (Lehotsky et al., 2009).

3.3.11. Knockdown of *uggt-1* by RNAi reduces the number and size of polyglutamine aggregates in a *C. elegans* model for Huntington Disease

Given the role of *uggt-1* in protein folding quality control, I was curious as to its role in neurodgeneration associated with protein aggregation, such as polyglutamine expansion models. When tested in an aggregation-prone model for Huntington Disease (polyQ82 peptide expressed in body wall muscles), knockdown of *uggt-1* activity by RNAi significantly reduced the number of poly-Q aggregates as well as the size of aggregates (Figure 27). Similarly, downregulation of UPR transducers *pek-1*, *ire-1*, and *atf-6* also reduced the number and size of aggregates. Interestingly, such effects are not conferred by *crt-1* RNAi, which might be due to the high concentration of calreticulin or might reflect different mechanisms of action.

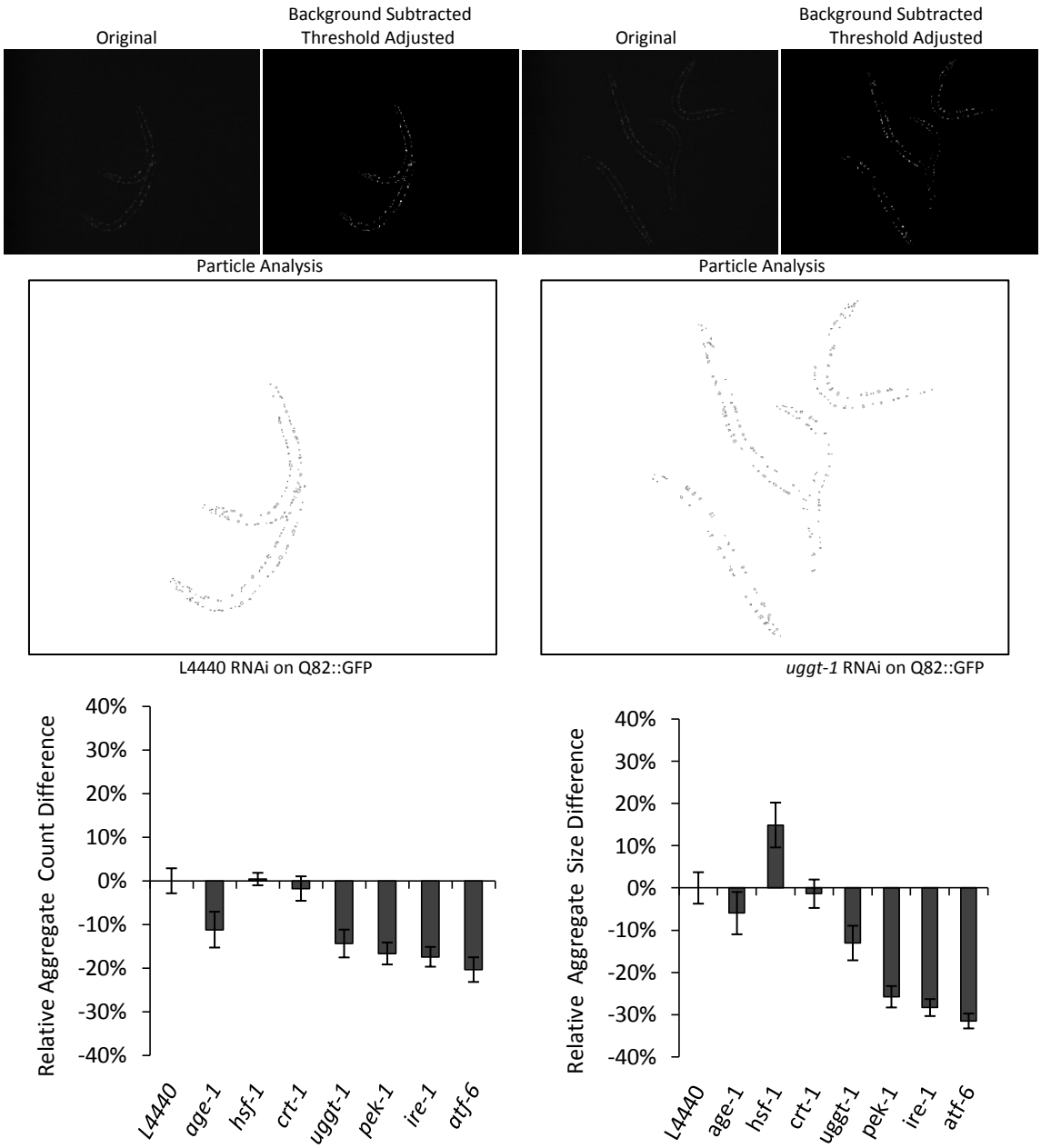

Figure 27. Loss of *uggt-1* and UPR transducers reduces the number and size of polyglutamine aggregates.

Pictures were taken using epifluorescence capabilities installed on Zeiss Axiovert 2 microscope. Number and size of aggregates was quantified using the Particle Analysis capability of NIH ImageJ software (shown in figure: raw, then subtracted background

and adjusted threshold, followed by analysis of particle images). Strains *age-1* and *hsf-1* are used as controls. Fifteen to twenty five pictures were analyzed per category. Error bars represent standard error. Statistical significant differences in aggregate count and size between L4440 control and *uggt-1*, *pek-1*, *ire-1*, and *atf-6* were demonstrated by Student's t-test ($P<0.01$).

3.3.12. Knockdown of *uggt-1* by RNAi partially suppresses paralysis in a *C. elegans* model for Alzheimer's Disease

Downregulation of *uggt-1* message by feeding RNAi on strain CL4176: *smg-1(cc546ts) I; dvIs27[pAF29(myo-3/human Aβ1-42/long3'UTR) + pRF4] X* (which induces Aβ peptide synthesis and aggregation) partially suppressed the paralysis phenotype observed 24 hours after the worms are switched to the non-permissive temperature (Figure 28). Together with the results from previous section 3.3.11, this data suggests that downregulation of *uggt-1* induces a protective response that can suppress detrimental effects of toxic protein aggregates.

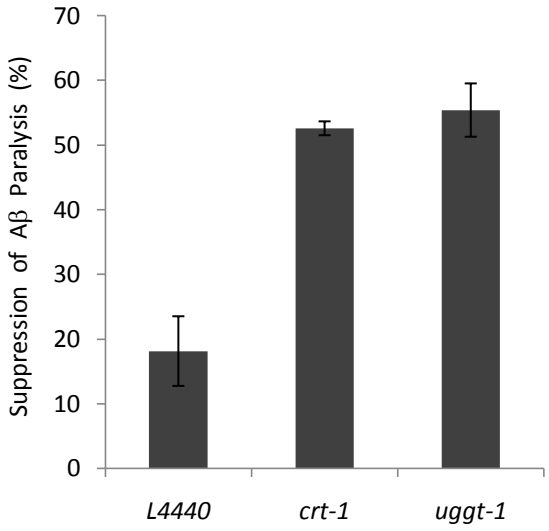

Figure 28. Knockdown expression (by RNAi) of *uggt-1* can suppress Aβ-induced paralysis.

Strain used was CL4176. Error bars represent standard error. Student's t-test used to evaluate statistical significance: P(*crt-1* vs. L4440)= 0.0245 and P(*uggt-1* vs. L4440)= 0.0315. Protocol used for paralysis quantification is described in section 4.2 of this thesis.

3.3.13. Health and life spans are enhanced in partial loss-of-function mutant *uggt-1(bz130)*

Exposure to a variety of mild stressors, including caloric restriction, thermal stress, or hyperbaric oxygen can induce an adaptive cellular and organismal response that increases lifespan in eukaryotes (Gems and Partridge, 2008; Saunders and Verdin, 2009; Westerheide et al., 2009). Recently, several authors described a novel role for ER signaling, via IRE-1 and PERK-1, in aging and dietary restriction-dependent lifespan

extension in *C. elegans* and yeast (Chen et al., 2009; Steffen et al., 2008). It has also been reported that with age, many of the key components of the UPR such as chaperones and enzymes display reduced expression and activity, which results in a dysfunctional ER (Naidoo, 2009a; Naidoo, 2009b). Given that the UPR appears mildly activated in the *uggt-1* mutant backgrounds, I wondered if the lifespan of these strains could consequently be affected.

As noted in Figure 29, healthspan as well as lifespan of the *uggt-1(bz130)* mutant is significantly enhanced compared to control N2 Bristol strain. The *uggt-1(bz146)* mutant, on the other hand, did not show any improvement in the respective measurements. These results suggest that the mildly enhanced levels of UPR activation observed in mutant strain *uggt-1(bz130)* are beneficial to the general well-being of the nematode, while the higher UPR activation levels induced in *uggt-1(bz146)* have probably surpassed the putative beneficial threshold level and, on the contrary, had gotten close to become detrimental. Although it is unlikely that opportunistic mutations other than *uggt-1* could be responsible for this phenotype (because these *uggt-1* strains had been outcrossed four times into the N2 Bristol background), I cannot rule out that possibility until transformation rescue experiments confirm the *uggt-1* role.

Our *uggt-1* mutant lines could represent valuable reagents for further studies aiming to better understand the differential effects of stress responses (the UPR in particular) in the nematode healthspan.

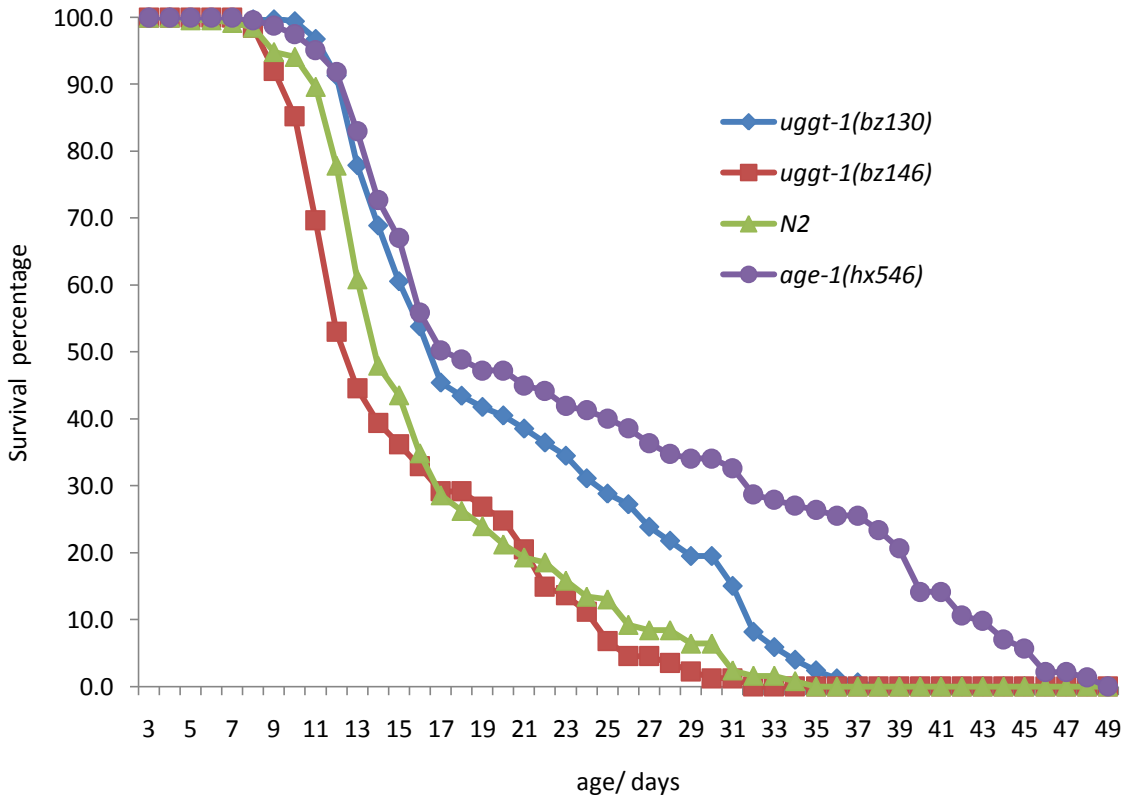

Figure 29. Lifespan is extended in mutant *uggt-1(bz130)*.

Young adult animals grown at 20 °C were followed daily during their respective life spans. About 20-25 young adults were distributed per plate, for a total of 75-100 per experiment. The experiment was repeated twice and an average percentage of surviving animals per day calculated.

3.3.14. Brood size is affected in *uggt-1* mutants

I found that brood size, as measured by the total amount of progeny produced in 6 days, is significantly reduced in both *uggt-1(bz130)* and *uggt-1(bz146)* mutant backgrounds (19% and 26% respectively) compared to wild type N2 Bristol strain (Figure 30). Since the UPR plays an important role during embryonic development, as indicated by the non-viability of UPR mutants in multiple species including C. elegans, this may indicate that the UPR activation levels in both the *uggt-1* mutants is detrimental to embryo development. This is in contrast to the case of mutant *uggt-1(bz130)*, with the beneficial effects on health and life span described in previous section, and may indicate that differential fine-tuning of stress responses play pivotal roles in organismal homeostasis.

Contrasting with these relatively mild effects of uggt-1 mutations on brood size at 20 °C, a highly detrimental effect on fertilization or germline viability was observed at 25 °C, at which temperature only five generations can be produced in the uggt-1 mutant backgrounds. Such detrimental effect is not noticeable at 20 °C. This reinforces the idea of putative threshold stress levels that need not to be surpassed in order to maintain organismal homeostasis and health.

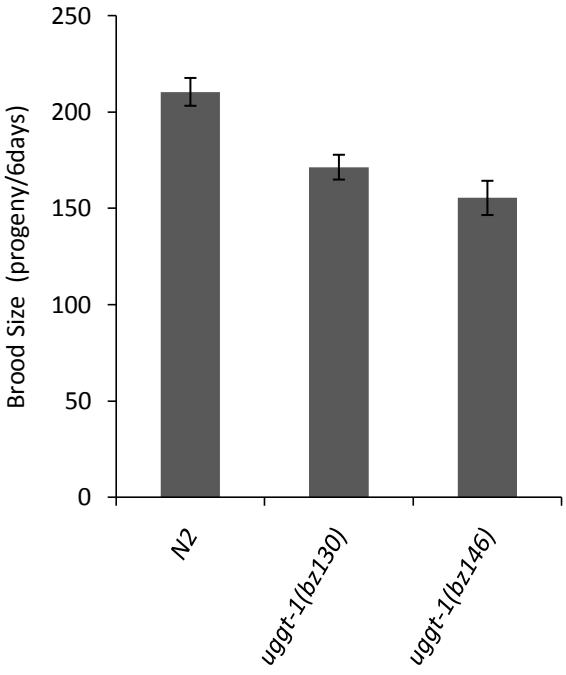

Figure 30. Brood size at 20 °C is reduced in *uggt-1* mutants.

Progeny from 14 isolated animals was scored and averaged for each strain. Significant differences in brood size were detected for both *uggt-1* mutants when compared to N2 strain (Student's t-test P<0.0005). No significant difference between the two uggt-1 alleles. L4-stage animals were transferred to individual plates and the number of progeny produced by each scored over a period of 6 days with daily transfer of the parent. Error bars represent standard error.

3.4. Discussion

My results indicate that *uggt-1* mutations can suppress necrotic cell death in *C. elegans*. The *uggt-1* mutations may induce suppression of necrosis by interfering with the death pathway rather than by affecting localization/trafficking or functionality of MEC-4 and MEC-4(d) channels. Such interference appears to be mediated in part by activation of the unfolded protein response (UPR) and downregulation of endoplasmic reticulum Ca^{2+} release. These results highlight the important contribution of ER homeostasis to cellular health. Interestingly, downregulation of *uggt-1* can counteract multiple degenerative insults, including hyperactivation of DEG/ENaC channels, Aβ toxicity, and aggregation of poly-glutamine containing proteins. Expression profiling experiments suggest that downregulation of *uggt-1* function induces a general reprogramming of cellular homeostasis, which may contribute to making the cells and the organism more resistant to stress.

Specific functions of the *uggt-1* gene in *C. elegans* remain to be determined, but the high sequence homology across kingdoms suggests an important and basic role for this protein in cellular function. Indeed, UDP-glucose:Glycoprotein Glucosyltransferases (UGGTs) have a conserved role in protein folding quality control in many organisms such as plasmodium, yeast, fruit fly, and humans (Guerin and Parodi, 2003; Parodi, 1999; Parodi, 2000; Tessier et al., 2000). This enzyme recognizes sub-optimally folded glycoproteins in the ER and adds a single glucose residue to a terminal mannose of their

asparagine-linked oligosaccharides (which have been previously and sequentially deglucosylated by the action of ER-resident glucosidase I and II in order for the glycoprotein to exit the ER and continue its transport through Golgi). The monoglucosylated glycoproteins serve then as substrate for the ER-resident lectins calnexin and calreticulin, which function as chaperones that help retain such misfolded proteins in the ER until they completely and correctly fold into their more stable conformations.

UGGTs transferase activity localizes to the highly conserved C-terminal region (catalytic domain), which represents about 20% of the protein (Taylor et al., 2004). The less conserved N-terminal region on the other hand, represents about 80% of the protein and is required to activate the catalytic domain and to sense folding defects on the substrates (Arnold and Kaufman, 2003; Taylor et al., 2004). It has been reported that UGGTs recognize clusters of surface-exposed hydrophobic residues that allow the enzyme to sense subtle conformational changes within structurally compact substrates (Caramelo et al., 2003; Ritter and Helenius, 2000; Ritter et al., 2005; Sousa and Parodi, 1995; Taylor et al., 2003; Totani et al., 2009).

Another potential issue to consider is that *C. elegans* UGGT-1, like its yeast relative, could be glycosylating proteins other than suboptimally folded ones (like a regular glycosyltransferase, independently from its folding quality control function) therefore

playing a more direct/specific role in the induction of cell death by directly modifying the structure of proteins involved in the death mechanism. Although such functional glycosylation has only been described for the yeast homolog (not for higher eukaryotes), this possibility should not be overlooked but addressed in future *C. elegans* UGGT-1 research. Most *uggt-1* alleles generated in this screen for suppressors of necrosis encode missense mutations that presumably produce truncated proteins that have lost the putative domains responsible for the enzymatic activity. Allele *bz130* appears to be the least affected, harboring an in frame deletion of 27 amino acids (Figure 10) right after the UDP-glucose:glycoprotein glucosyltransferase domain (the deletion removes the last amino acid of this domain). Even when the putative domains are still present in *bz130*, my suspicion is that the deletion dramatically affects the domain structure and consequently the function of the protein.

An adaptive state associated with *uggt-1* deficiency? In seminal work on cellular adaptation to ER stress, Rutkowski and collaborators showed that adaptation is mediated by activation of all proximal UPR sensors and is determined by the differential stabilities of pro-survival and pro-apoptotic mRNAs and proteins (Rutkowski et al., 2006). They found that despite eliciting UPR activation and ER perturbation, mild ER stress (either pharmacologically or genetically induced) allowed for net growth of cell populations, albeit initially slower, and for induction of resistance to the perturbing effects of mild disruption of protein folding in the ER. Cell survival did not require selective activation of the proximal UPR stress sensors but differential expression of

downstream proteins. Such differential expression was demonstrated to be the consequence of substantially different stabilities of mRNAs and proteins involved in either adaptative or apoptotic responses.

Rutkowski and colleagues also developed a highly relevant and informative *Uggt1*$^{-/-}$ knockout cell line that they used as a genetic paradigm for chronic stress. They demonstrated that in this knockout mouse embryonic fibroblast (MEF) line, the UPR is mildly activated and that these cells are able to adapt to the ER stress burden, mediated by UPR-dependent upregulation of ER chaperones. They found that as in pharmacologically adapted cells, *Uggt-1*$^{-/-}$ cells showed selective up-regulation of pro-survival proteins such as ER chaperones but not pro-apoptotic proteins (Rutkowski et al., 2006). The authors concluded that "while it might have been expected a priori that *Uggt1*$^{-/-}$ cells would be more sensitive to ER stress because of a compromised quality control system, the resistance of these cells is consistent with their having achieved an adapted state that parallels the state achieved in cells adapted to pharmacological stress", and supported a protective role for the upregulation of ER chaperones consequent to exposure to chronic stress.

In our mutant *uggt-1* genetic paradigm, now at the level of organismal physiology, I found evidence for a seemingly protective role for the activation of the UPR. My results show that this overall protective effect in *C. elegans* is partially mediated by two of the

proximal UPR transducers, *pek-1* and *ire-1*, which appear to promote necrosis-suppressing signals, while *atf-6* appears to promote necrosis-inducing ones (loss of *atf-6* function can, by itself, mildly suppress neuronal death in *C. elegans*). Expression profiling experiments indicated that the three UPR transducers were upregulated in the *uggt-1* mutant background, and epistasis analysis showed that there is genetic interaction among *pek-1, ire-1, atf-6,* and *uggt-1*. These results support and highlight an important role for the UPR in this case of necrosis suppression.

Interesting and puzzling is the fact that the effect of the UPR transducers in *C. elegans* necrosis appears to be contrary to their equivalent effects in mammalian apoptosis. For example, in mammalian apoptosis ATF6α is thought to be a main player controlling the transcriptional regulation of BiP, GRP94, calreticulin, and other chaperones, hence portraying a protective effect against stress-induced apoptotic death, while PERK signaling is thought to be the principal driver of CHOP expression, hence the main inducer of apoptosis. As described earlier, in our *mec-4(d)* channel hyperactivation necrosis paradigm, *atf-6* appears to promote necrosis-inducing signals, while *pek-1* appears to transduce death-suppressing ones. Although counterintuitive a priori, this could readily fit a model in which the UPR transducers have evolved opposed capacities to cope with extreme and opposed cellular events, as apoptosis and necrosis are. This would represent logical molecular multi-functionality and cellular economy, since apoptosis and necrosis are counteractive in nature.

An influence of *uggt-1* on intracellular calcium homeostasis? Observation of additional epistatic, necrosis-rescuing effects by upregulation of ER calcium release (induced by gain-of-function mutation in IP_3 receptor channel *itr-1*) in the *uggt-1* mutant background suggests that downregulation of ER calcium release could be another contributor to death-suppression. This idea is further supported by my expression profiling data indicating that both *itr-1* and *unc-68* transcripts are significantly downregulated in the *uggt-1* mutant background. Additional experiments with Ca^{2+}-activated chameleon reporters (Palmer et al., 2004; Rudolf et al., 2003) to profile ER and cytoplasmic Ca^{2+} concentration changes could be conducted in order to directly demonstrate modulation of Ca^{2+} signaling during necrosis induction in the *uggt-1* background.

These results fit well into our current understanding of *C. elegans* necrosis and contribute consolidating insights by bringing together the calpain/cathepsin and the autophagic branches of the death pathway into a congruent mechanism centered on a main event that is the induction of Ca^{2+} release from the endoplasmic reticulum (see proposed working model in Figure 31).

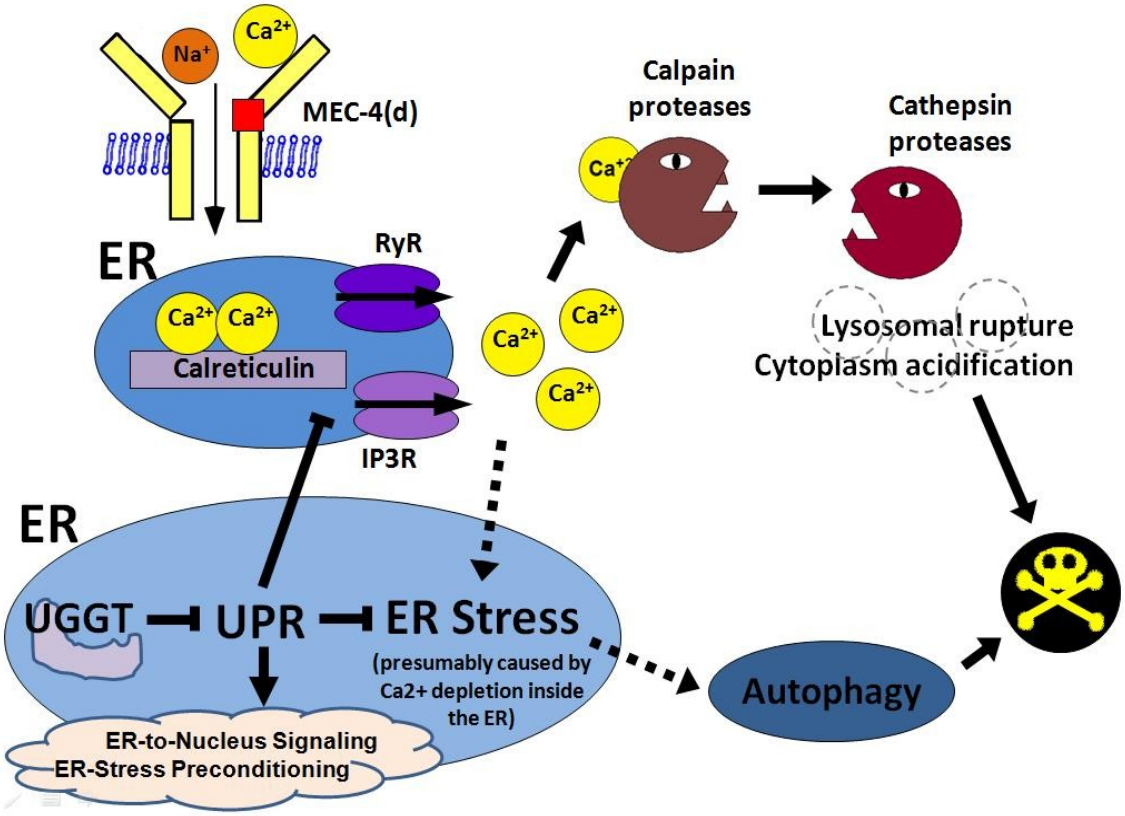

Figure 31. Proposed model of *mec-4(d)*-induced Necrotic Cell Death. See text for details.

It is well known that ER stress occurs under various physiological and pathological conditions (Berridge, 2002; Hoyer-Hansen and Jaattela, 2007; Huang et al., 2006), including those when the ER folding capacity becomes saturated or when too much Ca^{2+} is released across the ER membrane, increasing cytoplasmic Ca^{2+} concentration at the expense of lowering physiological ER Ca^{2+} concentration to levels that render ER chaperones and folding systems non-functional. The latter scenario is relevant to our necrotic model, where Ca^{2+} release from the ER and consequent activation of calpain/cathepsin proteases have been demonstrated (Xu et al., 2001). In addition,

autophagy has recently been implicated as a player in *C. elegans* necrosis (Samara et al., 2008; Toth et al., 2007). Since ER stress is a potent trigger of autophagy (Bernales et al., 2006; Bernales et al., 2007; Criollo et al., 2007; Fujita et al., 2007; Hoyer-Hansen and Jaattela, 2007; Ogata et al., 2006; Yorimitsu et al., 2006), it seems plausible that the initial Ca^{2+} release from the ER, in addition to activating the calpain/cathepsin cascade and lysosomal rupture, also induces ER stress, which consequently triggers autophagy and contributes to the necrotic demise.

It has been reported that during UPR-induced autophagy, ER membranes are selectively sequestered and tightly packed into autophagosomes, which do not fuse with the vacuole (in yeast) until the stress is eliminated (Bernales et al., 2006; Bernales et al., 2007). These observations suggest that sequestration of damaged ER is more important than its eventual degradation (Ron and Walter, 2007). I reason that the whorls observed in ultrastructural studies of necrotic neurons in *C. elegans* (Hall et al., 1997) may well represent ER stress-induced "sequestering" autophagosomes, which would provide additional support for our hypothesis suggesting that ER stress is contributing to necrosis in our model. The fact that *nsf-1*, an ATPase involved in vesicle fusion, is downregulated in the *uggt-1* background fits well into this model. NSF-1 was recently implicated in phagosome maturation during apoptotic corpse engulfment (Kinchen et al., 2008). It is interesting to speculate that *nsf-1* might play a similar role in autophagosome maturation during an autophagic response, which would have high relevance to our necrosis paradigm. Impairing or delaying autophagosome maturation

could directly interfere with necrosis progression while still allowing the formation of "sequestering" autophagosomes.

ER stress preconditioning as a necrosis-suppressing factor? My results suggest that early activation of an intact unfolded protein response can keep ER stress under control by directly maintaining ER homeostasis and interfering with Ca^{2+} release from the ER, hence keeping necrosis signaling under check. My expression profiling study in the *uggt-1* mutant background indicates that selective activation of pro-survival factors and general reprogramming of multiple transcriptional programs occur at the expense of metabolic functions. Recently, Dominguez-Cuevas and coworkers have shown that the induction of stress-related functions in *Pseudomonas putida* was accompanied by the inhibition of motility and repression of enzymes involved in metabolism, which appeared a tradeoff for activating stress tolerance genes at a minimal cost in terms of energy (Dominguez-Cuevas et al., 2006). Overall, the chronic mild activation of the UPR in *uggt-1* mutants and its associated necrosis-suppressing effects are reminiscent of preconditioned cellular states.

Referring to ischemic preconditioning, Dr. Gidday wrote: "The overall implication is that diverse families of pro-survival genes are activated and, in turn, encode proteins that serve to enhance the brain's resistance to ischemia. Protection is achieved by the attenuation of broad categories of injury-inducing mechanisms, including excitotoxicity,

ion/pH imbalance, oxidative and nitrosative stress, metabolic dysfunction, inflammation and, ultimately, necrotic and apoptotic cell death" (Gidday, 2006).

Interestingly, several authors have recently described protective effects of ER stress preconditioning in multiple paradigms (Hayashi et al., 2003; Hung et al., 2003; Inagi et al., 2008; Lehotsky et al., 2009; Peyrou and Cribb, 2007; Zhu et al., 2006). Lehotsky and collaborators, for example, found that higher proteins levels of GRP78 in preischemic animals were associated with improved resistance to ischemia/reperfusion. They also reported that ER stress preconditioning induced remarkable changes in the levels of ATF6 protein, which appear to underlie the neuroprotective effect by attenuating the ER stress response after acute ischemic/reperfusion insult (Lehotsky et al., 2009).

Other authors have reported that manipulations of the PERK/eIF2α subpathway such as pre-emptive phosphorylation of eIF2α (Lu et al., 2004b), selective chemical inhibition of eIF2α dephosphorylation (Boyce et al., 2005), and genetic manipulations that reduce the expression of eIF2α (therefore mimicking its phosphorylation) (Tan et al., 2001) can protect cells against subsequent exposure to ER stress, akin of preconditioning effects. On this same line of thought, Lu and collaborators found that "eIF2α phosphorylation can initiate signaling in a cytoprotective gene expression pathway independently of other parallel stress-induced signals and that activation of this pathway can single-handedly promote a stress-resistant preconditioned state" (Lu et al., 2004b). Tan and

colleagues, on the other hand, found that eIF2α is a "critical regulatory factor in the response of nerve cells to oxidative stress and in the control of the major intracellular antioxidant, GSH, and may play a central role in the many neurodegenerative diseases associated with oxidative stress" (Tan et al., 2001).

Mild UPR activation, as a preconditioning tool, may be relevant to general health and neurodegeneration in particular. As I have shown in this study, small increases in temperature could activate a protective response against neuronal necrosis, at least partially mediated by UPR transducers. Interestingly, epidemiological studies have reported that colder temperatures, as well as temperature changes, are associated with the onset of ischemic stroke, being the risk with temperature change greater in the winter than in summer (Chang et al., 2004; Hong et al., 2003). Although blood viscosity and coagulation may contribute to temperature effects in stroke, the possibility that protective cellular events such as benign, mild activation of the UPR (e.g. during summer time) could be additionally actuating at the cellular level and preconditioning tissues, should not be discarded.

To finish, I would like to call attention to the important implications that partial loss of *uggt-1* function could have in extending the health and life spans of the organism under controlled optimal ambient conditions (as inferred from lifespan experiments described in Figure 29). Such an approach could open new venues while addressing therapeutic

strategies for age-related conditions in general, provided that an appropriate UGGT inhibitor could be developed.

3.5. Summary and Future Prospects

Similar to mammalian excitotoxicity, *mec-4(d)*-dependent neuronal necrosis in *C. elegans* displays strikingly characteristic morphological and molecular events, which includes: increased cation influx, rise in cytoplasmic Ca^{2+} concentration, cell swelling, calpain and cathepsin activation, lysosomal rupture, degradation of cellular contents and eventual cell demise.

Our work in the Driscoll Lab over the last decade has implicated the endoplasmic reticulum as an important source of necrosis-inducing signaling and my more recent discoveries, additionally point towards an important role that the same compartment could play in eliciting a protective response (the UPR), allowing death suppression as a consequence of adaptation to chronic mild stress.

Recent implication of mammalian ASIC1a channels (mammalian homologs of *C. elegans* MEC-4) as main culprits in ischemic neuronal injury (Xiong et al., 2006; Xiong et al., 2004; Yermolaieva et al., 2004) underscores the utility that studies in simpler model organisms could have, and how they can dramatically impact our understanding of more complex biological phenomena. It is likely that our description of this neuroprotective

mechanism in the nematode will have direct relevance into human disease research, guiding new efforts in the development of novel therapeutic strategies that target, for example, partial or total inhibition of this particular UGGT enzyme.

Appendix 3.A. UGGT Sequence Alignment

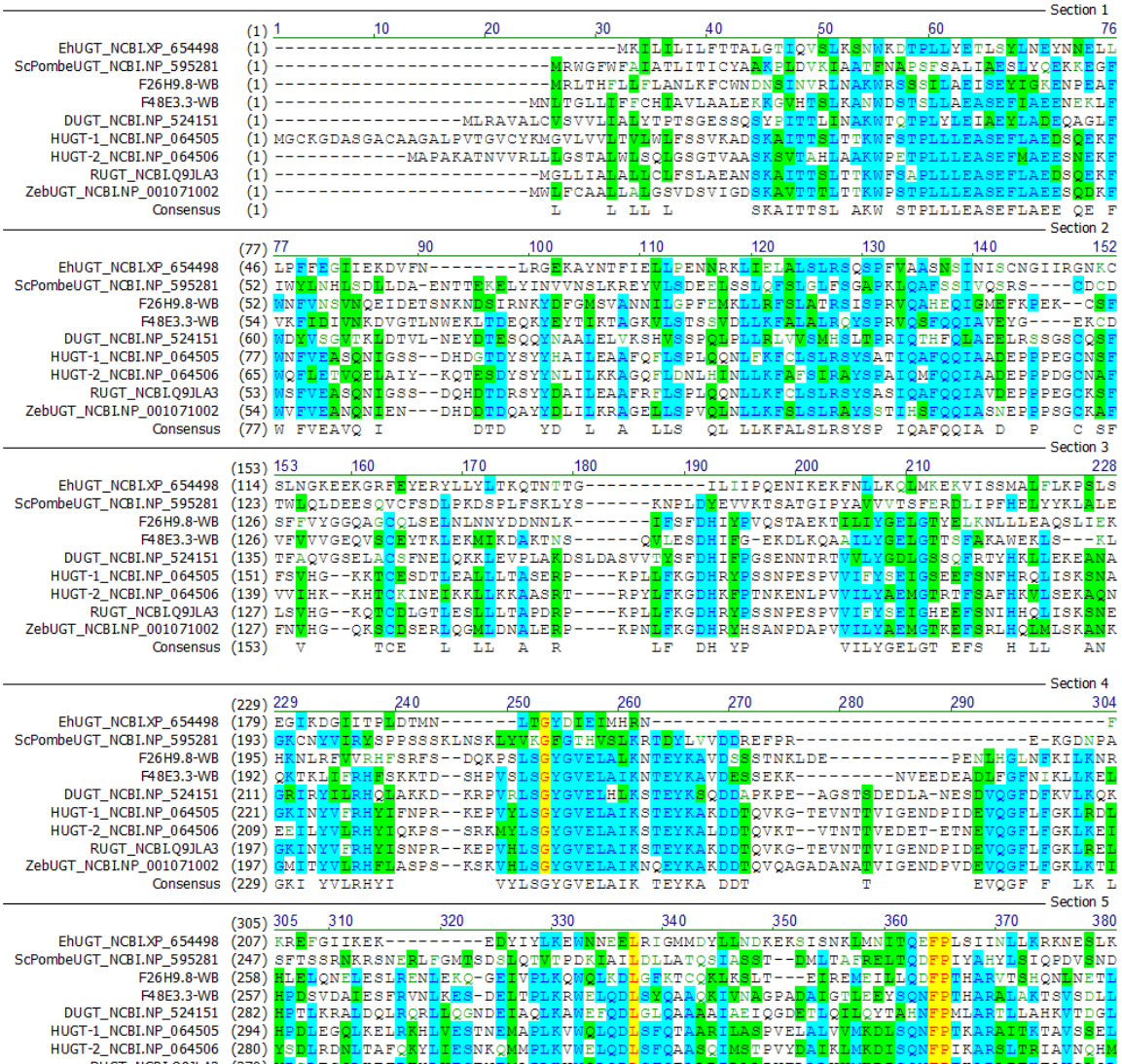


Section 7
Section 8
Section 9
Section 10
Section 11
Section 12
EhUGT_NCBI.XP_654498
ScPombeUGT_NCBI.NP_595281
F26H9.8-WB
F48E3.3-WB
DUGT_NCBI.NP_524151
HUGT-1_NCBI.NP_064505
HUGT-2_NCBI.NP_064506
RUGT_NCBIQ9JLA3
ZebUGT_NCBI.NP_001071002
Consensus

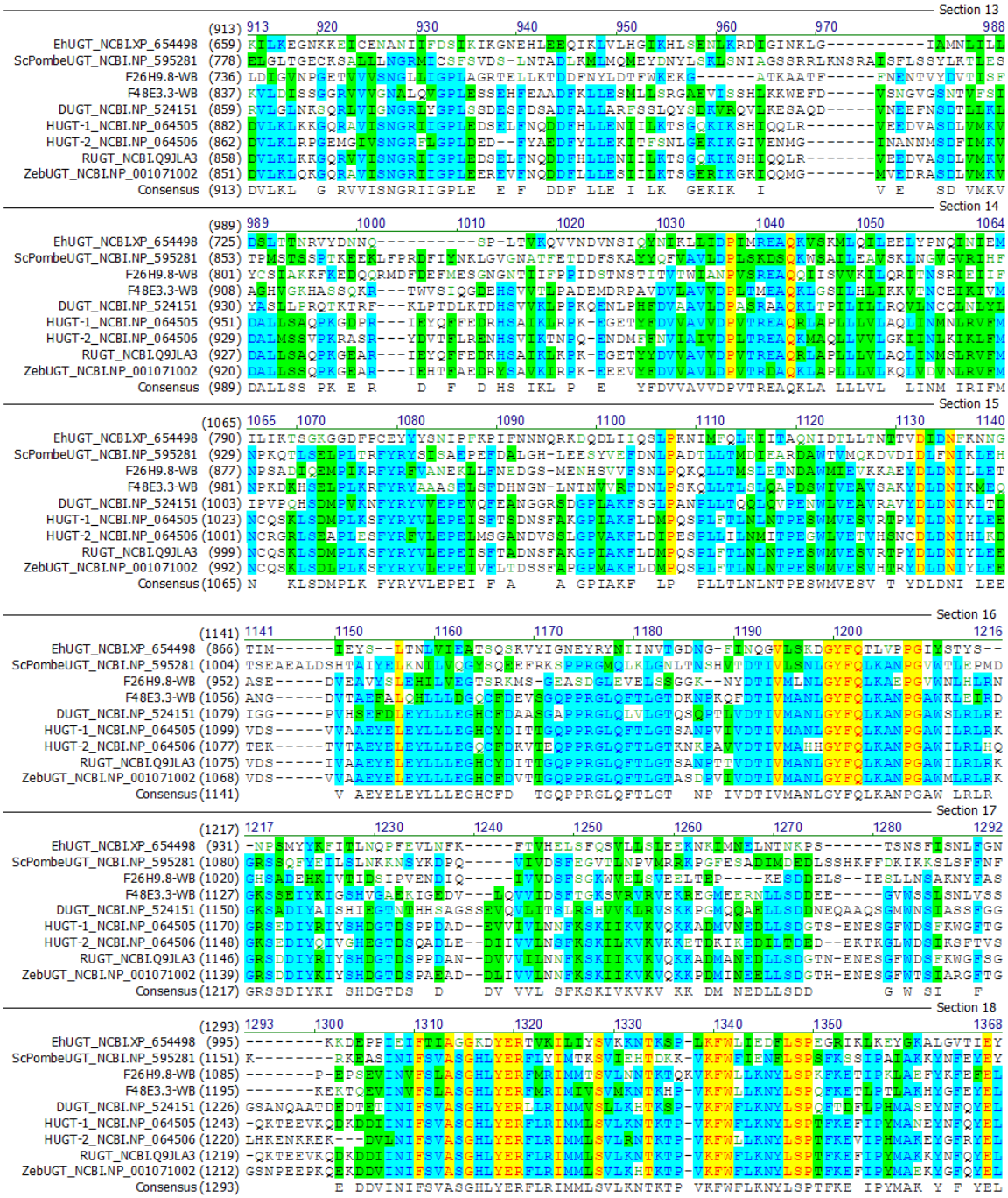
Section 13
Section 14
Section 15
Section 16
Section 17
Section 18
EhUGT_NCBI.XP_654498
ScPombeUGT_NCBI.NP_595281
F26H9.8-WB
F48E3.3-WB
DUGT_NCBI.NP_524151
HUGT-1_NCBI.NP_064505
HUGT-2_NCBI.NP_064506
RUGT_NCBIQ9JLA3
ZebUGT_NCBI.NP_001071002
Consensus

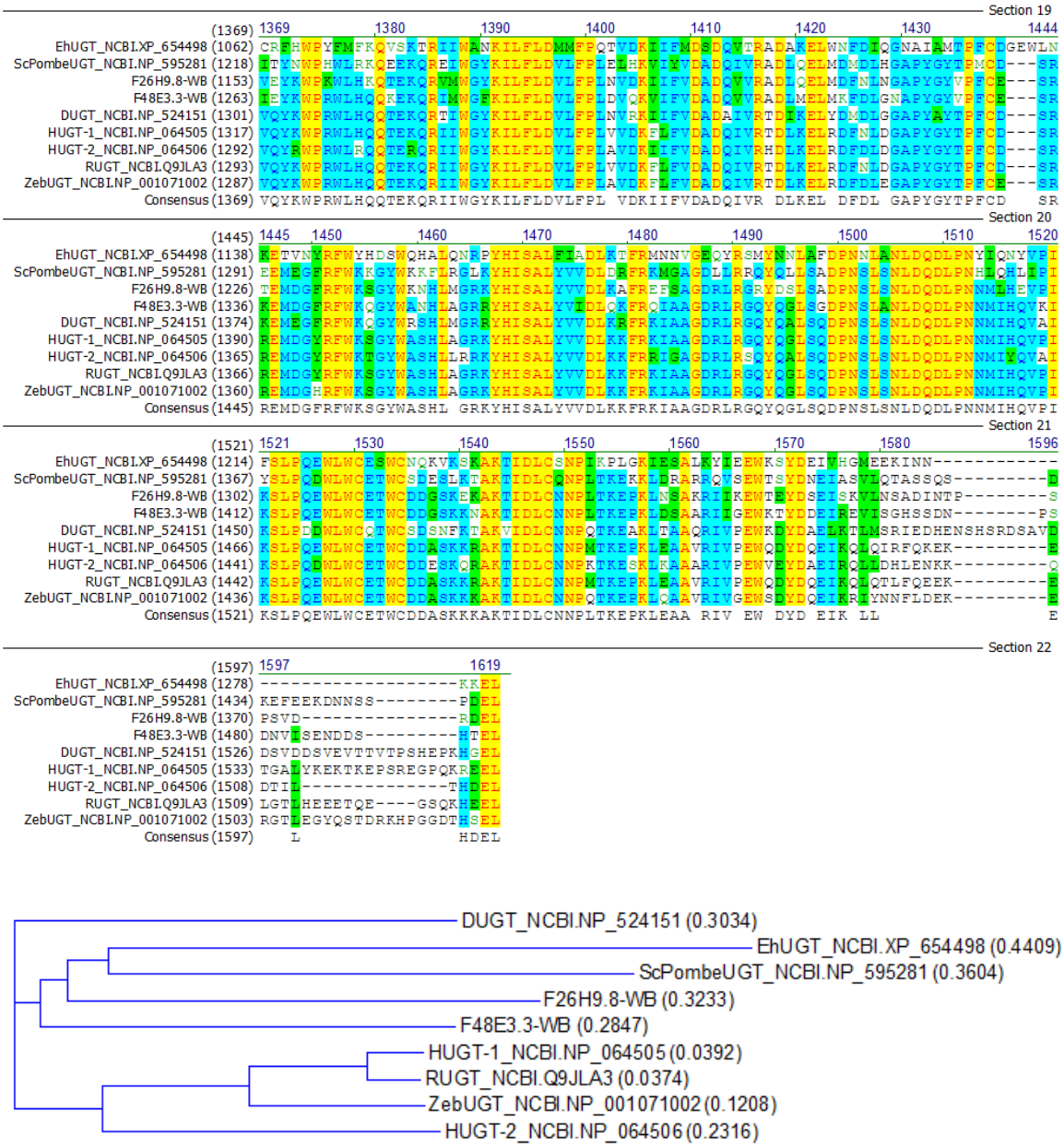

Sequence alignment was performed using AlignX (BLOSUM64 Matrix) from the Vector NTI Suit (Invitrogen, Carlsbad, CA). EhUGT: *Entamoeba hystolitica* UGGT, ScPombeUGT: *Saccharomyses Pombe* UGGT, DUGT: *Drosophila melanogaster* UGGT, HUGT: human UGGT, RUGT: rat UGGT, ZebUGT: *Danio Rerio* UGGT, F48E3.3 and F26H9.8: *C. elegans* UGGTs. Highlighted in yellow with red letters are identical residues; highlighted in blue are conserved residues; and highlighted in green are similar residues.

Appendix 3.B. F48E3.3 *in situ* hybridization pattern - The Nematode Expression Database (NEXTDB 4.0)

Cluster: CELK00454 - Clone : 112d12

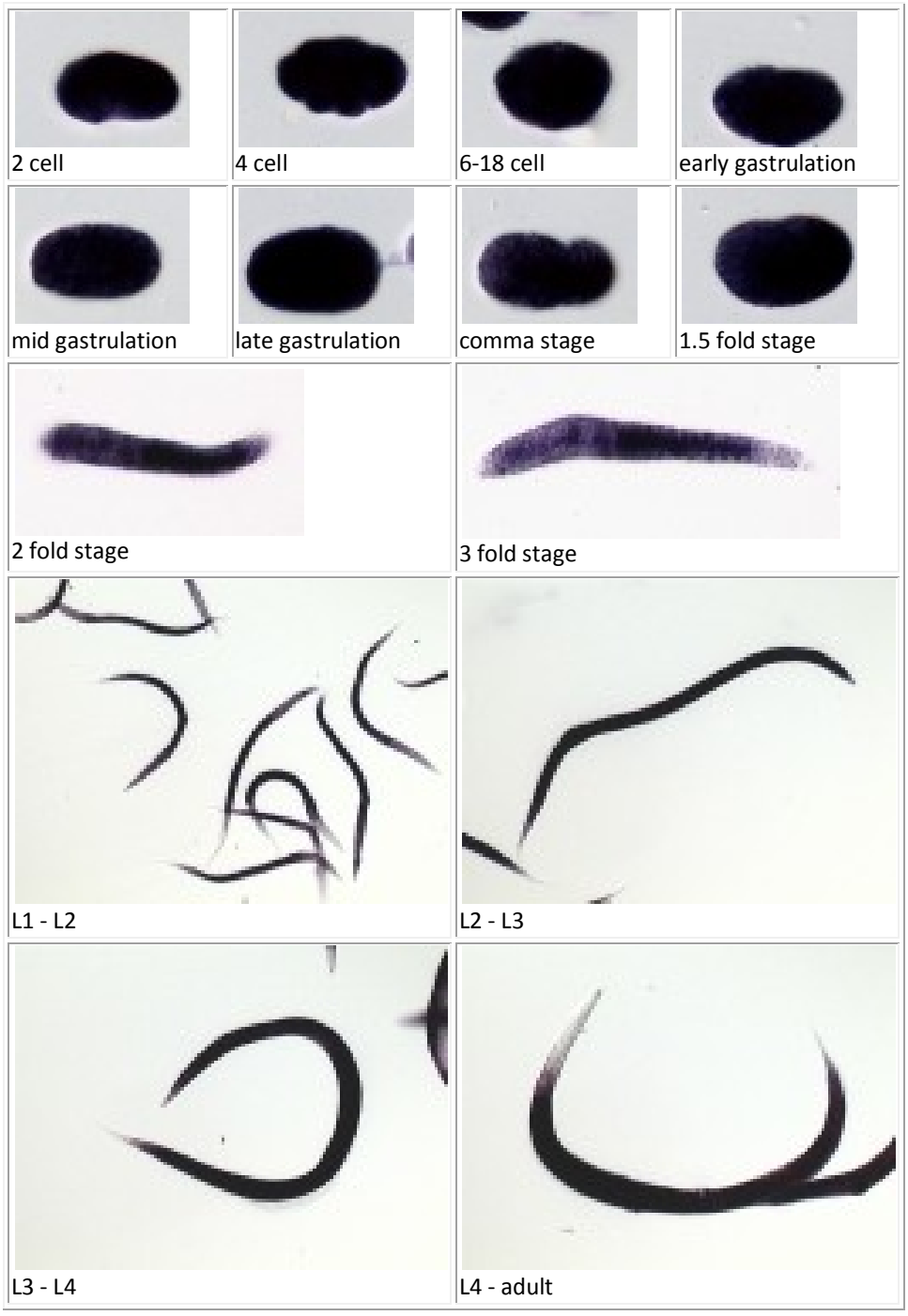

Reproduced with permission of Dr. Yuji Kohara, National Institute of Genetics, Japan

CHAPTER 4. RNAi SCREENING FOR SUPPRESSORS OF Aβ TOXICITY IN A *C. ELEGANS* MODEL ALZHEIMER'S DISEASE

4.1. Background and Significance

I want to start this chapter with a quote from the World Health Organization that highlights the importance of addressing the Alzheimer's Disease problem from all possible angles: "Alzheimer's Disease (AD) is a degenerative brain syndrome characterized by a progressive decline in memory, thinking, comprehension, calculation, language, learning capacity and judgement sufficient to impair personal activities of daily living. The rate of occurrence of AD doubles every five years for those between the 65 and 85 years of age, but if onset were delayed by five years, the number of cases worldwide would be halved. Thus serious attention needs to be paid to the risk factors and preventive measures that may be taken to postpone the onset, if not prevent the appearance of AD" (WHO, 2009).

The Alzheimer's Association (AA) has recently reported in its 2009 AD facts and figures that the number of deaths attributable to AD has been rising dramatically while deaths due to other major causes are decreasing. AD has become the sixth leading cause of all deaths in the United States, and the fifth leading cause of death in Americans 65 years of age and older (Association, 2009). The AA also reports that AD is the most common cause of age-related dementia, accounting for 60-80% of all cases.

The causes of AD are not well understood yet, but most experts agree that AD develops because of the influence of multiple factors rather than a single one. Most efforts in AD research have been focused on the genetic etiology of the disease, but recent epidemiological studies suggest that additional gene-environment interactions contribute to disease causation (WHO, 2009).

4.1.1. Genetics of Alzheimer's Disease

Two key pathological characteristics of AD are that nerve cells in the brain fill up with dense intracellular neurofibrillary tangles composed of hyperphosphorylated tau protein and with extracellular amyloid plaques composed of aggregated amyloid-beta peptide. Although the accumulation and aggregation of Aβ-42 is considered the central event in the pathogenesis of AD (Bu, 2009; Williamson et al., 2009), other important co-pathologies (such as Tau pathologies, diabetes, neuroinflamation, *etc*.) contribute to disease progression. Many of these co-pathologies appear in early phases of the disease, even preceding large-scale amyloidosis (Jakob-Roetne and Jacobsen, 2009).

Three autosomal human genes, mutations in which are dominantly inherited, have been associated with early-onset familial AD (FAD or EOAD): presenilin 1 (PSEN1), presenilin 2 (PSEN2), and amyloid precursor protein (APP), which are essential components of a protein complex responsible for γ-secretase activity (Bu, 2009; Selkoe and Kopan, 2003). γ-secretase is a key enzyme involved in the production of the so-called Aβ peptide,

which is in fact a group of peptides slightly differing in lengths (Jakob-Roetne and Jacobsen, 2009). From these, Aβ-40 (ca. 80 to 90%) and Aβ-42 (ca. 5 to 10%) represent the two major species, and Aβ-42 in particular readily aggregates and forms the seed for larger oligomers and fibrils that eventually produce the macroscopic amyloid plaques (Jakob-Roetne and Jacobsen, 2009). The above-mentioned mutations increase the amount of Aβ-42 at the expense of Aβ-40 peptide, raising the amount of aggregation-prone Aβ-42 peptide to up to 50% of the total Aβ (Citron et al., 1997).

On the other hand, only one gene (apolipoprotein E, APOE) has been confirmed as a major susceptibility/risk factor for late onset AD (LOAD). This type of AD is, however, responsible for the vast majority of AD cases. APOE is a major apolipoprotein and a cholesterol carrier in the brain, and has been shown to bind Aβ in the cerebrospinal fluid (Mahley, 1988; Strittmatter et al., 1993). Identifying additional genes involved in this complex disease has proven challenging, but several other susceptibility genes have been suggested to play a role in LOAD (Bertram et al., 2007; Gatz et al., 2006).

The amyloid hypothesis was introduced in the early 90's, and since then it has shaped the field to a large extent. This hypothesis basically states that the accumulation of amyloid β peptides in the CNS is the primary initiator of the pathogenic cascade of events conducing to AD. This proposal is founded on several lines of evidence including: disease pathology and genetics, cell biology of amyloid β peptides, and the more recent

introduction of transgenic animal models that recapitulate some important aspects of the disease.

There is much dispute in the AD field, however, regarding the key events underlying the disease. Some scientists say that “despite many unexplained aspects, there is a disproportionate amount of attention paid to the amyloid hypothesis that has prevented other ideas from flourishing”. These investigators warn about the need for new movements and new ideas in the field, to avoid focusing exclusively on one theory, which could be particularly imprudent in cases of complex diseases (Mandavilli, 2006).

Although there is a high correlation between amyloid pathology and disease, a major criticism of the amyloid hypothesis is the lack of a quantitative correlation between amyloid plaque load in the CNS and disease severity. Pathologists, for example, distinguish a sequence of five phases of Aβ deposition in the whole brain, yet there is no correlation between the degree of amyloid β-peptide deposition and the severity of dementia, and deposition of Aβ has also been observed in nondemented individuals (Jakob-Roetne and Jacobsen, 2009). As highlighted by Jakob-Roetne and Jacobsen, neuronal swelling occurs long before detectable Aβ deposition, which points to disturbances in axonal transport as potential role player in Aβ deposition. One of three classes of axonal defects distinguishable in AD, is neither spatially associated with amyloid nor with tangles, and shows focal axonal swelling as a result of abnormal

accumulation of axonally transported cargo (Stokin and Goldstein, 2006a; Stokin and Goldstein, 2006b; Stokin et al., 2005). Other hypotheses suggest that oxidative stress, inflammation, long-term response to injury or infection, and defects in normal brain maintenance such as clearance of defective proteins could be among the culprits triggering the disease (Mandavilli, 2006). Amid the criticisms, the Aβ amyloid hypothesis has undergone some revisions and, differently from the initial belief that the plaques were causing the disease, the emphasis is nowadays on oligomers and smaller aggregates of amyloid β proteins (Mandavilli, 2006).

4.1.2. Calcium homeostasis & Alzheimer's Disease

One of calcium's main functions inside the cell is to act as a second messenger to regulate many cellular processes. In neurons, for example, Ca^{2+} is used to control membrane excitability, trigger release of neurotransmitters, mediate activity-dependent changes in gene expression, and modulate growth, differentiation, and programmed cell death (Bezprozvanny and Mattson, 2008).

More than 20 years ago, it was suggested that Ca^{2+} dysregulation might play a role in AD and multiple studies have validated this hypothesis since then (Bezprozvanny and Mattson, 2008; Khachaturian, 1984; Thibault et al., 2007; Thibault et al., 1998). Studies of AD brain samples, for example, have revealed significant alterations in levels of genes and proteins directly involved with Ca^{2+} signaling (Emilsson et al., 2006). Others have

demonstrated that interaction of Aβ oligomers with the plasma membrane (PM) results in elevated cytoplasmic Ca^{2+} concentration and increased susceptibility to neuronal excitotoxicity, possibly due to insertion of the Aβ oligomers into the PM and formation of ion-conducting pores (Demuro et al., 2005; Haass and Selkoe, 2007; Mattson et al., 1992). Aβ can also perturb neuronal Ca^{2+} homeostasis by inducing membrane lipid peroxidation, which results in production of toxic lipid aldehydes that interfere with the functioning of ion-conducting ATPases and glutamate transporters, hence inducing Ca^{2+} overload, synaptic dysfunction, and neuronal degeneration (Mattson, 2004).

More recently, researchers found that a polymorphism in CALHM1 (presumably an essential component of a previously uncharacterized cerebral Ca^{2+} channel) influences Ca^{2+} homeostasis, Aβ levels, and susceptibility to late-onset AD (Dreses-Werringloer et al., 2008). Growing amounts of evidence suggest that Ca^{2+} might be the upstream factor inducing changes during aging and AD, which result in overproduction and aggregation of Aβ and additional alterations that induce differential neuronal vulnerability to degeneration (Bezprozvanny and Mattson, 2008).

4.1.3. *C. elegans* models of Alzheimer's Disease

Transgenic *C. elegans* models of Alzheimer's Disease, which recapitulate relevant disease features, have been engineered in order to exploit experimental approaches not possible or difficult to undertake in mammalian systems. These transgenic models

typically involve tissue-specific or inducible expression of human Aβ peptide (the worm does not produce an equivalent endogenous species) including an artificial signal peptide immediately upstream of the Aβ sequence to allow for secretion of the amyloid fragment and toxic accumulation of extracellular Aβ (Link, 2006).

Several transgenic lines expressing the Aβ minigene in *C. elegans* muscles showed a clear phenotype of progressive paralysis associated with extensive accumulation of Aβ deposits; nevertheless, the detectable Aβ aggregates were found in the muscle cytoplasm and not in the extracellular space, presumably because the Aβ peptide is recognized as an abnormal protein and retrotranslocated by the ER quality control machinery (Fonte et al., 2002; Link, 1995; Link et al., 2001). Notably, there was no consistent correlation between amyloid load and paralysis rates, which suggested that fibrillar amyloid was not the key toxic species (Fay et al., 1998). These models also allowed for the identification of cellular proteins, such as HSP70-related and HSP-16-related proteins, that directly interact with Aβ and could partially suppress Aβ-induced paralysis when overexpressed (Fonte et al., 2002; Link, 2006). Using transgenic lines with inducible expression of Aβ, Link and collaborators were also able to identify gene expression changes associated with the initial stages of Aβ toxicity, which are not detectable in postmortem brain material or in transgenic AD mouse models due to the fact that the assay point may be quite distant from the initial Aβ-dependent insults triggering the pathological cascade (Link et al., 2003).

Although these studies have relied mostly on transgenic worms with muscle-specific expression of Aβ peptide, the authors understand they are relevant to human disease because some human myopathies, such as Inclusion Body Miositis (IBM) for example, are characterized by intramuscular accumulation of Aβ. They also consider that many cell types are sensitive to Aβ accumulation and that "the most parsimonious explanation is that this is due to the same cell toxic mechanism" (Link, 2006). Dr. Link has noted that observations in human samples corroborate some of his findings, such as increased expression of αB-crystallin (a mammalian homolog of HSP-16) in AD brains (Link et al., 2003) and muscle tissue from IBM patients (Banwell and Engel, 2000).

Since a Ca^{2+} hypothesis of AD has recently gained support and attention from the scientific community (Bezprozvanny and Mattson, 2008; Thibault et al., 2007), I conducted an RNAi screen for Ca^{2+}-binding, EF-hand motif-containing suppressors of Aβ-dependent paralysis in *C. elegans*, in an effort to identify additional genes potentially involved in the development of AD.

The rationale for this approach relies in the fact that the Ca^{2+} that flows into the cytoplasm typically becomes bound to Ca^{2+}-binding proteins, which often contain a characteristic helix–loop–helix structural motif called the EF-hand motif (Grabarek, 2006). EF-hand motif-containing proteins can function as Ca^{2+} sensors (transducing signals in response to changes in Ca^{2+} concentration) or as Ca^{2+} buffers (removing

potentially harmful Ca^{2+} ions or helping to store it for subsequent signaling), and have been recognized as key players in all aspect of cellular function. Both sensor and buffering activities of calcium-binding EF-hand proteins could be important modulators of AD progression.

Interestingly, I found a handful of suppressors that on one hand validate this approach (since relevant homologs of human genes already known to play a role in AD were identified) and on the other, suggest interesting new gene interactions that could contribute fresh ideas to the field.

4.2. Materials and Methods

Strain CL4176: *smg-1(cc546ts) I; dvIs27 [pAF29(myo-3/AB1-42-long3'UTR)+pRF4] X*, which induces Aβ peptide synthesis and aggregation when temperature is up-shifted to 23°C or higher during larval stages (*myo-3* promoter expressed during development only), was used.

I used feeding RNAi following standard protocols (Kamath et al., 2001) for screening the EF-hand motif-containing clones available in the Ahringer Library (HGMP Resource Center, Cambridge, UK). EF-hand motif-containing genes were identified and previously reported by Wenying Zhang, a former graduate student in our laboratory (Zhang, 2009).

Gravid adults worms were bleached and eggs aliquoted on RNAi seeded plates (~100 eggs/plate, 3 replicates). Plates were maintained at 15°C for 3 days to generate a synchronized population of L3 larvae, at which time, plates were transferred to a 25°C incubator (non-permissive temperature that induces accumulation of Aβ aggregates in strain CL4176). Worms were maintained at the non-permissive temperature for 24 hours, then scored for suppression of paralysis. The percentage of non-paralyzed worms in each experiment was calculated as the average of at least two replica plate scores.

Paralysis scoring was straightforward, as affected worms cannot move their bodies and lay down in the agar in a straight position (paralyzed worms can move the head slowly and slightly, but the phenotype is self-evident; paralyzed worms do not make eggs either; see Figure 32a). Non-paralyzed worms can be found either sinusoidally moving or rolling, and often assuming a C shape position as they lay down in the agar (due to the presence of the *rol-6* coinjection marker in the transgenic background; see Figure 32b). I should point at here that response of CL4176 to the RNAi testing as performed in this screen on F1 generation exhibited high variance, hence required five repetitions of the screening methodology to attain statistical significance for the majority of the initially detected suppressor clones. RNAi clone for *crt-1* gene was used as positive control for the suppression of paralysis phenotype, while L4440 empty vector was used as negative control. RNAi clone for *bub-1* gene was used for RNAi quality control (*bub-1* knockdown induces sterility).

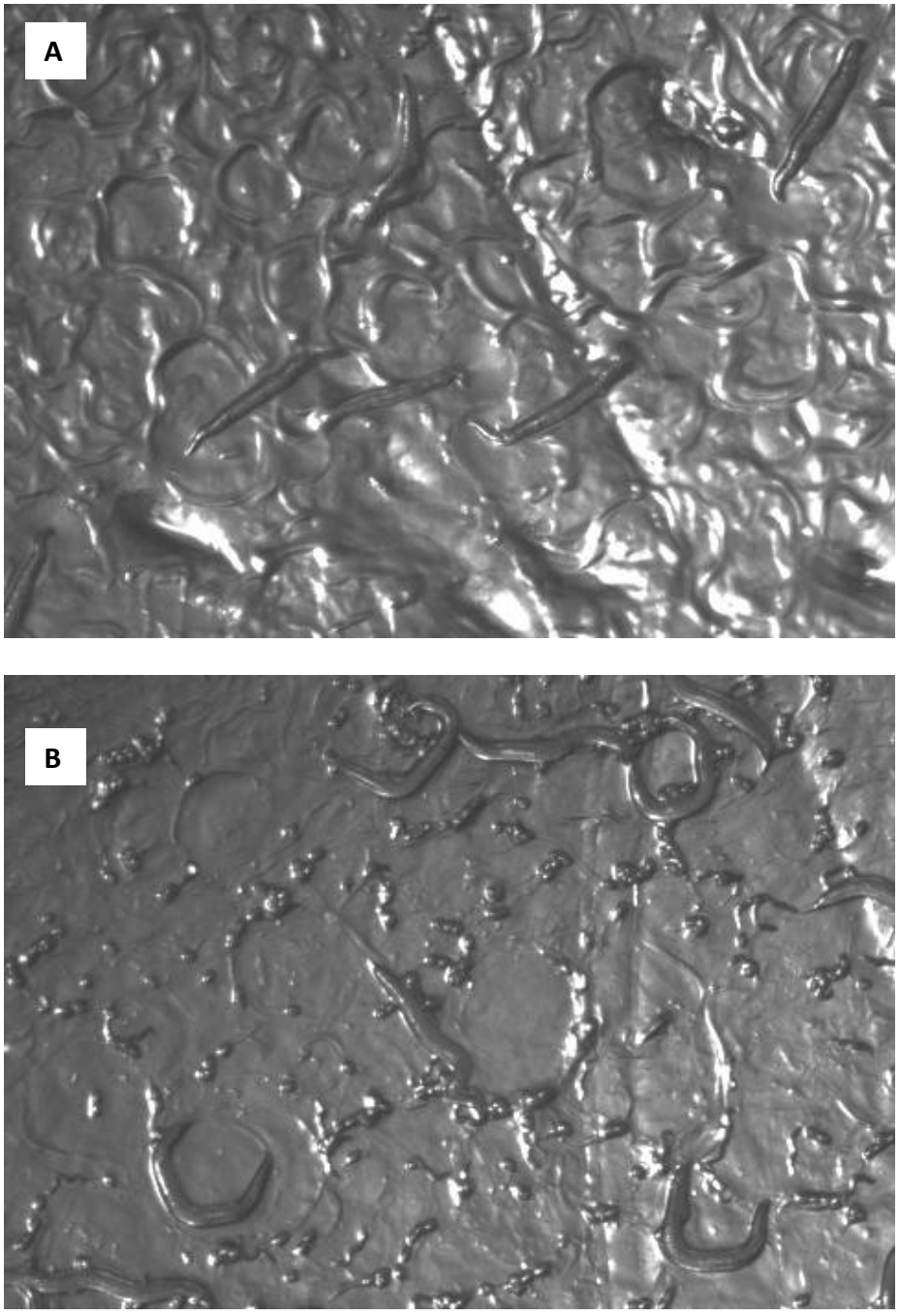

Figure 32. Phenotypes of strain CL4176.

CL4176: *smg-1(cc546ts) I; dvIs27 [pAF29(myo-3/AB1-42-long3'UTR)+pRF4] X* induces paralysis when temperature is up-shifted to 23°C or higher (A). Non-paralyzed worms and laid eggs are shown in (B).

4.3. Results and Discussion

Using strain CL4176: *smg-1(cc546ts) I; dvIs27[pAF29(myo-3/human Aβ1-42/long3'UTR) + pRF4] X*, I tested 129 RNAi clones that target known and putative *C. elegans* EF-hand motif-containing genes for knockdown. I induced RNA interference by feeding L1 larvae on agar plates and scored for suppression of the paralysis phenotype (induced by temperature upshift to the non-permissive temperature 25°C). Out of the 129 RNAi clones tested, 37 were either embryonic lethal or sterile. The 92 scored RNAi clones are listed in Table 9. A caveat of using strain CL4176 for this screening strategy is that suppression of paralysis may simply be caused by reduced transgene expression, e.g. by increasing mRNA surveillance, hence levels of general transgene expression should be monitored in order to determine which suppressor clones are directly interfering with the toxic Aβ pathway.

Ten clones appeared to dramatically suppress the Aβ-induced paralysis phenotype, but only six of them achieved statistical significance after five trials ($P<0.05$, Figure 33, Table 9). Those six genes were *ncs-3* (which codes for a muscular calcium sensor with neuronal paralogs), *tag-312* (which codes for a homolog of human Rab45), ORF C16H3.1 (which codes for a potassium channel interacting protein), *cna-1* (which is the worm homolog of phosphatase Calcineurin A), *letm-1* (which codes for a mitochondrial K^+/H^+ antiporter), and ORF T09B4.4 (which codes for a calmodulin-like protein). Since the t-Test calculations generated P values that decreased with each additional trial

considered (due to the incremental sample size effect), I believe the 4 clones that did not achieved statistical significance after five trials, might well achieve significance provided that enough additional trials are conducted to account for the high variance of the phenotype as assayed. For this reason, I included them and respective relevant information in Table 9.

Table 9. EF-hand motif-containing RNAi clones scored in the screen for suppressors of Aβ-induced paralysis.

EF #	gene name	EF #	gene name	EF #	gene name	EF #	gene name
1	**T03F1.11**	39	**R08F11.1**	76	**B0511.1**	121	**Y45F10A.6**
5	**F30A10.1**	41	**ZK856.8**	77	**F25H2.2**	122	**Y37A1B.1a**
7	**F10G8.5**	44	**T04F3.2**	78	**W02B9.1**	124	**C47A4.3**
8	**B0511.1**	46	**C13C12.1**	82	**T02G5.2**	125	**B0348.4**
11	**F23F1.2**	47	**E02A10.3**	83	**B0252.3b**	126	**K04F1.10**
12	**W09G10.3**	48	**C56A3.6**	84	**DH11.1**	127	**C03A7.13**
13	**F19B10.1**	50	**T09F5.10**	85	**F52H3.6**	128	**C09H5.7**
14	**F12A10.5**	51	**C44C1.3**	86	**ZK938.1**	129	**F25B3.4**
15	**F56D1.6**	52	**K03E6.3**	87	**C47D12.1**	130	**F40F9.8**
16	**C56C10.9**	54	**C33D12.6**	88	**F58G1.3**	131	**F58E6.1**
18	**T09A5.1**	55	**F43C9.2**	89	**Y48B6A.6a**	133	**W04D2.1**
19	**C18E9.1**	57	**K03A1.4**	90	**K10F12.3b**	134	**T10G3.5**
23	**C50C3.5**	58	**C47C12.4**	92	**C34C12.3**	135	**F53F4.14**
24	**C50C3.2**	59	**F16F9.3**	93	**F09F7.2**	136	**F58G11.1**
25	**F54G8.2**	60	**B0563.7**	99	**R13A5.11**	137	**F23B12.7**
26	**C07A9.5**	61	**F21A10.1**	100	**ZK686.2**	138	**F23B12.1**
27	**Y43F4B.1**	64	**C06G1.5**	101	**C48B4.2**	139	**Y40H4A.2**
31	**R05G6.8**	65	**C16H3.1**	102	**R10E11.6**	140	**Y75B12B.6**
32	**T07G12.1**	68	**T03F1.5**	103	**T16G12.7**	145	**K03A1.2**
33	**F13G11.2**	70	**T09B4.4**	107	**K08E3.3**	146	**F31B12.1**
34	**Y116A8C.36**	71	**F26B1.5**	113	**F42G8.8**	147	**T04F8.6**
35	**C54E10.2**	72	**K07G5.4**	117	**C02F4.2a**	148	**C04B4.2**
36	**F53F8.1**	75	**C25A1.9**	118	**Y69E1A.4**	149	**F11C7.4**

Clone EF-117, which knocks-down expression of *cna-1* (the *C. elegans* homolog of Calcineurin A), significantly suppressed Aβ-dependent paralysis in the worm, and serves as a validation point for my screening strategy. Calcineurin A has been widely reported to play an important role in the pathogenesis of Alzheimer's Disease as well as other Ca^{2+}-dependent disorders, presumably mediated by a role in astrogliosis (astrocyte activation) and brain neuroinflammation (Norris et al., 2005), as well as in activation of a calpain-calcineurin cascade that increases phosphatase activity and promotes caspase-mediated neuronal cell death (Wu et al., 2007). The fact that 9 out of the 10 suppressors of Aβ toxicity have human homologs additionally underscores the potential usefulness of the *C. elegans* model.

Clones EF-52, which targets *ncs-3* (a muscle-expressed paralog of neuronal Ca^{2+} sensors *ncs-1* and *ncs-2*, homologs of human NCS-1), and EF-65, which targets ORF C16H3.1 (a homolog of human Kv channel interacting protein 2, KChIP2) are two seemingly related novel suppressors discovered by this screen. Both genes products belong to the recoverin/frequenin protein family, which has been implicated in regulation of neuro-transmission by interacting with and modulating the activity of Kv ion channels (Guo et al., 2002; Patel et al., 2002; Ren et al., 2003; Zhang et al., 2003). K^+ channels has been implicated with normal and pathophysiological functions and various members of the family are recognized as potential therapeutic targets in the treatment of Alzheimer's disease, Parkinson's disease, multiple sclerosis, epilepsy, stroke, brain tumors, ischemia, pain and schizophrenia, migraine, *etc*. (Choi and Abbott, 2007; Etcheberrigaray et al.,

1993; Judge et al., 2007; Waters et al., 2006). In addition, interaction of human NCS-1 with IP3R channels (which increases Ca^{2+} release through the latter) has been reported an essential component of the pathological mechanism of bipolar disorder (Koh et al., 2003; Schlecker et al., 2006). The potential dual role in modulating K^{+} as well as IP3R channels makes these members of the recoverin/frequenin family interesting candidates as potential therapeutic targets, provided that their involvement in AD could be confirmed in mammalian models.

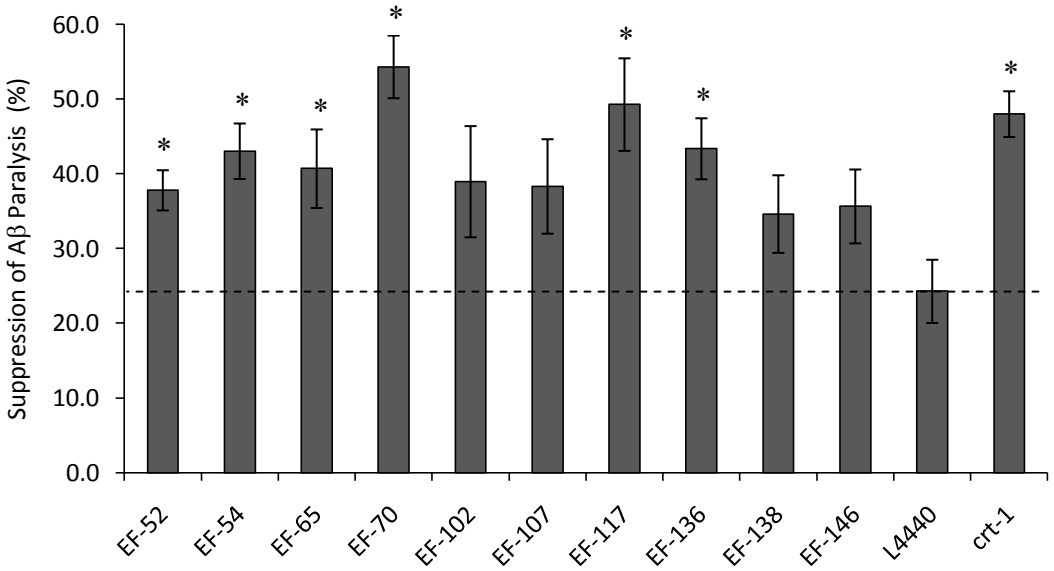

Figure 33. Knockdown expression (by RNAi) of selected EF-hand proteins can suppress Aβ-induced paralysis in strain CL4176.

Error bars represent standard error. Statistical significance as calculated by t-Test are: P(EF52 vs. L4440)= 0.0305, P(EF54 vs. L4440)= 0.0099, P(EF65 vs. L4440)= 0.0359, P(EF70 vs. L4440)= 0.0007, P(EF102 vs. L4440)= 0.1065, P(EF107 vs. L4440)= 0.0895, P(EF117 vs. L4440)= 0.0075, P(EF136 vs. L4440)= 0.0108, P(EF138 vs. L4440)= 0.1527, P(EF146 vs. L4440)= 0.1128.

Table 10. RNAi clones identified as suppressors of Aβ-induced paralysis

RNAi Clone	Human homolog	Notes on function
* EF-52 (*ncs-3*)	**Neuronal Ca^{2+} Sensor (NCS-1)**	Possibly regulates **IP3R** by interacting w/ phosphatidyl-inositol-4OH kinase. **IP3R/NCS-1** is essential to pathomechanism of Bipolar Disorder. Recoverin family interact with & modulates **Kv channels**.
* EF-54 (*tag-312*)	Rab45	Possibly involved in **membrane trafficking**
* EF-65 (*C16H3.1*)	**KChIP2**	**Kv channel** interacting protein. Belongs to Recoverin/frequenin family (like NCS-1)
* EF-70 (*T09B4.4*)	CALML4	Calmodulin like protein, only reported to be upregulated in mammalian tissue during chondrogenesis (cartilage development)
* EF-117 (*cna-1*)	**Calcineurin A**	Widely reported, important role in pathogenesis of Ca^{2+}-dependent disorders such as hypertension, heart disease, diabetes, cerebral ischemia, and Alzheimer's Disease.
* EF-136 (*letm-1*)	LETM1	LETM-1 is deleted in Wolf-Hischorn Syndrome and involved in mitochondrial volume regulation. Its downregulation causes **necrosis** in mammalian cells.
EF-102 (*R10E11.6*)	AP1γ-binding protein 1	Possibly involved in **vesicle trafficking**. R10E11.6 share operon w/ vha-1 & vha-2 (vacuolar proton translocating ATPases) and may be required for **lysosomal biogenesis**.
EF-107 (*toca-2*)	Cdc42 interacting protein 4 (CIP4)	TOCA-2 was found to interact with Huntingtin in Y2H screen. Thereafter, mammalian homolog was also found to interact with Huntingtin and to be overexpressed in HD brain striatum. CIP4 knockdown impaired **endocytosis**. Coupling of actin cytoskeleton reorganization & membrane deformation.
EF-146 (*plc-1*)	Phospholipase C epsilon (PLC-ε)	PLC-1 acts through ITR (*C. elegans* **IP3R**). PLC activation involved in **necrosis** induced by ischemia reperfusion stress. PLC-ε links the production of second messengers & small GTPases.
EF-138 (*F23B12.1*)	none	**Calcineurin-like**, serine/threonine protein phosphatase

* Statistical significance level $P<0.05$

Another interesting set of suppressors are EF-54 (which targets *tag-312*, a homolog of human Rab45), EF-102 (which targets ORF R10E11.6, a homolg of human AP1γ-binding protein 1, aka γ-synergin), and EF-107 (which targets toca-2, a homolog of human Cdc42-interacting protein 4), which have a common connection to membrane and vesicle trafficking, and endocytosis (Fernandez-Chacon et al., 2000; Mills et al., 2003; Shintani et al., 2007; Tsujita et al., 2006). Interestingly, TOCA-2 was found to interact with Huntingtin in a *C. elegans* yeast-two-hybrid screen and subsequently found overexpressed in brain tissue from Huntington's Disease (HD) patients (Holbert et al., 2003). These observations implicating vesicle trafficking and endocytosis in Aβ toxicity in *C. elegans* support the developing idea that AD could be closely associated with the entire endocytotic system, and that different stages of the system might play differential roles in the processing of the toxic Aβ peptide (Zhang, 2008). On the other hand, these observations are also in agreement with recent reports discussed in section 4.1.1, which implicate axonal cargo transport as an important contributor to AD (Jakob-Roetne and Jacobsen, 2009). RNAi clone EF-146, targeting *plc-1* (a homolog of human Phospholipase C epsilon, PLC-ε) could also belong to this same class of Aβ-toxicity suppressors, since PLC-ε links the production of second messengers and small GTPases, both of which events have particular importance to membrane trafficking and intracellular transport (Bunney et al., 2009; Bunney and Katan, 2006).

Clone EF-70, targeting ORF T09B4.4 (a homolog of human CALML4) may represent a muscle specific gene, since the human homolog has only been reported to be

upregulated in mammalian tissue during chondrogenesis (Chen et al., 2005a). Although this may not be relevant to neuronal AD, this observation might contribute to the study of human myopathies caused by β-amyloid depositions.

Suppression of Aβ-toxicity by clone EF-136, which targets *letm-1* (a homolog of human LETM1), came as a surprise since the human homolog is described to induce necrotic-like cell death when downregulated, and a similar phenomenon was observed by Wenying Zhang, a former graduate student in our laboratory, while conducting an RNAi screen for enhancers of *mec-10(d)*-induced necrosis in *C. elegans*. LETM1 is an evolutionary conserved mitochondrial protein involved in mitochondrial volume regulation in *C. elegans* and mammalian cells (Hasegawa and van der Bliek, 2007; Schlickum et al., 2004). The LETM1 gene is deleted in Wolf-Hirschhorn syndrome and downregulation of its expression leads to fragmentation of the mitochondrial network and activation of a caspase-independent type of cell death. LETM1 appears to work as a K^+/H^+ antiporter and, like its yeast ortholog Mdm38p, plays a role in the regulation of the expulsion of K^+ from the mitochondrial matrix (Dimmer et al., 2008; Nowikovsky et al., 2004). Although intriguing in this case (since induction of necrosis by LETM1 downregulation would rather be expected to enhance Aβ toxicity), the connection with K^+ homeostasis/signaling could be a recurrent theme relevant to suppression of Aβ toxicity (as suggested also in the case of RNAi clones EF-52 and EF-65).

Clone EF-138, targeting F23B12.1 (a gene coding for a calcineurin-like phosphatase) is of uncertain relevance at this time point since there is no human homolog and its significance level was the lowest of the group. However, this gene might modulate some phosphorylation event critical for toxicity; hence identifying such event will be advisable.

Future follow up of positive RNAi clones should address mutant availability at CGC and KO centers to analyze phenotype in real mutant backgrounds and conduct epistasis analysis (deletions alleles are available for *tag-312*, *can-1*, *letm-1*, R10E11.6, *toca-2*, and *plc-1*), and to test the effects of gene downregulation in other models of aggregation-dependent degeneration (e.g. PolyQ strains). I also want to comment on the fact that this screen was not designed to detect genes that enhance Aβ toxicity when downregulated, which would represent another informative group of paralysis modulators. Such a screen for paralysis enhancers could be readily implemented simply by shortening the time during which the CL4176 worms are exposed to the non-permissive temperature and screening for RNAi clones that increase the number of paralyzed animals. Additional experiments with Ca^{2+}-activated chameleon reporters to profile Ca^{2+} concentration changes (Palmer et al., 2004; Rudolf et al., 2003) could be informative while evaluating the potential of Ca^{2+} signaling modulation during Aβ toxicity. Another yet very interesting approach would be the examination of postmortem brain samples from AD patients, in an effort to determine whether any of the novel genes suggested by this screen are overexpressed in humans with the disease.

REFERENCES

Adams, C.M., Snyder, P.M., Price, M.P. and Welsh, M.J. (1998) Protons activate brain Na+ channel 1 by inducing a conformational change that exposes a residue associated with neurodegeneration. *J Biol Chem*, **273**, 30204-30207.

Arico, S., Petiot, A., Bauvy, C., Dubbelhuis, P.F., Meijer, A.J., Codogno, P. and Ogier-Denis, E. (2001) The tumor suppressor PTEN positively regulates macroautophagy by inhibiting the phosphatidylinositol 3-kinase/protein kinase B pathway. *J Biol Chem*, **276**, 35243-35246.

Arnold, S.M. and Kaufman, R.J. (2003) The noncatalytic portion of human UDP-glucose: glycoprotein glucosyltransferase I confers UDP-glucose binding and transferase function to the catalytic domain. *J Biol Chem*, **278**, 43320-43328.

Artal-Sanz, M., Samara, C., Syntichaki, P. and Tavernarakis, N. (2006) Lysosomal biogenesis and function is critical for necrotic cell death in Caenorhabditis elegans. *J Cell Biol*, **173**, 231-239.

Association, A.s. (2009) 2009 Alzheimer's disease facts and figures. *Alzheimers Dement*, **5**, 234-270.

Banwell, B.L. and Engel, A.G. (2000) AlphaB-crystallin immunolocalization yields new insights into inclusion body myositis. *Neurology*, **54**, 1033-1041.

Bargmann, C.I. (2001) High-throughput reverse genetics: RNAi screens in Caenorhabditis elegans. *Genome Biol*, **2**, REVIEWS1005.

Barkla, D.H. and Gibson, P.R. (1999) The fate of epithelial cells in the human large intestine. *Pathology*, **31**, 230-238.

Berger, A.J., Hart, A.C. and Kaplan, J.M. (1998) G alphas-induced neurodegeneration in Caenorhabditis elegans. *J Neurosci*, **18**, 2871-2880.

Bernales, S., McDonald, K.L. and Walter, P. (2006) Autophagy counterbalances endoplasmic reticulum expansion during the unfolded protein response. *PLoS Biol*, **4**, e423.

Bernales, S., Schuck, S. and Walter, P. (2007) ER-phagy: selective autophagy of the endoplasmic reticulum. *Autophagy*, **3**, 285-287.

Berridge, M.J. (2002) The endoplasmic reticulum: a multifunctional signaling organelle. *Cell Calcium*, **32**, 235-249.

Bertolotti, A., Zhang, Y., Hendershot, L.M., Harding, H.P. and Ron, D. (2000) Dynamic interaction of BiP and ER stress transducers in the unfolded-protein response. *Nat Cell Biol*, **2**, 326-332.

Bertram, L., McQueen, M.B., Mullin, K., Blacker, D. and Tanzi, R.E. (2007) Systematic meta-analyses of Alzheimer disease genetic association studies: the AlzGene database. *Nat Genet*, **39**, 17-23.

Beutler, B., Du, X. and Xia, Y. (2007) Precis on forward genetics in mice. *Nat Immunol*, **8**, 659-664.

Bezprozvanny, I. and Mattson, M.P. (2008) Neuronal calcium mishandling and the pathogenesis of Alzheimer's disease. *Trends Neurosci*, **31**, 454-463.

Bianchi, L., Gerstbrein, B., Frokjaer-Jensen, C., Royal, D.C., Mukherjee, G., Royal, M.A., Xue, J., Schafer, W.R. and Driscoll, M. (2004a) The neurotoxic MEC-4(d) DEG/ENaC sodium channel conducts calcium: implications for necrosis initiation. **7**, 1337-1344.

Bianchi, L., Gerstbrein, B., Frokjaer-Jensen, C., Royal, D.C., Mukherjee, G., Royal, M.A., Xue, J., Schafer, W.R. and Driscoll, M. (2004b) The neurotoxic MEC-4(d) DEG/ENaC sodium channel conducts calcium: implications for necrosis initiation. *Nat Neurosci*, **7**, 1337-1344.

Boya, P., Cohen, I., Zamzami, N., Vieira, H.L. and Kroemer, G. (2002) Endoplasmic reticulum stress-induced cell death requires mitochondrial membrane permeabilization. *Cell Death Differ*, **9**, 465-467.

Boyce, M., Bryant, K.F., Jousse, C., Long, K., Harding, H.P., Scheuner, D., Kaufman, R.J., Ma, D., Coen, D.M., Ron, D. and Yuan, J. (2005) A selective inhibitor of eIF2alpha dephosphorylation protects cells from ER stress. *Science*, **307**, 935-939.

Bredesen, D.E. (2008) Programmed cell death mechanisms in neurological disease. *Curr Mol Med*, **8**, 173-186.

Brenner, S. (1974) The genetics of Caenorhabditis elegans. *Genetics*, **77**, 71-94.

Bu, G. (2009) Apolipoprotein E and its receptors in Alzheimer's disease: pathways, pathogenesis and therapy. *Nat Rev Neurosci*, **10**, 333-344.

Bunney, T.D., Baxendale, R.W. and Katan, M. (2009) Regulatory links between PLC enzymes and Ras superfamily GTPases: signalling via PLCepsilon. *Adv Enzyme Regul*, **49**, 54-58.

Bunney, T.D. and Katan, M. (2006) Phospholipase C epsilon: linking second messengers and small GTPases. *Trends Cell Biol*, **16**, 640-648.

Cabral, C.M., Liu, Y., Moremen, K.W. and Sifers, R.N. (2002) Organizational diversity among distinct glycoprotein endoplasmic reticulum-associated degradation programs. *Mol Biol Cell*, **13**, 2639-2650.

Caldwell, G.A., Cao, S., Sexton, E.G., Gelwix, C.C., Bevel, J.P. and Caldwell, K.A. (2003) Suppression of polyglutamine-induced protein aggregation in Caenorhabditis elegans by torsin proteins

10.1093/hmg/ddg027. *Hum. Mol. Genet.*, **12**, 307-319.

Caramelo, J.J., Castro, O.A., Alonso, L.G., De Prat-Gay, G. and Parodi, A.J. (2003) UDP-Glc:glycoprotein glucosyltransferase recognizes structured and solvent accessible hydrophobic patches in molten globule-like folding intermediates. *Proc Natl Acad Sci U S A*, **100**, 86-91.

Caramelo, J.J., Castro, O.A., de Prat-Gay, G. and Parodi, A.J. (2004) The endoplasmic reticulum glucosyltransferase recognizes nearly native glycoprotein folding intermediates. *J Biol Chem*, **279**, 46280-46285.

Chalfie, M. and Wolinsky, E. (1990) The identification and suppression of inherited neurodegeneration in Caenorhabditis elegans. *Nature*, **345**, 410-416.

Chang, C.L., Shipley, M., Marmot, M. and Poulter, N. (2004) Lower ambient temperature was associated with an increased risk of hospitalization for stroke and acute myocardial infarction in young women. *J Clin Epidemiol*, **57**, 749-757.

Chautan, M., Chazal, G., Cecconi, F., Gruss, P. and Golstein, P. (1999) Interdigital cell death can occur through a necrotic and caspase-independent pathway. *Curr Biol*, **9**, 967-970.

Chen, D., Thomas, E.L. and Kapahi, P. (2009) HIF-1 modulates dietary restriction-mediated lifespan extension via IRE-1 in Caenorhabditis elegans. *PLoS Genet*, **5**, e1000486.

Chen, L., Fink, T., Zhang, X.Y., Ebbesen, P. and Zachar, V. (2005a) Quantitative transcriptional profiling of ATDC5 mouse progenitor cells during chondrogenesis. *Differentiation*, **73**, 350-363.

Chen, N., Harris, T.W., Antoshechkin, I., Bastiani, C., Bieri, T., Blasiar, D., Bradnam, K., Canaran, P., Chan, J., Chen, C.K., Chen, W.J., Cunningham, F., Davis, P., Kenny, E., Kishore, R., Lawson, D., Lee, R., Muller, H.M., Nakamura, C., Pai, S., Ozersky, P., Petcherski, A., Rogers, A., Sabo, A., Schwarz, E.M., Van Auken, K., Wang, Q., Durbin, R., Spieth, J., Sternberg, P.W. and Stein, L.D. (2005b) WormBase: a comprehensive data resource for Caenorhabditis biology and genomics. *Nucleic Acids Res*, **33**, D383-389.

Chen, W., Feng, Y., Chen, D. and Wandinger-Ness, A. (1998) Rab11 Is Required for Trans-Golgi Network-to-Plasma Membrane Transport and a Preferential Target for GDP Dissociation Inhibitor. *Mol. Biol. Cell*, **9**, 3241-3257.

Chesler, M. (2005) Failure and function of intracellular pH regulation in acute hypoxic-ischemic injury of astrocytes. *Glia*, **50**, 398-406.

Choi, E. and Abbott, G.W. (2007) The MiRP2-Kv3.4 potassium channel: muscling in on Alzheimer's disease. *Mol Pharmacol*, **72**, 499-501.

Chung, S., Gumienny, T.L., Hengartner, M.O. and Driscoll, M. (2000) A common set of engulfment genes mediates removal of both apoptotic and necrotic cell corpses in C. elegans. *Nat Cell Biol*, **2**, 931-937.

Citron, M., Westaway, D., Xia, W., Carlson, G., Diehl, T., Levesque, G., Johnson-Wood, K., Lee, M., Seubert, P., Davis, A., Kholodenko, D., Motter, R., Sherrington, R., Perry, B., Yao, H., Strome, R., Lieberburg, I., Rommens, J., Kim, S., Schenk, D., Fraser, P., St George Hyslop, P. and Selkoe, D.J. (1997) Mutant presenilins of Alzheimer's disease increase production of 42-residue amyloid beta-protein in both transfected cells and transgenic mice. *Nat Med*, **3**, 67-72.

Collins, T.J. (2007) ImageJ for microscopy. *Biotechniques*, **43**, 25-30.

Coulondre, C. and Miller, J.H. (1977) Genetic studies of the lac repressor. III. Additional correlation of mutational sites with specific amino acid residues. *J Mol Biol*, **117**, 525-567.

Crighton, D., Wilkinson, S., O'Prey, J., Syed, N., Smith, P., Harrison, P.R., Gasco, M., Garrone, O., Crook, T. and Ryan, K.M. (2006) DRAM, a p53-induced modulator of autophagy, is critical for apoptosis. *Cell*, **126**, 121-134.

Criollo, A., Maiuri, M.C., Tasdemir, E., Vitale, I., Fiebig, A.A., Andrews, D., Molgo, J., Diaz, J., Lavandero, S., Harper, F., Pierron, G., di Stefano, D., Rizzuto, R., Szabadkai, G. and Kroemer, G. (2007) Regulation of autophagy by the inositol trisphosphate receptor. *Cell Death Differ*, **14**, 1029-1039.

Dejgaard, S., Nicolay, J., Taheri, M., Thomas, D.Y. and Bergeron, J.J. (2004) The ER glycoprotein quality control system. *Curr Issues Mol Biol*, **6**, 29-42.

Delepine, M., Nicolino, M., Barrett, T., Golamaully, M., Lathrop, G.M. and Julier, C. (2000) EIF2AK3, encoding translation initiation factor 2-alpha kinase 3, is mutated in patients with Wolcott-Rallison syndrome. *Nat Genet*, **25**, 406-409.

Demuro, A., Mina, E., Kayed, R., Milton, S.C., Parker, I. and Glabe, C.G. (2005) Calcium dysregulation and membrane disruption as a ubiquitous neurotoxic mechanism of soluble amyloid oligomers. *J Biol Chem*, **280**, 17294-17300.

Dimmer, K.S., Navoni, F., Casarin, A., Trevisson, E., Endele, S., Winterpacht, A., Salviati, L. and Scorrano, L. (2008) LETM1, deleted in Wolf-Hirschhorn syndrome is required for normal mitochondrial morphology and cellular viability. *Hum Mol Genet*, **17**, 201-214.

Dominguez-Cuevas, P., Gonzalez-Pastor, J.E., Marques, S., Ramos, J.L. and de Lorenzo, V. (2006) Transcriptional tradeoff between metabolic and stress-response

programs in Pseudomonas putida KT2440 cells exposed to toluene. *J Biol Chem*, **281**, 11981-11991.

Dreses-Werringloer, U., Lambert, J.C., Vingtdeux, V., Zhao, H., Vais, H., Siebert, A., Jain, A., Koppel, J., Rovelet-Lecrux, A., Hannequin, D., Pasquier, F., Galimberti, D., Scarpini, E., Mann, D., Lendon, C., Campion, D., Amouyel, P., Davies, P., Foskett, J.K., Campagne, F. and Marambaud, P. (2008) A polymorphism in CALHM1 influences Ca2+ homeostasis, Abeta levels, and Alzheimer's disease risk. *Cell*, **133**, 1149-1161.

Driscoll, M. (1995) Methods for the study of cell death in the nematode Caenorhabditis elegans. *Methods Cell Biol*, **46**, 323-353.

Driscoll, M. and Chalfie, M. (1991) The mec-4 gene is a member of a family of Caenorhabditis elegans genes that can mutate to induce neuronal degeneration. *Nature*, **349**, 588-593.

Driscoll, M. and Gerstbrein, B. (2003) Dying for a cause: invertebrate genetics takes on human neurodegeneration. *Nat Rev Genet*, **4**, 181-194.

Emilsson, L., Saetre, P. and Jazin, E. (2006) Alzheimer's disease: mRNA expression profiles of multiple patients show alterations of genes involved with calcium signaling. *Neurobiol Dis*, **21**, 618-625.

Etcheberrigaray, R., Ito, E., Oka, K., Tofel-Grehl, B., Gibson, G.E. and Alkon, D.L. (1993) Potassium channel dysfunction in fibroblasts identifies patients with Alzheimer disease. *Proc Natl Acad Sci U S A*, **90**, 8209-8213.

Evans, T.C. (2006) Transformation and microinjection. *WormBook*, 1-16.

Fay, D. (2006) Genetic mapping and manipulation: chapter 1--Introduction and basics. *WormBook*, 1-12.

Fay, D.S., Fluet, A., Johnson, C.J. and Link, C.D. (1998) In vivo aggregation of beta-amyloid peptide variants. *J Neurochem*, **71**, 1616-1625.

Fernandez-Chacon, R., Achiriloaie, M., Janz, R., Albanesi, J.P. and Sudhof, T.C. (2000) SCAMP1 function in endocytosis. *J Biol Chem*, **275**, 12752-12756.

Festjens, N., Vanden Berghe, T. and Vandenabeele, P. (2006) Necrosis, a well-orchestrated form of cell demise: signalling cascades, important mediators and concomitant immune response. *Biochim Biophys Acta*, **1757**, 1371-1387.

Fewell, S.W., Travers, K.J., Weissman, J.S. and Brodsky, J.L. (2001) The action of molecular chaperones in the early secretory pathway. *Annu Rev Genet*, **35**, 149-191.

Fonte, V., Kapulkin, V., Taft, A., Fluet, A., Friedman, D. and Link, C.D. (2002) Interaction of intracellular beta amyloid peptide with chaperone proteins. *Proc Natl Acad Sci U S A*, **99**, 9439-9444.

Fujita, E., Kouroku, Y., Isoai, A., Kumagai, H., Misutani, A., Matsuda, C., Hayashi, Y.K. and Momoi, T. (2007) Two endoplasmic reticulum-associated degradation (ERAD) systems for the novel variant of the mutant dysferlin: ubiquitin/proteasome ERAD(I) and autophagy/lysosome ERAD(II). *Hum Mol Genet*, **16**, 618-629.

Garcia-Anoveros, J., Ma, C. and Chalfie, M. (1995) Regulation of Caenorhabditis elegans degenerin proteins by a putative extracellular domain. *Curr Biol*, **5**, 441-448.

Gatz, M., Reynolds, C.A., Fratiglioni, L., Johansson, B., Mortimer, J.A., Berg, S., Fiske, A. and Pedersen, N.L. (2006) Role of genes and environments for explaining Alzheimer disease. *Arch Gen Psychiatry*, **63**, 168-174.

Gems, D. and Partridge, L. (2008) Stress-response hormesis and aging: "that which does not kill us makes us stronger". *Cell Metab*, **7**, 200-203.

Gidday, J.M. (2006) Cerebral preconditioning and ischaemic tolerance. *Nat Rev Neurosci*, **7**, 437-448.

Golstein, P. and Kroemer, G. (2007) Cell death by necrosis: towards a molecular definition. *Trends Biochem Sci*, **32**, 37-43.

Goodman, M.B., Ernstrom, G.G., Chelur, D.S., O'Hagan, R., Yao, C.A. and Chalfie, M. (2002) MEC-2 regulates C. elegans DEG/ENaC channels needed for mechanosensation. *Nature*, **415**, 1039-1042.

Grabarek, Z. (2006) Structural basis for diversity of the EF-hand calcium-binding proteins. *J Mol Biol*, **359**, 509-525.

Green, D.R. and Kroemer, G. (2004) The pathophysiology of mitochondrial cell death. *Science*, **305**, 626-629.

Gregersen, N., Bross, P., Vang, S. and Christensen, J.H. (2006) Protein misfolding and human disease. *Annu Rev Genomics Hum Genet*, **7**, 103-124.

Grishok, A. (2005) RNAi mechanisms in Caenorhabditis elegans. *FEBS Lett*, **579**, 5932-5939.

Guerin, M. and Parodi, A.J. (2003) The UDP-glucose:glycoprotein glucosyltransferase is organized in at least two tightly bound domains from yeast to mammals. *J Biol Chem*, **278**, 20540-20546.

Guo, W., Malin, S.A., Johns, D.C., Jeromin, A. and Nerbonne, J.M. (2002) Modulation of Kv4-encoded K(+) currents in the mammalian myocardium by neuronal calcium sensor-1. *J Biol Chem*, **277**, 26436-26443.

Haas, A. (1998) NSF--fusion and beyond. *Trends Cell Biol*, **8**, 471-473.

Haas, A. and Wickner, W. (1996) Homotypic vacuole fusion requires Sec17p (yeast alpha-SNAP) and Sec18p (yeast NSF). *Embo J*, **15**, 3296-3305.

Haass, C. and Selkoe, D.J. (2007) Soluble protein oligomers in neurodegeneration: lessons from the Alzheimer's amyloid beta-peptide. *Nat Rev Mol Cell Biol*, **8**, 101-112.

Hall, D.H., Gu, G., Garcia-Anoveros, J., Gong, L., Chalfie, M. and Driscoll, M. (1997) Neuropathology of degenerative cell death in Caenorhabditis elegans. *J Neurosci*, **17**, 1033-1045.

Hampton, R.Y. (2002) ER-associated degradation in protein quality control and cellular regulation. *Curr Opin Cell Biol*, **14**, 476-482.

Hara, T., Nakamura, K., Matsui, M., Yamamoto, A., Nakahara, Y., Suzuki-Migishima, R., Yokoyama, M., Mishima, K., Saito, I., Okano, H. and Mizushima, N. (2006) Suppression of basal autophagy in neural cells causes neurodegenerative disease in mice. *Nature*, **441**, 885-889.

Harbinder, S., Tavernarakis, N., Herndon, L.A., Kinnell, M., Xu, S.Q., Fire, A. and Driscoll, M. (1997) Genetically targeted cell disruption in Caenorhabditis elegans. *Proc Natl Acad Sci U S A*, **94**, 13128-13133.

Harding, H.P., Zhang, Y. and Ron, D. (1999) Protein translation and folding are coupled by an endoplasmic-reticulum-resident kinase. *Nature*, **397**, 271-274.

Hasegawa, A. and van der Bliek, A.M. (2007) Inverse correlation between expression of the Wolfs Hirschhorn candidate gene Letm1 and mitochondrial volume in C. elegans and in mammalian cells. *Hum Mol Genet*, **16**, 2061-2071.

Hayashi, T., Saito, A., Okuno, S., Ferrand-Drake, M. and Chan, P.H. (2003) Induction of GRP78 by ischemic preconditioning reduces endoplasmic reticulum stress and prevents delayed neuronal cell death. *J Cereb Blood Flow Metab*, **23**, 949-961.

Haze, K., Yoshida, H., Yanagi, H., Yura, T. and Mori, K. (1999) Mammalian transcription factor ATF6 is synthesized as a transmembrane protein and activated by proteolysis in response to endoplasmic reticulum stress. *Mol Biol Cell*, **10**, 3787-3799.

Heintz, N. and Zoghbi, H.Y. (2000) Insights from mouse models into the molecular basis of neurodegeneration. *Annu Rev Physiol*, **62**, 779-802.

Hengartner, M.O. and Bryant, J.A. (2000) Apoptotic cell death: from worms to wombats ... but what about the weeds? *Symp Soc Exp Biol*, **52**, 1-12.

Henriquez, M., Armisen, R., Stutzin, A. and Quest, A.F. (2008) Cell death by necrosis, a regulated way to go. *Curr Mol Med*, **8**, 187-206.

Hirsch, C., Gauss, R. and Sommer, T. (2006) Coping with stress: cellular relaxation techniques. *Trends Cell Biol*, **16**, 657-663.

Hodgkin, J. (2005) Introduction to genetics and genomics. *WormBook*, 1-3.

Holbert, S., Dedeoglu, A., Humbert, S., Saudou, F., Ferrante, R.J. and Neri, C. (2003) Cdc42-interacting protein 4 binds to huntingtin: neuropathologic and biological evidence for a role in Huntington's disease. *Proc Natl Acad Sci U S A*, **100**, 2712-2717.

Hong, K. and Driscoll, M. (1994) A transmembrane domain of the putative channel subunit MEC-4 influences mechanotransduction and neurodegeneration in C. elegans. *Nature*, **367**, 470-473.

Hong, K., Mano, I. and Driscoll, M. (2000) In vivo structure-function analyses of Caenorhabditis elegans MEC-4, a candidate mechanosensory ion channel subunit. *J Neurosci*, **20**, 2575-2588.

Hong, Y.C., Rha, J.H., Lee, J.T., Ha, E.H., Kwon, H.J. and Kim, H. (2003) Ischemic stroke associated with decrease in temperature. *Epidemiology*, **14**, 473-478.

Horvitz, H.R. (1999) Genetic control of programmed cell death in the nematode Caenorhabditis elegans. *Cancer Res*, **59**, 1701s-1706s.

Hosokawa, N., Wada, I., Hasegawa, K., Yorihuzi, T., Tremblay, L.O., Herscovics, A. and Nagata, K. (2001) A novel ER alpha-mannosidase-like protein accelerates ER-associated degradation. *EMBO Rep*, **2**, 415-422.

Hoyer-Hansen, M. and Jaattela, M. (2007) Connecting endoplasmic reticulum stress to autophagy by unfolded protein response and calcium. *Cell Death Differ*, **14**, 1576-1582.

Huang, G., Yao, J., Zeng, W., Mizuno, Y., Kamm, K.E., Stull, J.T., Harding, H.P., Ron, D. and Muallem, S. (2006) ER stress disrupts Ca2+-signaling complexes and Ca2+ regulation in secretory and muscle cells from PERK-knockout mice. *J Cell Sci*, **119**, 153-161.

Hung, C.C., Ichimura, T., Stevens, J.L. and Bonventre, J.V. (2003) Protection of renal epithelial cells against oxidative injury by endoplasmic reticulum stress preconditioning is mediated by ERK1/2 activation. *J Biol Chem*, **278**, 29317-29326.

Inagi, R., Kumagai, T., Nishi, H., Kawakami, T., Miyata, T., Fujita, T. and Nangaku, M. (2008) Preconditioning with endoplasmic reticulum stress ameliorates mesangioproliferative glomerulonephritis. *J Am Soc Nephrol*, **19**, 915-922.

Jakob-Roetne, R. and Jacobsen, H. (2009) Alzheimer's disease: from pathology to therapeutic approaches. *Angew Chem Int Ed Engl*, **48**, 3030-3059.

Jin, H., Yan, Z., Nam, K.H. and Li, J. (2007) Allele-specific suppression of a defective brassinosteroid receptor reveals a physiological role of UGGT in ER quality control. *Mol Cell*, **26**, 821-830.

Judge, S.I., Smith, P.J., Stewart, P.E. and Bever, C.T., Jr. (2007) Potassium channel blockers and openers as CNS neurologic therapeutic agents. *Recent Pat CNS Drug Discov*, **2**, 200-228.

Kaletta, T. and Hengartner, M.O. (2006) Finding function in novel targets: C. elegans as a model organism. *Nat Rev Drug Discov*, **5**, 387-398.

Kamath, R.S., Fraser, A.G., Dong, Y., Poulin, G., Durbin, R., Gotta, M., Kanapin, A., Le Bot, N., Moreno, S., Sohrmann, M., Welchman, D.P., Zipperlen, P. and Ahringer, J. (2003) Systematic functional analysis of the Caenorhabditis elegans genome using RNAi. *Nature*, **421**, 231-237.

Kamath, R.S., Martinez-Campos, M., Zipperlen, P., Fraser, A.G. and Ahringer, J. (2001) Effectiveness of specific RNA-mediated interference through ingested double-stranded RNA in Caenorhabditis elegans. *Genome Biol*, **2**, RESEARCH0002.

Kang, S.W., Rane, N.S., Kim, S.J., Garrison, J.L., Taunton, J. and Hegde, R.S. (2006) Substrate-specific translocational attenuation during ER stress defines a pre-emptive quality control pathway. *Cell*, **127**, 999-1013.

Khachaturian, Z.S. (1984) Scientific challenges and opportunities related to Alzheimer's disease. *Clin Pharm*, **3**, 522-523.

Kinchen, J.M., Doukoumetzidis, K., Almendinger, J., Stergiou, L., Tosello-Trampont, A., Sifri, C.D., Hengartner, M.O. and Ravichandran, K.S. (2008) A pathway for phagosome maturation during engulfment of apoptotic cells. *Nat Cell Biol*, **10**, 556-566.

Klionsky, D.J. (2007) Autophagy: from phenomenology to molecular understanding in less than a decade. *Nat Rev Mol Cell Biol*, **8**, 931-937.

Koh, P.O., Undie, A.S., Kabbani, N., Levenson, R., Goldman-Rakic, P.S. and Lidow, M.S. (2003) Up-regulation of neuronal calcium sensor-1 (NCS-1) in the prefrontal cortex of schizophrenic and bipolar patients. *Proc Natl Acad Sci U S A*, **100**, 313-317.

Komatsu, M., Waguri, S., Chiba, T., Murata, S., Iwata, J., Tanida, I., Ueno, T., Koike, M., Uchiyama, Y., Kominami, E. and Tanaka, K. (2006) Loss of autophagy in the central nervous system causes neurodegeneration in mice. *Nature*, **441**, 880-884.

Korswagen, H.C., Park, J.H., Ohshima, Y. and Plasterk, R.H. (1997) An activating mutation in a Caenorhabditis elegans Gs protein induces neural degeneration. *Genes Dev*, **11**, 1493-1503.

Lee, W., Kim, K.R., Singaravelu, G., Park, B.J., Kim, D.H., Ahnn, J. and Yoo, Y.J. (2006) Alternative chaperone machinery may compensate for calreticulin/calnexin deficiency in Caenorhabditis elegans. *Proteomics*, **6**, 1329-1339.

Lehotsky, J., Urban, P., Pavlikova, M., Tatarkova, Z., Kaminska, B. and Kaplan, P. (2009) Molecular Mechanisms Leading to Neuroprotection/Ischemic Tolerance: Effect of Preconditioning on the Stress Reaction of Endoplasmic Reticulum. *Cell Mol Neurobiol*.

Levine, B. and Klionsky, D.J. (2004) Development by self-digestion: molecular mechanisms and biological functions of autophagy. *Dev Cell*, **6**, 463-477.

Levine, B. and Yuan, J. (2005) Autophagy in cell death: an innocent convict? *J Clin Invest*, **115**, 2679-2688.

Link, C.D. (1995) Expression of human beta-amyloid peptide in transgenic Caenorhabditis elegans. *Proc Natl Acad Sci U S A*, **92**, 9368-9372.

Link, C.D. (2006) C. elegans models of age-associated neurodegenerative diseases: lessons from transgenic worm models of Alzheimer's disease. *Exp Gerontol*, **41**, 1007-1013.

Link, C.D., Johnson, C.J., Fonte, V., Paupard, M., Hall, D.H., Styren, S., Mathis, C.A. and Klunk, W.E. (2001) Visualization of fibrillar amyloid deposits in living, transgenic Caenorhabditis elegans animals using the sensitive amyloid dye, X-34. *Neurobiol Aging*, **22**, 217-226.

Link, C.D., Taft, A., Kapulkin, V., Duke, K., Kim, S., Fei, Q., Wood, D.E. and Sahagan, B.G. (2003) Gene expression analysis in a transgenic Caenorhabditis elegans Alzheimer's disease model. *Neurobiol Aging*, **24**, 397-413.

Liu, C.L., Siesjo, B.K. and Hu, B.R. (2004) Pathogenesis of hippocampal neuronal death after hypoxia-ischemia changes during brain development. *Neuroscience*, **127**, 113-123.

Lu, P.D., Harding, H.P. and Ron, D. (2004a) Translation reinitiation at alternative open reading frames regulates gene expression in an integrated stress response. *J Cell Biol*, **167**, 27-33.

Lu, P.D., Jousse, C., Marciniak, S.J., Zhang, Y., Novoa, I., Scheuner, D., Kaufman, R.J., Ron, D. and Harding, H.P. (2004b) Cytoprotection by pre-emptive conditional phosphorylation of translation initiation factor 2. *Embo J*, **23**, 169-179.

Luke, C.J., Pak, S.C., Askew, Y.S., Naviglia, T.L., Askew, D.J., Nobar, S.M., Vetica, A.C., Long, O.S., Watkins, S.C., Stolz, D.B., Barstead, R.J., Moulder, G.L., Bromme, D. and Silverman, G.A. (2007) An intracellular serpin regulates necrosis by inhibiting the induction and sequelae of lysosomal injury. *Cell*, **130**, 1108-1119.

Ma, Y., Brewer, J.W., Diehl, J.A. and Hendershot, L.M. (2002) Two distinct stress signaling pathways converge upon the CHOP promoter during the mammalian unfolded protein response. *J Mol Biol*, **318**, 1351-1365.

Mahley, R.W. (1988) Apolipoprotein E: cholesterol transport protein with expanding role in cell biology. *Science*, **240**, 622-630.

Maiuri, M.C., Zalckvar, E., Kimchi, A. and Kroemer, G. (2007) Self-eating and self-killing: crosstalk between autophagy and apoptosis. *Nat Rev Mol Cell Biol*, **8**, 741-752.

Mandavilli, A. (2006) The amyloid code. *Nat Med*, **12**, 747-751.

Mano, I. and Driscoll, M. (2009) Caenorhabditis elegans glutamate transporter deletion induces AMPA-receptor/adenylyl cyclase 9-dependent excitotoxicity. *J Neurochem*, **108**, 1373-1384.

Mattson, M.P. (2004) Pathways towards and away from Alzheimer's disease. *Nature*, **430**, 631-639.

Mattson, M.P., Cheng, B., Davis, D., Bryant, K., Lieberburg, I. and Rydel, R.E. (1992) beta-Amyloid peptides destabilize calcium homeostasis and render human cortical neurons vulnerable to excitotoxicity. *J Neurosci*, **12**, 376-389.

McKay, S.J., Johnsen, R., Khattra, J., Asano, J., Baillie, D.L., Chan, S., Dube, N., Fang, L., Goszczynski, B., Ha, E., Halfnight, E., Hollebakken, R., Huang, P., Hung, K., Jensen, V., Jones, S.J., Kai, H., Li, D., Mah, A., Marra, M., McGhee, J., Newbury, R., Pouzyrev, A., Riddle, D.L., Sonnhammer, E., Tian, H., Tu, D., Tyson, J.R., Vatcher, G., Warner, A., Wong, K., Zhao, Z. and Moerman, D.G. (2003) Gene expression profiling of cells, tissues, and developmental stages of the nematode C. elegans. *Cold Spring Harb Symp Quant Biol*, **68**, 159-169.

Metzstein, M.M., Stanfield, G.M. and Horvitz, H.R. (1998) Genetics of programmed cell death in C. elegans: past, present and future. *Trends Genet*, **14**, 410-416.

Michalak, M., Corbett, E.F., Mesaeli, N., Nakamura, K. and Opas, M. (1999) Calreticulin: one protein, one gene, many functions. *Biochem J*, **344 Pt 2**, 281-292.

Mills, I.G., Praefcke, G.J., Vallis, Y., Peter, B.J., Olesen, L.E., Gallop, J.L., Butler, P.J., Evans, P.R. and McMahon, H.T. (2003) EpsinR: an AP1/clathrin interacting protein involved in vesicle trafficking. *J Cell Biol*, **160**, 213-222.

Molinari, M., Galli, C., Piccaluga, V., Pieren, M. and Paganetti, P. (2002) Sequential assistance of molecular chaperones and transient formation of covalent complexes during protein degradation from the ER. *J Cell Biol*, **158**, 247-257.

Naidoo, N. (2009a) The endoplasmic reticulum stress response and aging. *Rev Neurosci*, **20**, 23-37.

Naidoo, N. (2009b) ER and aging-Protein folding and the ER stress response. *Ageing Res Rev*, **8**, 150-159.

Nakamura, N., Morinaga, H., Kikuchi, M., Yonekura, S., Ishii, N., Yamamoto, K., Yonei, S. and Zhang, Q.M. (2008) Cloning and characterization of uracil-DNA glycosylase and the biological consequences of the loss of its function in the nematode Caenorhabditis elegans. *Mutagenesis*, **23**, 407-413.

Nichols, W.C., Seligsohn, U., Zivelin, A., Terry, V.H., Hertel, C.E., Wheatley, M.A., Moussalli, M.J., Hauri, H.P., Ciavarella, N., Kaufman, R.J. and Ginsburg, D. (1998) Mutations in the ER-Golgi intermediate compartment protein ERGIC-53 cause combined deficiency of coagulation factors V and VIII. *Cell*, **93**, 61-70.

Nishitoh, H. and Ichijo, H. (2004) [Molecular mechanisms of ER stress-induced apoptosis]. *Tanpakushitsu Kakusan Koso*, **49**, 1006-1009.

Nishitoh, H., Matsuzawa, A., Tobiume, K., Saegusa, K., Takeda, K., Inoue, K., Hori, S., Kakizuka, A. and Ichijo, H. (2002) ASK1 is essential for endoplasmic reticulum stress-induced neuronal cell death triggered by expanded polyglutamine repeats. *Genes Dev*, **16**, 1345-1355.

Norris, C.M., Kadish, I., Blalock, E.M., Chen, K.C., Thibault, V., Porter, N.M., Landfield, P.W. and Kraner, S.D. (2005) Calcineurin triggers reactive/inflammatory processes in astrocytes and is upregulated in aging and Alzheimer's models. *J Neurosci*, **25**, 4649-4658.

Nowikovsky, K., Froschauer, E.M., Zsurka, G., Samaj, J., Reipert, S., Kolisek, M., Wiesenberger, G. and Schweyen, R.J. (2004) The LETM1/YOL027 gene family encodes a factor of the mitochondrial K+ homeostasis with a potential role in the Wolf-Hirschhorn syndrome. *J Biol Chem*, **279**, 30307-30315.

Oda, Y., Okada, T., Yoshida, H., Kaufman, R.J., Nagata, K. and Mori, K. (2006) Derlin-2 and Derlin-3 are regulated by the mammalian unfolded protein response and are required for ER-associated degradation. *J Cell Biol*, **172**, 383-393.

Ogata, M., Hino, S., Saito, A., Morikawa, K., Kondo, S., Kanemoto, S., Murakami, T., Taniguchi, M., Tanii, I., Yoshinaga, K., Shiosaka, S., Hammarback, J.A., Urano,

F. and Imaizumi, K. (2006) Autophagy is activated for cell survival after endoplasmic reticulum stress. *Mol Cell Biol*, **26**, 9220-9231.

Orrenius, S., Zhivotovsky, B. and Nicotera, P. (2003) Regulation of cell death: the calcium-apoptosis link. *Nat Rev Mol Cell Biol*, **4**, 552-565.

Palmer, A.E., Jin, C., Reed, J.C. and Tsien, R.Y. (2004) Bcl-2-mediated alterations in endoplasmic reticulum Ca2+ analyzed with an improved genetically encoded fluorescent sensor. *Proc Natl Acad Sci U S A*, **101**, 17404-17409.

Papadopulos, F., Spinelli, M., Valente, S., Foroni, L., Orrico, C., Alviano, F. and Pasquinelli, G. (2007) Common tasks in microscopic and ultrastructural image analysis using ImageJ. *Ultrastruct Pathol*, **31**, 401-407.

Parodi, A.J. (1999) Reglucosylation of glycoproteins and quality control of glycoprotein folding in the endoplasmic reticulum of yeast cells. *Biochim Biophys Acta*, **1426**, 287-295.

Parodi, A.J. (2000) Protein glucosylation and its role in protein folding. *Annu Rev Biochem*, **69**, 69-93.

Patel, S.P., Campbell, D.L. and Strauss, H.C. (2002) Elucidating KChIP effects on Kv4.3 inactivation and recovery kinetics with a minimal KChIP2 isoform. *J Physiol*, **545**, 5-11.

Peyrou, M. and Cribb, A.E. (2007) Effect of endoplasmic reticulum stress preconditioning on cytotoxicity of clinically relevant nephrotoxins in renal cell lines. *Toxicol In Vitro*, **21**, 878-886.

Plasterk, R.H. (1992) Reverse genetics of Caenorhabditis elegans. *Bioessays*, **14**, 629-633.

Praitis, V., Casey, E., Collar, D. and Austin, J. (2001) Creation of low-copy integrated transgenic lines in Caenorhabditis elegans. *Genetics*, **157**, 1217-1226.

Ren, X., Shand, S.H. and Takimoto, K. (2003) Effective association of Kv channel-interacting proteins with Kv4 channel is mediated with their unique core peptide. *J Biol Chem*, **278**, 43564-43570.

Riddle, D.L., Blumenthal, T., Meyer, B.J. and Priess, J.R. (1997) Introduction to C. elegans. In Riddle, D.L., Blumenthal, T., Meyer, B.J. and Priess, J.R. (eds.), *C. elegans II*. Cold Spring Harbor Laboratory Press.

Ritter, C. and Helenius, A. (2000) Recognition of local glycoprotein misfolding by the ER folding sensor UDP-glucose:glycoprotein glucosyltransferase. *Nat Struct Biol*, **7**, 278-280.

Ritter, C., Quirin, K., Kowarik, M. and Helenius, A. (2005) Minor folding defects trigger local modification of glycoproteins by the ER folding sensor GT. *Embo J*, **24**, 1730-1738.

Roach, H.I. and Clarke, N.M. (2000) Physiological cell death of chondrocytes in vivo is not confined to apoptosis. New observations on the mammalian growth plate. *J Bone Joint Surg Br*, **82**, 601-613.

Ron, D. and Hampton, R.Y. (2004) Membrane biogenesis and the unfolded protein response. *J Cell Biol*, **167**, 23-25.

Ron, D. and Walter, P. (2007) Signal integration in the endoplasmic reticulum unfolded protein response. *Nat Rev Mol Cell Biol*, **8**, 519-529.

Rose, C.R. and Konnerth, A. (2001) Stores not just for storage. intracellular calcium release and synaptic plasticity. *Neuron*, **31**, 519-522.

Rothstein, J.D. (1996) Excitotoxicity hypothesis. *Neurology*, **47**, S19-25; discussion S26.

Royal, D.C., Bianchi, L., Royal, M.A., Lizzio, M., Jr., Mukherjee, G., Nunez, Y.O. and Driscoll, M. (2005) Temperature-sensitive mutant of the Caenorhabditis elegans neurotoxic MEC-4(d) DEG/ENaC channel identifies a site required for trafficking or surface maintenance. *J Biol Chem*, **280**, 41976-41986.

Rudolf, R., Mongillo, M., Rizzuto, R. and Pozzan, T. (2003) Looking forward to seeing calcium. *Nat Rev Mol Cell Biol*, **4**, 579-586.

Rutkowski, D.T., Arnold, S.M., Miller, C.N., Wu, J., Li, J., Gunnison, K.M., Mori, K., Sadighi Akha, A.A., Raden, D. and Kaufman, R.J. (2006) Adaptation to ER stress is mediated by differential stabilities of pro-survival and pro-apoptotic mRNAs and proteins. *PLoS Biol*, **4**, e374.

Rutkowski, D.T. and Kaufman, R.J. (2004) A trip to the ER: coping with stress. *Trends Cell Biol*, **14**, 20-28.

Samara, C., Syntichaki, P. and Tavernarakis, N. (2008) Autophagy is required for necrotic cell death in Caenorhabditis elegans. *Cell Death Differ*, **15**, 105-112.

Sarkar, S., Davies, J.E., Huang, Z., Tunnacliffe, A. and Rubinsztein, D.C. (2007) Trehalose, a novel mTOR-independent autophagy enhancer, accelerates the clearance of mutant huntingtin and alpha-synuclein. *J Biol Chem*, **282**, 5641-5652.

Saunders, L.R. and Verdin, E. (2009) CELL BIOLOGY: Stress Response and Aging

10.1126/science.1170007. *Science*, **323**, 1021-1022.

Schlecker, C., Boehmerle, W., Jeromin, A., DeGray, B., Varshney, A., Sharma, Y., Szigeti-Buck, K. and Ehrlich, B.E. (2006) Neuronal calcium sensor-1 enhancement of InsP3 receptor activity is inhibited by therapeutic levels of lithium. *J Clin Invest*, **116**, 1668-1674.

Schlickum, S., Moghekar, A., Simpson, J.C., Steglich, C., O'Brien, R.J., Winterpacht, A. and Endele, S.U. (2004) LETM1, a gene deleted in Wolf-Hirschhorn syndrome, encodes an evolutionarily conserved mitochondrial protein. *Genomics*, **83**, 254-261.

Scorrano, L., Oakes, S.A., Opferman, J.T., Cheng, E.H., Sorcinelli, M.D., Pozzan, T. and Korsmeyer, S.J. (2003) BAX and BAK regulation of endoplasmic reticulum Ca2+: a control point for apoptosis. *Science*, **300**, 135-139.

Selkoe, D. and Kopan, R. (2003) Notch and Presenilin: regulated intramembrane proteolysis links development and degeneration. *Annu Rev Neurosci*, **26**, 565-597.

Shen, X., Ellis, R.E., Sakaki, K. and Kaufman, R.J. (2005) Genetic interactions due to constitutive and inducible gene regulation mediated by the unfolded protein response in C. elegans. *PLoS Genet*, **1**, e37.

Shimizu, S., Kanaseki, T., Mizushima, N., Mizuta, T., Arakawa-Kobayashi, S., Thompson, C.B. and Tsujimoto, Y. (2004) Role of Bcl-2 family proteins in a non-apoptotic programmed cell death dependent on autophagy genes. *Nat Cell Biol*, **6**, 1221-1228.

Shintani, M., Tada, M., Kobayashi, T., Kajiho, H., Kontani, K. and Katada, T. (2007) Characterization of Rab45/RASEF containing EF-hand domain and a coiled-coil motif as a self-associating GTPase. *Biochem Biophys Res Commun*, **357**, 661-667.

Shreffler, W., Magardino, T., Shekdar, K. and Wolinsky, E. (1995) The unc-8 and sup-40 genes regulate ion channel function in Caenorhabditis elegans motorneurons. *Genetics*, **139**, 1261-1272.

Solda, T., Galli, C., Kaufman, R.J. and Molinari, M. (2007) Substrate-specific requirements for UGT1-dependent release from calnexin. *Mol Cell*, **27**, 238-249.

Sonnichsen, B., Koski, L.B., Walsh, A., Marschall, P., Neumann, B., Brehm, M., Alleaume, A.M., Artelt, J., Bettencourt, P., Cassin, E., Hewitson, M., Holz, C., Khan, M., Lazik, S., Martin, C., Nitzsche, B., Ruer, M., Stamford, J., Winzi, M., Heinkel, R., Roder, M., Finell, J., Hantsch, H., Jones, S.J., Jones, M., Piano, F., Gunsalus, K.C., Oegema, K., Gonczy, P., Coulson, A., Hyman, A.A. and Echeverri, C.J. (2005) Full-genome RNAi profiling of early embryogenesis in Caenorhabditis elegans. *Nature*, **434**, 462-469.

Sousa, M. and Parodi, A.J. (1995) The molecular basis for the recognition of misfolded glycoproteins by the UDP-Glc:glycoprotein glucosyltransferase. *Embo J*, **14**, 4196-4203.

Sriburi, R., Jackowski, S., Mori, K. and Brewer, J.W. (2004) XBP1: a link between the unfolded protein response, lipid biosynthesis, and biogenesis of the endoplasmic reticulum. *J Cell Biol*, **167**, 35-41.

Steffen, K.K., MacKay, V.L., Kerr, E.O., Tsuchiya, M., Hu, D., Fox, L.A., Dang, N., Johnston, E.D., Oakes, J.A., Tchao, B.N., Pak, D.N., Fields, S., Kennedy, B.K. and Kaeberlein, M. (2008) Yeast life span extension by depletion of 60s ribosomal subunits is mediated by Gcn4. *Cell*, **133**, 292-302.

Stokin, G.B. and Goldstein, L.S. (2006a) Axonal transport and Alzheimer's disease. *Annu Rev Biochem*, **75**, 607-627.

Stokin, G.B. and Goldstein, L.S. (2006b) Linking molecular motors to Alzheimer's disease. *J Physiol Paris*, **99**, 193-200.

Stokin, G.B., Lillo, C., Falzone, T.L., Brusch, R.G., Rockenstein, E., Mount, S.L., Raman, R., Davies, P., Masliah, E., Williams, D.S. and Goldstein, L.S. (2005) Axonopathy and transport deficits early in the pathogenesis of Alzheimer's disease. *Science*, **307**, 1282-1288.

Strittmatter, W.J., Saunders, A.M., Schmechel, D., Pericak-Vance, M., Enghild, J., Salvesen, G.S. and Roses, A.D. (1993) Apolipoprotein E: high-avidity binding to beta-amyloid and increased frequency of type 4 allele in late-onset familial Alzheimer disease. *Proc Natl Acad Sci U S A*, **90**, 1977-1981.

Sulston, J.E., Schierenberg, E., White, J.G. and Thomson, J.N. (1983) The embryonic cell lineage of the nematode Caenorhabditis elegans. *Dev Biol*, **100**, 64-119.

Syntichaki, P., Samara, C. and Tavernarakis, N. (2005) The vacuolar H+ -ATPase mediates intracellular acidification required for neurodegeneration in C. elegans. *Curr Biol*, **15**, 1249-1254.

Syntichaki, P., Xu, K., Driscoll, M. and Tavernarakis, N. (2002) Specific aspartyl and calpain proteases are required for neurodegeneration in C. elegans. *Nature*, **419**, 939-944.

Takacs-Vellai, K., Bayci, A. and Vellai, T. (2006) Autophagy in neuronal cell loss: a road to death. *Bioessays*, **28**, 1126-1131.

Tan, S., Somia, N., Maher, P. and Schubert, D. (2001) Regulation of antioxidant metabolism by translation initiation factor 2alpha. *J Cell Biol*, **152**, 997-1006.

Tavernarakis, N., Shreffler, W., Wang, S. and Driscoll, M. (1997) unc-8, a DEG/ENaC family member, encodes a subunit of a candidate mechanically gated channel that modulates C. elegans locomotion. *Neuron*, **18**, 107-119.

Tawe, W.N., Eschbach, M.L., Walter, R.D. and Henkle-Duhrsen, K. (1998) Identification of stress-responsive genes in Caenorhabditis elegans using RT-PCR differential display. *Nucleic Acids Res*, **26**, 1621-1627.

Taylor, S.C., Ferguson, A.D., Bergeron, J.J. and Thomas, D.Y. (2004) The ER protein folding sensor UDP-glucose glycoprotein-glucosyltransferase modifies substrates distant to local changes in glycoprotein conformation. *Nat Struct Mol Biol*, **11**, 128-134.

Taylor, S.C., Thibault, P., Tessier, D.C., Bergeron, J.J. and Thomas, D.Y. (2003) Glycopeptide specificity of the secretory protein folding sensor UDP-glucose glycoprotein:glucosyltransferase. *EMBO Rep*, **4**, 405-411.

Teckman, J.H. and Perlmutter, D.H. (2000) Retention of mutant alpha(1)-antitrypsin Z in endoplasmic reticulum is associated with an autophagic response. *Am J Physiol Gastrointest Liver Physiol*, **279**, G961-974.

Tessier, D.C., Dignard, D., Zapun, A., Radominska-Pandya, A., Parodi, A.J., Bergeron, J.J. and Thomas, D.Y. (2000) Cloning and characterization of mammalian UDP-glucose glycoprotein: glucosyltransferase and the development of a specific substrate for this enzyme. *Glycobiology*, **10**, 403-412.

Thibault, O., Gant, J.C. and Landfield, P.W. (2007) Expansion of the calcium hypothesis of brain aging and Alzheimer's disease: minding the store. *Aging Cell*, **6**, 307-317.

Thibault, O., Porter, N.M., Chen, K.C., Blalock, E.M., Kaminker, P.G., Clodfelter, G.V., Brewer, L.D. and Landfield, P.W. (1998) Calcium dysregulation in neuronal aging and Alzheimer's disease: history and new directions. *Cell Calcium*, **24**, 417-433.

Thierry-Mieg, D. and Thierry-Mieg, J. (2006) AceView: a comprehensive cDNA-supported gene and transcripts annotation. *Genome Biol*, **7 Suppl 1**, S12 11-14.

Thorburn, A. (2004) Death receptor-induced cell killing. *Cell Signal*, **16**, 139-144.

Thorburn, A. (2008) Apoptosis and autophagy: regulatory connections between two supposedly different processes. *Apoptosis*, **13**, 1-9.

Thorell, W.E., Leibrock, L.G. and Agrawal, S.K. (2002) Role of RyRs and IP3 receptors after traumatic injury to spinal cord white matter. *J Neurotrauma*, **19**, 335-342.

Timmons, L., Court, D.L. and Fire, A. (2001) Ingestion of bacterially expressed dsRNAs can produce specific and potent genetic interference in Caenorhabditis elegans. *Gene*, **263**, 103-112.

Tirasophon, W., Welihinda, A.A. and Kaufman, R.J. (1998) A stress response pathway from the endoplasmic reticulum to the nucleus requires a novel bifunctional

protein kinase/endoribonuclease (Ire1p) in mammalian cells. *Genes Dev*, **12**, 1812-1824.

Totani, K., Ihara, Y., Matsuo, I., Tsujimoto, T. and Ito, Y. (2009) The Recognition Motif of the Glycoprotein-Folding Sensor Enzyme, UDP-Glc: Glycoprotein Glucosyltransferase. *Biochemistry*.

Toth, M.L., Simon, P., Kovacs, A.L. and Vellai, T. (2007) Influence of autophagy genes on ion-channel-dependent neuronal degeneration in Caenorhabditis elegans. *J Cell Sci*, **120**, 1134-1141.

Treinin, M. and Chalfie, M. (1995) A mutated acetylcholine receptor subunit causes neuronal degeneration in C. elegans. *Neuron*, **14**, 871-877.

Trusina, A., Papa, F.R. and Tang, C. (2008) Rationalizing translation attenuation in the network architecture of the unfolded protein response. *Proc Natl Acad Sci U S A*, **105**, 20280-20285.

Tsujita, K., Suetsugu, S., Sasaki, N., Furutani, M., Oikawa, T. and Takenawa, T. (2006) Coordination between the actin cytoskeleton and membrane deformation by a novel membrane tubulation domain of PCH proteins is involved in endocytosis. *J Cell Biol*, **172**, 269-279.

van der Linden, A.M. and Plasterk, R.H. (2004) Shotgun Cloning of Transposon Insertions in the Genome of Caenorhabditis elegans. *Comp Funct Genomics*, **5**, 225-229.

Vanlangenakker, N., Berghe, T.V., Krysko, D.V., Festjens, N. and Vandenabeele, P. (2008) Molecular mechanisms and pathophysiology of necrotic cell death. *Curr Mol Med*, **8**, 207-220.

Wang, S.S., Denk, W. and Hausser, M. (2000) Coincidence detection in single dendritic spines mediated by calcium release. *Nat Neurosci*, **3**, 1266-1273.

Waters, M.F., Minassian, N.A., Stevanin, G., Figueroa, K.P., Bannister, J.P., Nolte, D., Mock, A.F., Evidente, V.G., Fee, D.B., Muller, U., Durr, A., Brice, A., Papazian, D.M. and Pulst, S.M. (2006) Mutations in voltage-gated potassium channel KCNC3 cause degenerative and developmental central nervous system phenotypes. *Nat Genet*, **38**, 447-451.

Wei, C., Lamesch, P., Arumugam, M., Rosenberg, J., Hu, P., Vidal, M. and Brent, M.R. (2005) Closing in on the C. elegans ORFeome by cloning TWINSCAN predictions. *Genome Res*, **15**, 577-582.

Westerheide, S.D., Anckar, J., Stevens, S.M., Jr., Sistonen, L. and Morimoto, R.I. (2009) Stress-inducible regulation of heat shock factor 1 by the deacetylase SIRT1. *Science*, **323**, 1063-1066.

White, J., Southgate, E., Thomson, J. and Brenner, S. (1986) The Structure of the Nervous System of the Nematode Caenorhabditis elegans. *Philosophical Transactions of the Royal Society of London. Series B, Biological Sciences (1934-1990)*, **314**, 1-340.

White, J.G., Southgate, E., Thomson, J.N. and Brenner, S. (1976) The structure of the ventral nerve cord of Caenorhabditis elegans. *Philos Trans R Soc Lond B Biol Sci*, **275**, 327-348.

WHO. (2009) Mental Health and Substance Abuse. Facts and Figures. Alzheimer's Disease. *Available at: www.searo.who.int/en/section1174/section1199/section1567_6740.htm. Accessed 2009*.

Williamson, J., Goldman, J. and Marder, K.S. (2009) Genetic aspects of Alzheimer disease. *Neurologist*, **15**, 80-86.

Wilm, T., Demel, P., Koop, H.U., Schnabel, H. and Schnabel, R. (1999) Ballistic transformation of Caenorhabditis elegans. *Gene*, **229**, 31-35.

Wu, H.Y., Tomizawa, K. and Matsui, H. (2007) Calpain-calcineurin signaling in the pathogenesis of calcium-dependent disorder. *Acta Med Okayama*, **61**, 123-137.

Wu, J. and Kaufman, R.J. (2006) From acute ER stress to physiological roles of the Unfolded Protein Response. *Cell Death Differ*, **13**, 374-384.

Xiong, Z.G., Chu, X.P. and Simon, R.P. (2006) Ca2+ -permeable acid-sensing ion channels and ischemic brain injury. *J Membr Biol*, **209**, 59-68.

Xiong, Z.G., Zhu, X.M., Chu, X.P., Minami, M., Hey, J., Wei, W.L., MacDonald, J.F., Wemmie, J.A., Price, M.P., Welsh, M.J. and Simon, R.P. (2004) Neuroprotection in ischemia: blocking calcium-permeable acid-sensing ion channels. *Cell*, **118**, 687-698.

Xu, K., Tavernarakis, N. and Driscoll, M. (2001) Necrotic cell death in C. elegans requires the function of calreticulin and regulators of Ca(2+) release from the endoplasmic reticulum. *Neuron*, **31**, 957-971.

Yamashima, T. (2004) Ca2+-dependent proteases in ischemic neuronal death: a conserved 'calpain-cathepsin cascade' from nematodes to primates. *Cell Calcium*, **36**, 285-293.

Yermolaieva, O., Leonard, A.S., Schnizler, M.K., Abboud, F.M. and Welsh, M.J. (2004) Extracellular acidosis increases neuronal cell calcium by activating acid-sensing ion channel 1a. *Proc Natl Acad Sci U S A*, **101**, 6752-6757.

Yorimitsu, T. and Klionsky, D.J. (2005) Autophagy: molecular machinery for self-eating. *Cell Death Differ*, **12 Suppl 2**, 1542-1552.

Yorimitsu, T., Nair, U., Yang, Z. and Klionsky, D.J. (2006) Endoplasmic reticulum stress triggers autophagy. *J Biol Chem*, **281**, 30299-30304.

Yoshida, H., Okada, T., Haze, K., Yanagi, H., Yura, T., Negishi, M. and Mori, K. (2000) ATF6 activated by proteolysis binds in the presence of NF-Y (CBF) directly to the cis-acting element responsible for the mammalian unfolded protein response. *Mol Cell Biol*, **20**, 6755-6767.

Yu, H., Pretot, R.F., Burglin, T.R. and Sternberg, P.W. (2003) Distinct roles of transcription factors EGL-46 and DAF-19 in specifying the functionality of a polycystin-expressing sensory neuron necessary for C. elegans male vulva location behavior. *Development*, **130**, 5217-5227.

Yuan, J. (2009) Neuroprotective strategies targeting apoptotic and necrotic cell death for stroke. *Apoptosis*, **14**, 469-477.

Yue, Z., Jin, S., Yang, C., Levine, A.J. and Heintz, N. (2003) Beclin 1, an autophagy gene essential for early embryonic development, is a haploinsufficient tumor suppressor. *Proc Natl Acad Sci U S A*, **100**, 15077-15082.

Zhang, M. (2008) Endocytic mechanisms and drug discovery in neurodegenerative diseases. *Front Biosci*, **13**, 6086-6105.

Zhang, S., Arnadottir, J., Keller, C., Caldwell, G.A., Yao, C.A. and Chalfie, M. (2004) MEC-2 is recruited to the putative mechanosensory complex in C. elegans touch receptor neurons through its stomatin-like domain. *Curr Biol*, **14**, 1888-1896.

Zhang, W. (2009) Molecular and genetic dissection of neuronal necrotic-like death in *Caenorhabditis elegans*. *PhD Thesis*. Rutgers, The State University of New Jersey, New Brunswick, p. 236.

Zhang, Y., MacLean, J.N., An, W.F., Lanning, C.C. and Harris-Warrick, R.M. (2003) KChIP1 and frequenin modify shal-evoked potassium currents in pyloric neurons in the lobster stomatogastric ganglion. *J Neurophysiol*, **89**, 1902-1909.

Zhou, Z., Yamamoto, Y., Sugai, F., Yoshida, K., Kishima, Y., Sumi, H., Nakamura, H. and Sakoda, S. (2004) Hepatoma-derived growth factor is a neurotrophic factor harbored in the nucleus. *J Biol Chem*, **279**, 27320-27326.

Zhu, X.M., Liu, X.H., Cai, L.R. and Xu, F.F. (2006) [Hypoxic preconditioning induces endoplasmic reticulum stress-related cardioprotection mediated by p38 mitogen-activated protein kinase]. *Sheng Li Xue Bao*, **58**, 463-470.

Zinszner, H., Kuroda, M., Wang, X., Batchvarova, N., Lightfoot, R.T., Remotti, H., Stevens, J.L. and Ron, D. (1998) CHOP is implicated in programmed cell death in response to impaired function of the endoplasmic reticulum. *Genes Dev*, **12**, 982-995.

Zoghbi, H.Y. and Orr, H.T. (2000) Glutamine repeats and neurodegeneration. *Annu Rev Neurosci*, **23**, 217-247.

Zong, W.X. and Thompson, C.B. (2006) Necrotic death as a cell fate. *Genes Dev*, **20**, 1-15.

CURRICULUM VITAE

Yury Orlando Nunez Lopez

EDUCATION

2002 – 2009: Ph.D. Cell & Developmental Biology. Joint Graduate Program in Molecular Biosciences. Rutgers University–UMDNJ, Piscataway, NJ.

1989-1994: Summa Cum Laude, Licentiate in Radiochemistry (5-year University Degree). Higher Institute of Nuclear Sciences and Technology. Havana, Cuba. Equivalency granted in USA: Bachelor in Sciences in Applied Chemistry, by the World Education Service, Inc., New York, NY, July 27, 1999.

EMPLOYMENT HISTORY & EXPERIENCE

Sept. 2002 – Sept. 2009: Graduate Fellow/ Ph.D. Candidate. Joint Program in Molecular Biosciences/ Cell and Developmental Biology Program. Rutgers University-UMDNJ, Piscataway, NJ. Dr. Monica Driscoll's Laboratory (*C. elegans* Genetics and Neurodegeneration).

Nov.2000 – Aug. 2002: Sr. Research Technician. Memorial Sloan-Kettering Cancer Center (MSKCC), New York, NY. Dr. Elizabeth Lacy's Laboratory (Molecular Mouse Embryology). Molecular Biology Program.

Mar.2000 – Nov. 2000: Research Associate. Yale University School of Medicine, Epidemiology and Public Health Department. New Haven, CT. Dr. Debra E. Bessen's Laboratory (Streptococcus pyogenes Molecular Microbiology).

Nov.1994 – Mar. 1998: Research Assistant/Associate. Institute of Tropical Medicine Pedro Kouri (IPK), Parasitology and Vector Control Department, Havana, Cuba.

PUBLICATIONS

- Royal DC, Bianchi L, Royal MA, Lizzio M, Mukherjee G, Nunez YO, and Driscoll M. Temperature-sensitive mutant of the *Caenorhabditis elegans* neurotoxic MEC-4(D) DEG/ENaC channel identifies a site required for trafficking or surface maintenance. **J. Biol. Chem., December 23, 2005; 280(51): 41976 - 41986.**

- Nunez YO, Fernandez MA, Torres-Nunez D, Silva JA, Maestre JL, and Fonte LA. Multiplex PCR amplification and differentiation of *Entamoeba histolytica*/ *E. dispar* DNA from stool samples. **Am. J. Trop. Med. Hyg. 2001, 64(3): 293-297.**

- Fonte LA, Fernandez MA, Sanchez L, Marin H, Montano I, and Nunez YO. Demonstration using ENZYMEBA test of the overdiagnosis of intestinal amoebiosis associated with microscopic examination of feces. Report of a study in Cienfuegos, Cuba. **Rev. Patol. Trop. 1998, 27(2): 195-200.**

- Fernandez MA, Sanchez L, Marin H, Montano I, Nunez YO, and Fonte LA. Knowledge, beliefs, and practices in relation to intestinal amoebiosis. **Rev. Cubana Med. 1998, 37(3): 147-156.**